
[All ETDs from UAB](#)

[UAB Theses & Dissertations](#)

2017

Development And Assessment Of Nonsense Suppression Therapies To Ameliorate Disease Progression In A Nonsense Mouse Model Of Mps I Hurler Syndrome

Gwendolyn G. Gunn
University of Alabama at Birmingham

Follow this and additional works at: <https://digitalcommons.library.uab.edu/etd-collection>

Recommended Citation

Gunn, Gwendolyn G., "Development And Assessment Of Nonsense Suppression Therapies To Ameliorate Disease Progression In A Nonsense Mouse Model Of Mps I Hurler Syndrome" (2017). *All ETDs from UAB*. 1810.

<https://digitalcommons.library.uab.edu/etd-collection/1810>

This content has been accepted for inclusion by an authorized administrator of the UAB Digital Commons, and is provided as a free open access item. All inquiries regarding this item or the UAB Digital Commons should be directed to the [UAB Libraries Office of Scholarly Communication](#).

DEVELOPMENT AND ASSESSMENT OF NONSENSE SUPPRESSION
THERAPIES TO AMELIORATE DISEASE PROGRESSION IN A NONSENSE
MOUSE MODEL OF MPS I HURLER SYNDROME

by

GWEN GUNN

DAVID M. BEDWELL, COMMITTEE CHAIR
KIM M. KEELING
ROBERT A. KESTERSON
TRENTON R. SCHOEB
JOHN J. SHACKA

A DISSERTATION

Submitted to the graduate faculty of The University of Alabama at Birmingham,
in partial fulfillment of the requirements for the degree of
Doctor of Philosophy

BIRMINGHAM, ALABAMA

2017

DEVELOPMENT AND ASSESSMENT OF NONSENSE SUPPRESSION THERAPIES
TO AMELIORATE DISEASE PROGRESSION IN A NONSENSE MOUSE MODEL
OF MPS I HURLER SYNDROME

GWEN GUNN

CELL, MOLECULAR, AND DEVELOPMENTAL BIOLOGY

ABSTRACT

Nonsense mutations introduce a premature termination codon (PTC) into the open reading frame of an mRNA resulting in premature translation termination, loss of functional protein, and rapid degradation of the mutant mRNA. Approximately 11% of human genetic disorders are attributable to a nonsense mutation. Several small molecules have been identified as potential nonsense suppression compounds. These compounds increase the frequency of PTC recognition by near-cognate aminoacyl tRNAs resulting in PTC “readthrough” and restored protein production.

Mucopolysaccharidosis type I-Hurler (MPS IH) is the severe form of the autosomal recessive lysosomal storage disorder caused by mutations in the iduronidase (IDUA) gene. 60-80% of the MPS IH patient population have a nonsense mutation in at least one allele of the gene. Preliminary studies in our laboratory indicated that the designer aminoglycoside NB84 could restore functional enzyme and alleviate GAG accumulation both *in vitro* and *in vivo* in a nonsense model of MPS IH. Long-term, early intervention treatment with NB84 in the W402X mouse model resulted in sustained restoration of enzyme activity, reduced GAG accumulation, slowed disease progression in multiple tissues, and no evidence of toxicity. These results demonstrate that nonsense suppression therapy can effectively ameliorate disease progression and that designer

aminoglycosides represent a safe and more effective alternative to traditional aminoglycosides.

The non-aminoglycoside compounds PTC124, 414, and 415 were identified by high throughput screening as candidates for nonsense suppression therapy. Extensive evidence demonstrates that PTC124 is orally bioavailable and induces nonsense mutation readthrough in a variety of disease contexts. We evaluated drug mechanism, safety and efficacy of these three compounds using heterologous reporter assays, *in vitro*, and *in vivo* studies in the context of MPS IH. We found that all three compounds resulted in decreased GAG accumulation *in vitro*. PTC124 produced modest but statistically significant improvements *in vitro* after both short- and long-term administration.

Our results demonstrate that nonsense suppression therapy is a viable approach for the treatment of genetic disorders but that, due to its modest efficacy, it may be best used in combination with existing or new therapies.

ACKNOWLEDGEMENTS

I would like to thank my mentor Dr. David M Bedwell for his extraordinary example of the creative, honest, and avid practice of research science. I would like to thank the members of my graduate committee, Dr. Robert Kesterson, Dr. Trenton Schoeb, and Dr. John Shacka, for their insightful guidance and consistent support. I would particularly like to thank Dr. Kim Keeling for her incredible guidance in scientific study design, scientific writing, and generosity of time and energy.

I would like express my great appreciate for Wayne Bradley for his contribution to our work and his enthusiastic willingness to teach, help, and learn. I would also like to thank Dr. Terry Lewis and Dr. Thomas Van Groen for their generosity of time, energy and expertise.

Thank you so very much to all the members of the Bedwell/Keeling Lab, past and present, who have made each day enjoyable and productive.

Last, I would like to acknowledge and honor the support of my friends and family. Marc Gunn, Heather Gunn, Inara Gunn, Robert Gisiner, Anne Phelps, Daphne Boggs and Matt Weaver, without each and every one of you this journey would have been exponentially more difficult and unfathomably less beautiful. Thank you.

TABLE OF CONTENTS

	<i>Page</i>
ABSTRACT	ii
ACKNOWLEDGMENTS	iv
LIST OF TABLES	vi
LIST OF FIGURES	vii
INTRODUCTION	1
Eukaryotic Translation	2
Elongation and Translational Fidelity	3
Translation Termination	5
Premature Termination Codons (PTCs) vs. Natural Stop Codons	6
Nonsense Suppression Therapy	8
Aminoglycosides	8
Synthetic Aminoglycoside Derivatives	9
Non-Aminoglycoside Compounds	10
Hurler Syndrome (MPS I-H)	11
Clinical Manifestations, Detection, and Diagnosis	11
Current Treatments	13
Nonsense Suppression Therapy and MPS I-H	14
LONG-TERM NONSENSE SUPPRESSION THERAPY MODERATES MPS I-H DISEASE PROGRESSION	16
ASSESSMENT OF NON-AMINOGLYCOSIDE COMPOUNDS AS NONSENSE SUPPRESSION AGENTS IN AN <i>IDUA</i> -W402X MOUSE MODEL OF MPS I-H	46
SUMMARY	93
Major Findings and Significance	93
Future Directions	98
GENERAL LIST OF REFERENCES	103
APPENDIX: IACUC APPROVAL FOR ANIMAL STUDIES	108

LIST OF TABLES

<i>Table</i>	<i>Page</i>
LONG-TERM NONSENSE SUPPRESSION THERAPY MODERATES MPS I-H DISEASE PROGRESSION	
1 Comprehensive Serum Clinical Chemistry Analysis to Evaluate NB84 Toxicity	45
ASSESSMENT OF NON-AMINOGLYCOSIDE COMPOUNDS AS NONSENSE SUPPRESSION AGENTS IN AN <i>IDUA</i> -W402X MOUSE MODEL OF MPS I-H	
1 <i>In vivo</i> study design details and study endpoints	92

LIST OF FIGURES

<i>Figure</i>	<i>Page</i>
LONG-TERM NONSENSE SUPPRESSION THERAPY MODERATES MPS I-H DISEASE PROGRESSION	
1 NB84 treatment alleviates MPS I-H biochemical endpoints in mouse brain	37
2 NB84 treatment alleviates MPS I-H biochemical endpoints in mouse spleen	38
3 NB84 treatment moderates neuropathology in MPS I-H mice	39
4 NB84 treatment moderates progression of heart defects in MPS I-H mice	41
5 NB84 treatment moderates progress of bone defects in MPS I-H mice	42
6 NB84 treatment improves activity levels in MPS I-H mice	44
ASSESSMENT OF NON-AMINOGLYCOSIDE COMPOUNDS AS NONSENSE SUPPRESSION AGENTS IN AN <i>IDUA</i> -W402X MOUSE MODEL OF MPS I-H	
1 Characterization of the ability of non-aminoglycoside compounds to suppress the <i>Idua</i> - W402X nonsense mutation <i>in vitro</i>	77
2 Examination of compound efficacy and tolerability after 4 weeks of treatment in <i>Idua</i> - W402X mice	79
3 Examination of compound specificity after 2 weeks of treatment in <i>Idua</i> -W402X and KO MPS I-H mice	81
4 Examination of biochemical endpoints after 28 weeks of treatment in <i>Idua</i> -W402X mice	82
5 Mass spectrometry analysis of liver GAGs in response to PTC124	83
6 Functional and morphological heart analysis after 28 weeks of treatment in <i>Idua</i> - W402X mice	85

LIST OF FIGURES (CONTINUED)

7	Bone morphological parameters after 28 weeks of treatment in <i>Idua-W402X</i> mice	86
8	Examination of PTC124 metabolites in mouse urine	88
S1	Four-week treatment does not reduce GAG accumulation in heart and brain	89
S2	Additional bone morphological and histological parameters after 28-week treatment in <i>Idua-W402X</i> mice	90
S3	Behavioral analysis after 28-week treatment in <i>Idua-W402X</i> mice	91

SUMMARY

1	Opportunities for enhancing or modifying nonsense suppression therapy	101
---	---	-----

INTRODUCTION

Mucopolysaccharidosis type I (MPS I) is an autosomal recessive lysosomal storage disorder (LSD) caused by deficiency of the lysosomal enzyme alpha-L-iduronidase. Approximately 70% of the patient population with the severe Hurler form of the disease carry a nonsense mutation in at least one allele of the iduronidase gene [1], but restoration of less than 1% of normal enzyme activity could drastically improve the disease progression, as evidenced by the markedly reduced disease severity seen in patients with the milder Scheie form of the disease [2]. In this study, we investigated potential nonsense suppression compounds in a nonsense mouse model of Hurler disease. We first evaluated early intervention through both short- and long-term administration of the designer aminoglycoside NB84. We found that this compound restored and maintained enzyme activity resulting in significant amelioration of disease progression without any evidence of toxicity. We then evaluated the non-aminoglycoside compounds PTC124, 414, and 415. PTC124 is the only compound so far that has been approved, albeit conditionally, for the treatment of a disease caused by a nonsense mutation [3]. PTC414 is a derivative of PTC124 with *in vitro* evidence of greater nonsense suppression activity [4] and PTC415 is a structurally unrelated compound identified by PTC Therapeutics as a potential nonsense suppression compound with greater blood-brain barrier penetrance (private communication from PTC Therapeutics). Using heterologous reporters, we evaluated the effect of these compounds on read-through induction and

nonsense-mediated mRNA decay (NMD) inhibition. We then evaluated efficacy and safety with *in vitro* and short term *in vivo* administration. The two safest compounds, PTC124 and PTC414, were administered in a long-term study and showed modest therapeutic efficacy. We determined that the efficacy of PTC124 is limited because the majority of the compound is modified and excreted in the Hurler mouse model.

Eukaryotic Translation

Translation is the step in the so-called central dogma wherein an mRNA message is read as tri-nucleotide codons, each encoding a single amino acid, that ultimately generates a polypeptide chain forming a functional protein. This process is highly regulated due to the demanding use of resources and the risk of erroneously formed protein products. The process is often divided into stages, namely initiation, elongation, termination and recycling, based on participating factors and process regulation. The general process of initiation in eukaryotes begins with the formation of the 43S preinitiation complex, comprised of the 40S ribosomal subunit, the eIF2 ternary complex (eIF2-GTP-Met-tRNA^{Met}_i), eIF3 and several other factors [5]. The 43S complex is recruited to the capped 5' end of the message through the interaction of eIF3 and the scaffolding protein eIF4G, which binds eIF4E on the 5' cap. The 43S complex then unwinds and scans the 5' UTR for the initiation codon, a process dependent upon eIF1A [6]. Start codon recognition and eIF2 hydrolysis mark the formation of the 48S initiation complex which then binds the 60S ribosomal subunit to form the 80S initiation complex. The 80S complex is capable of reading the mRNA and incorporating subsequent amino acids into the growing polypeptide chain in a process known as elongation. Elongation is

a cyclic phase wherein aminoacyl-tRNAs are sampled based on codon-anticodon pairing and rejected or incorporated into the growing polypeptide chain [7]. tRNAs initially enter the ribosome at the A site for evaluation of codon-anticodon pairing, are translocated to the P site for peptide bond formation, and then released from the E site for recycling. Termination occurs when the ribosome reaches one of the stop codons (UGA, UAA, or UAG) for which there are no complementary aminoacyl-tRNAs. These codon sequences are recognized by the eukaryotic release factors eRF1 and eRF3 which facilitate peptide release and dissociation of the nascent peptide. Finally, recycling of the translational machinery occurs in which subunits are dissociated from the mRNA so that they may be recycled or reassembled onto new messages to perform additional rounds of translation [8]. Concomitantly, errors in translation are monitored by a number of mRNA surveillance pathways such as no-go decay (NGD), non-stop decay (NSD) and nonsense-mediated decay (NMD) which target, respectively, stalled ribosomes, messages lacking termination codons, and premature termination events [9]. These pathways each preferentially target defective mRNAs for rapid degradation.

Elongation and Translational Fidelity

During elongation, the initial codon of the ORF successfully paired with its aminoacyl-tRNA (Met-tRNA_i) resides in the P site of the 80S ribosome. The next codon now resides in the A (acceptor) site of the ribosome where it will act as the template with which a new aminoacyl-tRNA must pair, directed by eukaryotic elongation factor eEF1A-GTP. This phase is cyclic and involves random sampling of tRNAs in the A site of the ribosome for each subsequent codon of the mRNA template. At the base of the A

site lies the ribosomal decoding center consisting of rRNA and ribosomal proteins that participate in sampling, proofreading, and accommodating tRNAs at the A site based on the accuracy of codon-anticodon pairing. The initial identification of a cognate tRNA must be quick and accurate. This step is monitored by several key nucleotides of the 18s rRNA, A1824, A1825 and G626 oriented around the decoding center of the ribosome. These residues undergo conformational changes in response to correct codon-anticodon pairing at positions 1 and 2 of the codon, and loose interaction with the third “wobble” position forming stabilizing hydrogen bonds with the tRNA followed by further eukaryotic-specific stabilizing interactions with residues on the eS30 ribosomal protein to reinforce cognate pairing during initial tRNA sampling [10]. Once the cognate interaction has been stabilized through these key residues, the resulting conformational change “opens” a hydrophobic barrier allowing hydrolysis of GTP on eEF1A changing the ribosomal A site conformation from “open” to “closed”, more firmly securing the peptidyl-tRNA in the P site while reducing interaction with eEF1A-GDP allowing for its release from the ribosome [11]. This causes the tRNA to undergo a final conformational change that enables differentiation between true cognates and near-cognates (codons that differ at a single nucleotide). If the match is good then rapid accommodation of the tRNA occurs with the aminoacyl end of the tRNA shifting toward the peptidyl transferase center where a peptide bond is established between the first and second amino acids. This then triggers ratcheting of the ribosomal subunits to move the acceptor ends of the tRNAs over to the P/E sites from the A/P sites. eEF2 GTPase then binds the ribosome resulting in rapid hydrolysis of GTP, conformational change, release of eEF2-GDP and complete translocation of the tRNAs into the E and P sites so that a new codon is now

positioned in the A site and sampling of aminoacyl-tRNAs can begin again. This process is repeated until a termination codon enters the A site.

Translation Termination

Translation termination occurs when the translating ribosome encounters one of three stop codons (UAA, UAG, UGA) for which no cognate tRNAs exist. Instead these three codons are all recognized, in eukaryotes, by a single class 1 release factor, eRF1. eRF1 is targeted to the ribosome in complex with eRF3-GTP where accommodation of eRF1 through recognition of the stop codon results in GTP hydrolysis and dissociation of eRF3-GDP. Specificity is achieved through conserved motifs of eRF1 which have long been implicated in stop codon recognition. Recent work utilizing cryo-EM has demonstrated that the TASNIKS motif of eRF1 is responsible for constraining the identity of the first base (+1) of a stop codon to uridine [12]. Upon dissociation of eRF3-GDP, eRF1 is then bound by ABCE1/Rli1 which induces a second conformational change essential for identification of bases 2 and 3 of the stop codon and peptide release from the ribosome [13]. These roles are mediated through two other conserved domains on eRF1; YxCxxxF was shown to interact with the 2+ and 3+ purines of stop codons thus participating directly in stop codon discrimination and the GGQ motif of eRF1 extends into the peptide transfer center of the ribosome and hydrolyses the ester bond between the tRNA and the polypeptide chain facilitating its release from the ribosome. Stop codon recognition is enhanced by a number of contextual factors. Cytoplasmic poly(A)-binding protein (PABPC1) associates with the poly(A)-tail of mRNAs. It has been long been known that this protein associates with the translation initiation factors, namely eIF4G, to

produce circularization of the mRNA during translation [14]. More recently it has been shown that PABPC1, in close proximity to a stop codon, enhances translation termination through recruitment and association of termination factors, namely eRF3 [15]. This recruitment of termination factors serves to increase local concentrations near a termination codon, thereby reducing the sampling of tRNAs, accelerating recognition of the stop codon by release factors, and minimizing the time the ribosome resides at the stop codon prior to polypeptide release and ribosome recycling. Subsequent to stop codon recognition, ABCE1 binds and hydrolyzes ATP to split the ribosome into the 60S and 40S subunits, which is essential for ribosome recycling for additional rounds of translation. ABCE1 remains associated with the 40S subunit and is found to be present on the 43S initiation complex leading to a cohesive model of translation termination, ribosome release, and recycling of the ribosome to begin new rounds of translation [16].

Premature Termination Codons (PTCs) vs. Natural Stop Codons

Premature termination codons (PTCs) are the result of a single nucleotide change in the coding sequence of the gene that alters a sense codon to one of the three eukaryotic stop codons. PTCs cause premature translation termination, resulting in production of a truncated, and often non-functional, protein product. Through premature translation termination, PTCs also cause the mRNA to be targeted for rapid degradation by a surveillance pathway known as the nonsense-mediated mRNA decay (NMD) pathway. NMD results in reduced abundance and half-life of the erroneous mRNA. In 2008, a meta-analysis of the Human Gene Mutation Database found that nonsense mutations (in-frame PTCs) account for over 20% of the reported disease-associated single base pair

mutations and nearly 11% of disease lesions resulting in heritable genetic disease [17].

PTCs are subject to differences in the local context, structure, and associated proteins of the mRNA compared to a natural stop codon. The two primary differences that signify a PTC-containing transcript, and target the transcript for NMD, are a long 3' untranslated region (UTR) and/or the presence of exon junction complexes (EJCs) downstream of a PTC-arrested ribosome. In these instances, long 3' UTRs are the result of translation termination 5' to the natural stop codon, thus synthetically increasing the distance of the region between the translational stop site and the start of the poly(A) tail and PABPC1 proteins. These 3' UTRs are coated with enhanced levels of UPF1, a key component of the NMD pathway, and act as a recruiting signal for additional NMD components including nucleases [18]. EJCs consist of a variety of RNA-associated proteins, including UPF2/3, and are deposited on eukaryotic messages as they undergo splicing and during exit from the nucleus. These RNA-bound proteins are removed during the pioneer round of translation as the ribosome physically displaces them during translation. If the ribosome is prematurely stopped at a PTC, then downstream UPF1 and EJCs are not displaced and act as recruiting signals for components of the NMD pathway that degrade the mRNA [19, 20]. Additionally, PTCs result in increased distance between the stop codon and the poly(A) tail and associated PABPC1. Simply tethering of PABPC1 in closer proximity to PTCs can prevent or reduce NMD [21]. Termination suppression occurs when a tRNA is accommodated at the site of a stop codon resulting in amino acid insertion and translation elongation 3' of the stop codon. Termination suppression is much more common at PTCs where it occurs with a frequency of <1.0% [22] compared to a frequency of <0.1% at natural stops [23]. These differences between

PTCs and native stops provide a basis for therapeutic approaches to address diseases resulting from PTCs.

Nonsense Suppression Therapy

Nonsense suppression therapy consists of approaches aimed at restoring protein production from PTC-containing mRNA that result in disease. These approaches include read-through drugs, NMD inhibition, suppressor tRNAs, and RNA-directed pseudouridylation. Small molecule therapies are able to alter rates of termination suppression and NMD efficiency, and represent the most easily-adaptable approach to therapeutic administration. Small molecule nonsense suppression works by inducing read-through as a result of increasing the rate at which PTCs are recognized by near cognate tRNAs whose anticodon is a mismatch at only one of the three nucleotide residues. This results in incorporation of a predictable and finite set of alternative amino acids [24] at the site of the PTC, allowing translation of the full message and restoration of lost protein product.

Aminoglycosides

The most well-known class of nonsense suppression compounds are aminoglycosides (AGs). These compounds were originally discovered as powerful antibiotics in the 1960s. Subsequent work showed that these compounds interact with the 16S subunit of the prokaryotic ribosome, thus interfering with normal translation [25]. A subset of AGs was shown to induce misincorporation of near-cognate aminoacyl-tRNAs at PTCs in eukaryotes [26]. More recent work has been able to verify that, although the

compounds show much lower affinity for eukaryotic versus prokaryotic ribosomes, in both systems they bind to a conserved loop (helix 44) of the 16S prokaryotic and 18S eukaryotic rRNA of the 30S ribosomal subunit resulting in reduced proofreading capacity and increased acceptance of near-cognate tRNAs at premature stop codons [27]. Gentamicin is historically one of the most widely investigated AGs for nonsense suppression. It was first demonstrated in an *in vitro* model of cystic fibrosis that gentamicin and G418 could be used as therapeutic compounds to treat nonsense-associated disease by inducing translation of full-length mRNA from which functional protein was produced [28]. Shortly after, gentamicin was evaluated both *in vitro* and *in vivo* using a mouse model of Duchenne Muscular Dystrophy (DMD) in a study that provided the first definitive evidence that nonsense suppression could restore protein in a disease model and effectively ameliorate the disease phenotype [29]. Clinical trials of gentamicin were conducted in both DMD [30] and CF patients [31] with enough success to demonstrate proof of principle, but with significant incidence of toxicity. It is well-documented that high dose, long-term or repeat administration of AGs results in ototoxicity and nephrotoxicity due primarily to disproportionate accumulation of the compound at those sites with concomitant induction of lysosomal phospholipidosis, and a greater affinity for mitochondrial ribosomes than eukaryotic ribosomes [32-35].

Synthetic Aminoglycoside Derivatives

The reduced affinity of AGs for eukaryotic ribosomes results in a much higher dose requirement to produce beneficial levels of read-through compared to prokaryotes. Designer aminoglycosides with increased specificity for eukaryotic cytoplasmic

ribosomes show higher levels of read-through induction at lower doses [36]. By employing this “mechanism-based drug redesign strategy” compounds like NB74 and NB84 were found to have greater affinity for cytoplasmic, rather than mitochondrial, ribosomes resulting in greatly decreased ototoxicity [37]. NB54 and NB124 were able to restore CF function, both *in vitro* and *in vivo*, to a greater extent than traditional aminoglycosides with reduced ototoxicity [38, 39]. The reduced toxicity and increased efficacy of these designer compounds encourage further investigation of aminoglycosides as nonsense suppression agents.

Non-Aminoglycoside Compounds

There are also alternative small molecules emerging as potential nonsense suppression compounds, termed collectively “non-aminoglycosides”. Whereas the mechanism of action for AGs has been well-investigated and characterized, most other compounds of interest have uncharacterized therapeutic mechanisms and are diverse in their chemical structures. The most promising of these compounds is ataluren aka PTC124, a 1,2,4-oxadiazole derivative marketed by PTC Therapeutics as Translarna™. PTC124 was identified in a high throughput screen and originally validated using luciferase-based reporter assays, cell culture, and the *mdx* mouse model [40]. Subsequently the ability of PTC124 to restore functional enzyme was validated in *Cftr* *-/-* *hCFTR*-G542X mice expressing the G542X PTC-containing human CFTR, demonstrating the broad applicability of PTC124 in treating diseases of nonsense mutations [41]. Phase I clinical trials of PTC124 demonstrated excellent safety and bioavailability [42]. Based on Phase II trials, PTC124 was conditionally approved for the

treatment of DMD by the European Union in 2014 with renewal of that approval in 2016 [43] and Phase III clinical trials for CF. Modest efficacy in the DMD trial and lack of benefit in the Phase II CF study led to failure of PTC124 approval in the United States.

Hurler Syndrome (MPS I-H)

Mucopolysaccharidosis (MPS) type I is an autosomal recessive lysosomal storage disease characterized by severe deficiency of the lysosomal enzyme α -L-iduronidase. This enzyme is a glycosidase involved in the catabolism of the glycosaminoglycans (GAG) dermatan sulfate and heparan sulfate. These GAGs have diverse functions as cell surface signaling molecules or “biological response modifiers” in pathways as diverse as wound repair, growth and development, and infection [44]. Insufficient enzyme activity results in accumulation of GAGs in most organ systems leading to complex somatic and neurological manifestations. Enzyme deficiency can be the result of a number of different types of genetic and regulatory dysfunctions. However, in approximately 70% of patients suffering from the severe Hurler form of MPS I, a nonsense mutation is present in at least one allele of the gene and the two most common nonsense alleles, W402X and Q70X account for approximately 60-80% of those mutations [1, 45].

Clinical Manifestations, Detection, and Diagnosis

MPS type I is divided into three subgroups (Hurler, Hurler-Scheie, and Scheie syndrome) according to clinical manifestations and phenotypic severity. However, this disease truly represents a spectrum disorder where disease severity generally correlates with residual enzyme activity such that enzyme levels less than 0.2% of normal are

associated with the most severe (Hurler) form of the disease whereas enzyme levels nearer 1.0% of WT are associated with the mild non-cognitive Scheie disease phenotype [2]. Scheie patients have normal cognitive abilities and a normal lifespan. Thus, a small amount of normal enzyme function can significantly improve the quality of life and lifespan of Hurler syndrome patients. Some of the organ systems most notably affected in Hurler syndrome patients include airway, pulmonary, cardiac, neurologic, ophthalmologic, and orthopedic systems. Children with metabolic disorders are frequently born healthy with no obvious sign of any disease. However, as accumulation of the disease-causing substrate progresses, so does disease manifestation. In the severe Hurler form of MPS I children begin to exhibit symptoms including corneal clouding, hepatosplenomegaly, coarse facial features, and bone deformities within the first year. Within the second year there is an observable decline in cognitive ability. Without intervention, these patients usually die within the first decade from obstructive airway, respiratory infection, spinal compression, and cardiac complications [1].

Because most patients with metabolic defects are born apparently healthy, detection usually comes well after the presentation of disease phenotypes which indicate to caregivers, or the patients themselves, that something is not right. Official diagnosis occurs through evaluation of urine GAGs and residual leukocyte or fibroblast enzyme activity [46]. However, due to the development of therapies to address LSDs, along with growing evidence supporting early therapeutic intervention [2, 46, 47], programs to include LSDs, such as MPS I, on newborn screens are active or under way in many US states and several other countries around the world [48, 49].

Current Treatments

The first treatment available for MPS I was hematopoietic stem cell transplantation (HSCT). This treatment is currently the recommended treatment of choice for patients with the severe form of MPS I (Hurler) who are diagnosed before 2.5 years of age with negligible to moderate cognitive impairment, or any patient for which there is a suitable donor when there is evidence of cognitive decline [47]. This option is expensive, invasive and carries a 10-15% risk of death but it has been demonstrated to preserve cognitive function and prevent further somatic deterioration.

Enzyme replacement therapy (ERT) represents the newest successful method of treatment for MPS I. Recombinant human alpha-L-iduronidase (laronidase, Aldurazyme) was approved for use in 2003 and has transformed the prognosis for MPS I patients [50]. However, it is delivered through intravenous infusion and treatment must be continued indefinitely so that the cost of this form of treatment throughout a lifetime can be staggering. Additionally, the compound does not cross the blood-brain barrier and therefore does not provide a viable option for attenuating cognitive decline [51], although in combination with a therapy that does benefit the CNS, like HSCT, patient outcome is even more favorable [47]. Both HSCT and ERT are expensive and require access to relatively advanced medical care and facilities. Furthermore, neither treatment fully addresses the abnormalities found in the brain, bone, cornea or heart valves, which are the least responsive to HSCT or ERT.

Nonsense Suppression Therapy and MPS I-Hurler

The first evidence of the potential ability of nonsense suppression therapy to benefit MPS I Hurler patients was supplied by a study of patient fibroblasts heterozygous for the Q70X and W402X mutations. Fibroblasts exhibited increased enzyme activity and reduced GAG storage in response to gentamicin treatment [52]. The development of a nonsense mouse model of Hurler syndrome, carrying a PTC analogous to the most common W402X mutation found in human patients, has allowed greater analysis of nonsense suppression therapies [53]. This animal model was used to assess the designer aminoglycosides NB54 and NB84. NB84 was able to reduce urine GAG excretion and tissue GAG storage to a greater extent than NB54 and traditional aminoglycosides [54]. Administration of the non-aminoglycoside compound PTC124 in this animal model provided promising preliminary evidence of GAG reduction in a distinct dose-dependent manner [55]. An ongoing Phase II clinical trial was approved by the European Medicines Agency in 2014 and began in 2015 to evaluate safety and pharmacokinetics of PTC124 in Hurler patients.

There is now excellent evidence for the therapeutic potential of nonsense suppression compounds. Preliminary data in a nonsense Hurler animal model showed short aminoglycoside administration resulted in reduced GAG accumulation and increased enzyme activity [54]. However, Hurler disease is a progressive disorder with a complex phenotypic presentation. My research aimed to identify and validate potential nonsense suppression compounds in the Hurler nonsense mouse model. To this end, I investigated the long-term therapeutic efficacy and safety of the designer aminoglycoside NB84 in the W402X mouse model. The consensus in evaluating MPS IH disease and

intervention is that disease progression can be prevented but not corrected. To this end, we designed the studies so that treatment was begun at a far earlier time point, three weeks of age, to provide the greatest therapeutic benefit. Additionally, Hurler disease is a progressive disorder and the aminoglycosides are associated with toxicity. Therefore, we designed a long-term treatment to evaluate the safety profile of the designer aminoglycoside NB84 and to evaluate some of the diverse phenotypic presentations of the disease only detectable in older animals (Chapter 2). We next evaluated a group of non-aminoglycoside compounds, PTC124, 414, and 415, in a similarly designed animal study. However, we first evaluated these compounds using heterologous reporter assays and *in vitro* systems to investigate the as-yet uncharacterized mechanisms of action and therapeutic potential of the new compounds PTC414 and 415 (Chapter 3).

LONG-TERM NONSENSE SUPPRESSION THERAPY MODERATES MPS I-H
DISEASE PROGRESSION

by

GWEN GUNN, YANYING DAI, MING DU, VALERY BELAKHOV, JEYAKUMAR
KANDASAMY, TRENTON R. SCHOEB, TIMOR BAASOV, DAVID M. BEDWELL,
AND KIM M. KEELING

Molecular Genetics and Metabolism 111 (2014) 374-381

Copyright
2014
by
Elsevier, Inc.

Used by permission

Format adapted and errata corrected for dissertation

ABSTRACT

Nonsense suppression therapy is a therapeutic approach aimed at treating genetic diseases caused by in-frame premature termination codons (PTCs; also commonly known as nonsense mutations). This approach utilizes compounds that suppress translation termination at PTCs, which allows translation to continue and partial levels of deficient protein function to be restored. We hypothesize that suppression therapy can attenuate the lysosomal storage disease mucopolysaccharidosis type I-Hurler (MPS I-H), the severe form of α -L-iduronidase deficiency. α -L-iduronidase participates in glycosaminoglycan (GAG) catabolism and its insufficiency causes progressive GAG accumulation and onset of the MPS I-H phenotype, which consists of multiple somatic and neurological defects. 60-80% of MPS I-H patients carry a nonsense mutation in the *IDUA* gene. We previously showed that 2-week treatment with the designer aminoglycoside NB84 restored enough α -L-iduronidase function via PTC suppression to reduce tissue GAG accumulation in the *Idua*^{tm1Kmke} MPS I-H mouse model, which carries a PTC homologous to the human *IDUA-W402X* nonsense mutation. Here we report that long-term NB84 administration maintains α -L-iduronidase activity and GAG reduction in *Idua*^{tm1Kmke} mice throughout a 28-week treatment period. Examination of more complex MPS I-H phenotypes in *Idua*^{tm1Kmke} mice following 28-week NB84 treatment revealed significant moderation of the disease in multiple tissues, including the brain, heart and bone, that are resistant to current MPS I-H therapies. This study represents the first demonstration that long-term nonsense suppression therapy can moderate progression of a genetic disease.

Keywords: nonsense suppression; readthrough; premature termination codons; nonsense mutations; mucopolysaccharidosis I-Hurler; lysosomal storage disease

INTRODUCTION

Nonsense suppression therapy is a therapeutic approach aimed at treating diseases caused by nonsense mutations. Suppression of translation termination at nonsense mutations occurs when an aminoacyl-tRNA base pairs with a premature termination codon (PTC) and the amino acid carried by the aminoacyl-tRNA is incorporated into the nascent polypeptide at the site of the PTC. This allows translation elongation to continue in the original ribosomal reading frame and results in the production of full-length polypeptide. A number of drugs have been found to stimulate nonsense suppression and restore partial function of deficient proteins associated with a variety of genetic diseases [1].

In this study, we examined whether nonsense suppression therapy can moderate the progression of the lysosomal storage disease mucopolysaccharidosis I-Hurler (MPS I-H). MPS I-H is caused by a severe deficiency of the enzyme α -L-iduronidase, which is encoded by the *IDUA* gene. Loss of α -L-iduronidase function results in an inability to degrade the glycosaminoglycans (GAGs) dermatan sulfate and heparan sulfate. This leads to progressive accumulation of these GAGs and onset of the MPS I-H phenotype that consists of multiple somatic and neurological defects [2]. MPS I-H patients are born without symptoms; however, presentation of the disease manifests during infancy with frequent respiratory and/or ear infections, hernia development, restricted joint movement, altered facial features and skeletal deformities. Developmental delay usually becomes

apparent by 12 to 24 months of age followed by a progressive cognitive decline and onset of multiple neurological abnormalities. Progressive joint and skeletal disease leads to significant disability. Furthermore, MPS I-H patients develop progressive valvular and cardiac disease. Without therapeutic intervention, most MPS I-H patients succumb to the disease in their first decade due to cardiorespiratory failure and neurologic disease.

MPS I-H is an excellent candidate disease for nonsense suppression therapy. First, genotype/phenotype correlation studies indicate that MPS I-H has a low threshold for correction since as little as 0.3-1% of normal α -L-iduronidase function significantly alleviates the MPS I-H phenotype [3, 4]. Second, nonsense mutations are prevalent among MPS I-H patients, where it is estimated that 60-80% of MPS I-H patients carry a nonsense mutation [5].

We previously found that the aminoglycoside gentamicin restored enough α -L-iduronidase via PTC suppression to normalize GAG accumulation and lysosomal morphology in cultured primary MPS I-H patient fibroblasts [6]. However, current clinical aminoglycosides are prohibited from long-term use for suppression therapy due to their toxicity [7, 8]. Recently, a novel rational drug design strategy was devised to generate new aminoglycosides that are more effective in mediating PTC suppression and less toxic than conventional aminoglycosides [9]. One of the aminoglycoside derivatives created by this drug design strategy, NB84, restored enough α -L-iduronidase activity to reduce GAG accumulation by 15-65% in *Idua*^{tm1Kmke} mouse tissues after two weeks of administration [10, 11]. Fibroblasts from patients with attenuated forms of MPS I (Scheie; Hurler-Scheie) have been reported to retain 20–70% fewer GAGs than cells from MPS I-H patients [4]. Based on these values, the level of GAG reduction observed

in *Idua*^{tm1Kmke} mice treated with NB84 may be sufficient to attenuate the severe MPS I-H phenotype in multiple tissues.

In the current study, we examined whether long-term NB84 treatment can reduce or prevent progression of morphological and functional defects associated with MPS I-H in *Idua*^{tm1Kmke} mice. We found that the restoration of α -L-iduronidase function and the corresponding decrease in GAG accumulation associated with NB84 treatment could be maintained for 28 weeks in *Idua*^{tm1Kmke} mice. Furthermore, *Idua*^{tm1Kmke} mice treated with NB84 for 28 weeks exhibited moderation of the MPS I-H phenotype in multiple tissues including the CNS, heart and bone, which are resistant to current MPS I therapies. This suggests that nonsense suppression therapy, alone or in combination with other MPS I therapies, may be effective in treating MPS I-H in patients that carry nonsense mutations.

MATERIALS AND METHODS

Animal Treatment. The Baasov lab (Technion-Israel Institute of Technology) synthesized NB84 [9]. NB84 was dissolved in sterilized PBS and administered at a dose of 30 mg/kg via daily subcutaneous injections to 10-week-old mice daily for 2 weeks and to 3-week-old mice three times weekly (M/W/F) for either 9 or 28 weeks. Age-matched untreated mutant and wild-type control cohorts were included for each treatment group. Clinical chemistry analysis of blood and urine samples was conducted by Antech Diagnostics. All animal work was conducted according to relevant national and international guidelines. All animal protocols used in this study were reviewed and approved by the UAB IACUC (APN#120109344).

Biochemical Assays. Assays to determine α -L-iduronidase, β -hexosaminidase, and β -glucuronidase activities and sulfated GAG levels were performed as previously described [10]. Enzyme specific activities were calculated as picomoles of released substrate per mg of total protein per hour. Enzyme activities remained linear over the incubation times. Tissue sulfated GAG levels were calculated as μ g of GAGs per mg of defatted, dried tissue using a dye-binding assay (Blyscan), where chondroitin 6-sulfate was used as a reference.

Elevated Zero Maze. The apparatus consists of a circular maze, 70 centimeters in diameter, raised 40 cm above the platform, and divided into four equal sections. Two opposite sections have 15 cm high sides of non-transparent material, and the other two have only a 0.5 cm high wall. The animal is put in the arena at the juncture of a high wall and a low wall, and observed for 4 minutes, with a camera driven tracker system, (Ethovision, Noldus, The Netherlands). The system records the position of the animal in the arena at 5 frames/second. The test was performed once per animal to prevent habituation. After each testing day and in between animals the apparatus is wiped down with chlorhexidine and 70% ethanol and allowed to air-dry.

Western blotting. Fifty micrograms of total protein lysate were subjected to SDS-PAGE and transferred to Immobolone-P membrane (Millipore). Blots were incubated with antibodies to GFAP (EMD Millipore), IBA-1 (Wako Chemicals), LAMP-1 (DSHB), or tubulin (Abcam) according to manufacturer instructions. 125 I-Protein A (GE)-bound proteins were detected and quantified using a Storm PhosphoImager and ImageQuant software (GE).

Immunohistochemistry. The right brain hemisphere was collected in 4% paraformaldehyde (PFA) at sacrifice after 5 minutes of perfusion with PBS. After 18-24 hours in PFA the tissue was rinsed twice for 1 hour each in 70% ethanol and then maintained in 70% ethanol. Tissue was subsequently processed, paraffin-embedded, and sectioned on a microtome at 9 μ m thickness. Sections were then stained using fluorescent antibodies to GFAP (EMD Millipore), IBA-1 (Wako Chemicals), LAMP-1 (DSHB), then amplified using HRP-conjugated secondary antibodies (VectorLabs ImmPress anti-mouse and Invitrogen Superpic anti-rabbit) and TSA amplification (Perkin Elmer Cy3+ and Fit-C+); bis-benzamide DNA. Sections were imaged on a Nikon A1 Confocal Scanning Laser microscope and images generated using version 4.13 Nikon Elements Software at UAB's High Resolution Imaging Facility.

Ultrasound Echocardiography. Doppler transthoracic echocardiography was performed by an experienced sonographer using a Visual Sonics Vevo 2100 Imaging System and 30MHz MS400 MicroScan transducer (FUJIFILM VisualSonics, Inc., Toronto). Mice were anesthetized initially with 5% isoflurane and then maintained with 1% to 2% isoflurane. Core temperatures and heart rate were continuously monitored and maintained at ~37 degrees and ~500 beats per minute, respectively. The chests of the mice were treated with a chemical hair remover to reduce ultrasound attenuation. B-mode guided M-mode measurements of left ventricular wall thickness of the septum and posterior walls were made at the papillary muscle level. An apical four-chamber B-mode color Doppler view was used to position pulse wave Doppler measurement of flow at the tips of the mitral valve leaflets. M-mode was also used to measure ascending aorta lumen diameter and wall thickness at the midpoint between the aortic sinus and the innominate

artery. Flow was measured at the aortic root using M-mode Doppler and evaluation of flow turbulence in the aorta was evaluated with color Doppler. When possible, measurements were made on three consecutive beats.

Micro-computed tomography. Excised mouse femurs were scanned using the Scanco uCT40 desktop cone-beam micro-CT scanner. Bones were placed vertically into 12mm diameter holders and scanned at 12 μm resolution, 70kVp, 114 μA with an integration time of 200ms. Cortical bone was scanned at the midshaft and consisted for 25 slices, 12 μm in thickness. Fewer scans are needed for cortical bone due to its uniformity. Scans were reconstructed and the region of interest was drawn at the outside of the cortical bone such that all of the cortical bone and marrow were included. No trabecular bone was included. The threshold for cortical bone was set at 282 and the 3-D reconstruction was performed on all 25 slices. Data was obtained on bone volume (BV), total volume (TV), BV/TV, and cortical thickness. The trabecular bone was scanned from the growth plate consisted of 200 slices, with each slice 12 μM in thickness. Scans were reconstructed into 2-D slices and 100 slices were analyzed using the μCT Evaluation Program (v5.0A, Sanco Medical). The region of interest was drawn on each of the 100 slices just inside the cortical bone to include only trabecular bone and marrow. The threshold for trabecular bone was set at 212 to distinguish it from the marrow. The 3-D reconstruction was performed using all the outlined slices. No cortical bone was included in the analysis. Data was obtained on bone volume (BV), total volume (TV), BV/TV, trabecular number (number of intersections between bone and non-bone components), trabecular thickness, trabecular separation (space between trabeculae), connectivity density (density of trabecular connections), and structural model index

(trabecular bone structure characterization: plate-like (SMI=0); rod-like (SMI=3); sphere-like (SMI=4).

Osteoclast TRAP staining. Mouse femurs were excised and fixed in 70% ethanol, decalcified, embedded in paraffin, and longitudinally sectioned into 5 μ m sections. Osteoclasts within femur sections were stained for tartrate-resistant acid phosphatase (TRAP) as previously described [12]. Areas of bone and TRAP staining were measured in red and green channel images, respectively, using ImagePro Plus v6.2 software (Media Cybernetics, Rockville, MD). TRAP-stained material was quantitated per area (mm²) of bone examined.

Statistics. All statistics were calculated with two-tailed unpaired t-tests using InStat or GraphPad Prism software.

RESULTS

Long-term NB84 treatment attenuates MPS I-H CNS phenotypes. MPS I-H patients develop intellectual disability; however, patients with attenuated forms of MPS I (Scheie; Hurler-Scheie) have normal intellect. Genotype-phenotype correlations among MPS I patients indicate that only 0.3-1% of normal α -L-iduronidase activity can preclude neurodegeneration and normalize lifespan [3, 4]. Systemic enzyme replacement therapy (ERT) cannot prevent neurodegeneration in MPS I-H patients because the recombinant enzyme cannot enter the central nervous system (CNS) [13]. In contrast, aminoglycosides enter the CNS at ~10-20% of their serum concentration [14, 15]. We therefore evaluated whether long-term NB84 administration alleviated CNS phenotypes in *Idua*^{tm1Kmke} mice. Compared to wild-type controls, less than 0.02% of residual α -L-

iduronidase activity is present in whole brain lysates from untreated *Idua*^{tm1Kmke} mice (**Figure 1A**). Similar to the level of α -L-iduronidase function restored after 2-week or 9-week NB84 treatment [11], we found ~0.4% of normal α -L-iduronidase function was restored in *Idua*^{tm1Kmke} mouse whole brain lysates after 28 weeks of NB84 treatment. We next determined whether this enzyme level reduced GAG accumulation (**Figure 1B**). Remarkably, we found that GAG levels were reduced ~60% in whole brain lysates from *Idua*^{tm1Kmke} mice treated with NB84 for 9 or 28 weeks compared to untreated controls, a ~2-fold greater GAG reduction than observed after 2-week NB84 treatment [10, 11]. This enhancement in GAG reduction may be the result of longer administration and/or the earlier initiation of NB84 treatment for the long-term studies (begun in 3-week-old mice for the long-term studies as opposed to 10-week-old mice for the 2-week study).

In addition, excessive GAG accumulation has been shown to be associated with an increase in lysosomal proliferation for many MPS diseases [6, 10, 11, 16]. Consistent with this observation, increased lysosomal proliferation was also found in *Idua*^{tm1Kmke} mice as indicated by an elevation in the activity of multiple lysosomal enzymes, including β -hexosaminidase (**Figure 1C**) and β -glucuronidase (**Figure 1D**). However, a significant reduction in the activity of these lysosomal enzymes was observed in brain lysates of NB84-treated *Idua*^{tm1Kmke} mice, indicating that the GAG reduction mediated by NB84 treatment is able to reduce secondary lysosomal proliferation. Together, these results indicate that NB84 enters the CNS, restores enough α -L-iduronidase activity to reduce GAG storage, and can maintain the improvements observed in MPS I-H biochemical endpoints for >6 months. Similar results were also observed for MPS I-H

biochemical endpoints in other tissues, including the spleen (**Figure 2**) and heart (**Figure 4A**).

Evidence of neuropathology was previously reported in MPS I and MPS III knockout mice [17, 18]. We evaluated neuropathology in *Idua*^{tm1Kmke} mice by examining the following CNS markers using immunohistochemistry (IHC) and western blotting: LAMP-1, a lysosomal marker increased during lysosomal proliferation; IBA-1, an activated macrophage/microglia marker indicative of neuroinflammation; and GFAP, an activated astrocyte marker upregulated in response to CNS distress/disturbance. IHC staining of brain sections indicated elevations in the abundance of all three markers in untreated 31-week-old MPS I-H mice compared to age-matched WT controls. This upregulation was partially relieved in MPS I-H mice treated with NB84 treatment for 28 weeks (**Figure 3A-C**). Quantification of the three CNS markers in whole brain lysates using western blotting indicated their levels were increased 2.5 to 5-fold in untreated MPS I-H mice relative to wild-type controls (**Figure 3D-G**). However, the abundance of all three CNS markers decreased ~80% in *Idua*^{tm1Kmke} mice treated with NB84 for 28 weeks relative to untreated controls, suggesting that NB84 treatment significantly moderated the progression of neuropathology associated with MPS I-H.

Long-term NB84 treatment attenuates MPS I-H cardiac phenotypes. GAG accumulation in the heart tissues of MPS I patients leads to cardiomyopathy, thickened cardiac valves, progressive narrowing and occlusion of epicardial coronary arteries, and eventual congestive heart failure [19]. ERT and hematopoietic stem cell transplantation (HSCT) alleviate much of the MPS I cardiac phenotype, but cannot prevent valvular disease [13, 20]. Whole heart lysates from untreated *Idua*^{tm1Kmke} mice revealed a 4 to 8

fold increase in GAG accumulation (**Figure 4A**, which leads to significant thickening of the aorta, aortic valve, and atrioventricular valves [21]. Doppler echocardiography assessments of 31-week-old *Idua*^{tm1Kmke} mice recapitulated previous reports evaluating MPS I animal models and MPS I patients [19, 22, 23]. Abnormalities were observed only in male *Idua*^{tm1Kmke} mice and included dilation of the ascending aorta with concomitant turbulent blood flow. Morphological and functional measures revealed increases in aortic lumen diameter (**Figure 4B**), left ventricular stroke volume (**Figure 4C**), and aortic wall thickness (**Figure 4D**). Treatment with NB84 for 2, 9 or 28 weeks reduced GAG storage in whole heart lysates by ~15-20% relative to untreated controls (**Figure 4A**). In male *Idua*^{tm1Kmke} mice treated with NB84 for 28 weeks, the modest GAG reduction contributed to a 38-46% reduction in aortic lumen diameter, a 93% decrease in left ventricular stroke volume, and a 64% decrease in aortic wall thickness relative to male *Idua*^{tm1Kmke} controls (**Figure 4B-D**). Together, these results demonstrate that suppression therapy reduced MPS I-H progression in the hearts of male *Idua*^{tm1Kmke} mice.

Long-term NB84 treatment attenuates MPS I-H bone phenotypes.

Musculoskeletal defects are a major cause of morbidity among the various MPS diseases. MPS I patients develop severe abnormalities in bone structure as well as articular cartilage and joints [24] that cannot be prevented by ERT or HSCT [13, 20]. Skeletal abnormalities that develop in MPS I-H patients include short stature, spinal misalignment, long bone deformation, macrocephaly, hip dysplasia, chest deformity, and facial dysmorphism. *Idua*^{tm1Kmke} mice recapitulate many of the clinical skeletal defects observed in MPS I-H patients, including facial dysmorphism, thickening of their digits, and thoracolumbar kyphosis as well as thickening of the zygotic arch, broadening of the

ribs, and shortening and thickening of the long bones [21]. Micro-computed tomography (micro-CT) analysis of the three-dimensional architecture of femurs from 31-week-old male *Idua*^{tm1Kmke} mice (relative to wild-type controls) indicated abnormalities in both cortical and trabecular bone (**Figure 5A-G**) that are consistent with defects reported in other MPS animal models [25] and in MPS patients [24]. In agreement with findings in MPS I-H knockout mice [12, 26], a 4-fold elevation in osteoclast number was observed in the femoral growth plates of *Idua*^{tm1Kmke} mice relative to wild-type controls (**Figure 5H**). Consistent with the accumulation of aminoglycosides in bone-forming tissues at 10-20% of their serum concentration [27], we found significant improvements in multiple bone parameters in *Idua*^{tm1Kmke} mice treated with NB84 for 28 weeks compared to untreated controls. Micro-CT analyses indicate a ~40-60% improvement in cortical and trabecular bone parameters (**Figure 5A-G**). Osteoclast abundance was also reduced by ~40% (**Figure 5H**). These data indicate that NB84 treatment attenuates progression of MPS I-H bone abnormalities.

Long-term NB84 treatment improves MPS I-H mouse activity. Behavioral defects have been reported in MPS I and MPS III knockout mice [28-30]. Using the elevated zero maze assay, we found a significant decrease in activity (distance traveled) in 31-week-old *Idua*^{tm1Kmke} mice relative to age-matched wild-type controls (**Figure 6**). However, in *Idua*^{tm1Kmke} mice treated with NB84 for 28 weeks, distance traveled was restored to wild-type levels, indicating a general improvement in phenotype. This activity assay might be considered analogous to the “six minute walk test”, an endpoint used in clinical trials to assess functional improvement [31].

Long-term NB84 treatment did not induce toxicity in mice. Traditional aminoglycosides are associated with nephrotoxicity and ototoxicity [7, 8]. To determine whether long-term NB84 treatment induced toxicity in mice, sera from mice treated with NB84 for 28 weeks and untreated controls were subjected to clinical chemistry analyses that included multiple endpoints for liver and kidney function (Antech Diagnostics). Of the 18 parameters evaluated, only three (alkaline phosphatase, bilirubin, creatinine) changed significantly in NB84-treated mice relative to untreated controls (**Table 1**). However, comparison of these endpoint values relative to averages reported for C57BL/6 mice (the genetic background of *Idua*^{tm1Kmkc} mice) in the Jackson Laboratories Mouse Phenome Database [32] indicated that these differences are within normal parameters. No anomalies attributable to NB84 treatment were found during histological analysis of liver, kidney, lung, brain, or heart. Also, no significant changes in weight or food consumption were observed. These results indicate that long-term NB84 administration did not induce significant toxicity in mice.

DISCUSSION

Current treatments for MPS I include enzyme replacement therapy (ERT) and hematopoietic stem cell transplantation (HSCT). ERT, the intravenous administration of recombinant α -L-iduronidase protein (AldurazymeTM), treats many somatic defects associated with MPS I, but cannot prevent development of bone, heart valve and ocular abnormalities [2]. In addition, Aldurazyme is unable to penetrate the CNS, and therefore does not prevent onset of neurological abnormalities associated with MPS I-H. HSCT treats many features of MPS I, including neurological defects, but only if treatment is

initiated at an early age (≤ 2 yrs) [2]. However, heart valve, bone and ocular abnormalities persist. The limitations, cost and potential risks associated with current MPS I treatments indicate that more effective treatment options are needed. In this report, we investigate the potential of nonsense suppression therapy to treat MPS I-H. We found that long-term administration of the nonsense suppression drug NB84 restored enough α -L-iduronidase function to reduce GAG accumulation and ameliorate MPS I-H progression in multiple tissues of the *Idua*^{tm1Kmkc} MPS I-H mouse, including the CNS, heart and bone. Consistent with previous studies that have shown early intervention increases the therapeutic benefit of ERT or HSCT for treating MPS I-H [33-37], we also found that more robust improvements in MPS I-H biochemical endpoints were observed in the CNS when suppression therapy was administered to younger mice. This may be due to the ability of drugs to penetrate the blood-brain barrier at a greater level in younger mice [38] and/or the prevention of GAG accumulation during early ages. Overall, these results suggest suppression therapy may be a viable treatment for MPS I-H, either alone or in combination with other MPS I treatments.

The concept of PTC suppression as a treatment for diseases caused by nonsense mutations was introduced almost two decades ago [39]. Subsequently, ~100 studies have shown that nonsense suppression can partially restore expression of deficient proteins associated with ~40 different diseases [1]. However, no study to date has demonstrated that suppression therapy can prevent or alleviate progression of a disease phenotype. The meager progress in the development of suppression therapy may be attributed to the lack of: 1) safe, effective drugs; 2) relevant animal models; and 3) adequate disease endpoints to effectively assess therapeutic efficacy. The current study addresses each of these

limitations and makes significant contributions to the advancement of nonsense suppression therapy. First, MPS I-H represents an excellent candidate disease for suppression therapy due to its low threshold for correction and the high frequency of nonsense mutations in MPS I-H patients. Furthermore, the *Idua*^{tm1K^{mk}e} MPS I-H mouse is a superb animal model to test suppression therapy because it closely recapitulates the human MPS I-H phenotype and has abundant quantifiable disease endpoints. In addition, NB84 represents a major step forward in the development of safer, more effective nonsense suppression drugs. The toxicity associated with aminoglycosides is unrelated to their ability to suppress PTCs associated with cytoplasmic ribosomes, but rather is due to off-target binding of aminoglycosides to membrane lipids [40] and their affinity for mitochondrial ribosomes [41]. NB84 was designed using a rational drug design to better target eukaryotic cytoplasmic ribosomes in order to increase the effectiveness of PTC suppression and to decrease toxicity compared to conventional aminoglycosides [9]. In support of this design rationale, not only was NB84 found to suppress PTCs more effectively than traditional aminoglycosides [9-11], it was also shown to be significantly less toxic (~5 fold) in mammalian cells [9]. In addition, we found no evidence of toxicity in mice treated with NB84 for 28 weeks.

The data generated from this study using the MPS I-H model represents a critical proof of concept that demonstrates the feasibility of using suppression therapy to treat genetic diseases attributable to nonsense mutations. Based on information from the National Institutes of Health (NIH) Office of Rare Disease Research (<http://rarediseases.info.nih.gov>) and the National Organization for Rare Disorders (<http://www.rarediseases.org>), over 7,000 distinct genetic diseases have been identified

that affect roughly 300 million people worldwide. Approximately 11% of the gene lesions that caused inherited human disease are nonsense mutations [42]. This indicates that millions of individuals could potentially benefit from nonsense suppression therapy. We anticipate that the advancement of personalized medicine and the continued development of safe, effective drugs will allow suppression therapy to progress into a treatment for many genetic diseases.

ACKNOWLEDGEMENTS

We thank the following UAB core facilities for assistance in phenotypic analyses: Terry Lewis, UAB Neuroscience Molecular Detection Core, P30 NS47466; Thomas Van Groen, UAB Neuroscience Behavioral Assessment Core, P30 NS47466; Shawn Williams, UAB High Resolution Imaging Facility, P30 CA013148; Maria Johnson, UAB Small Animal Phenotyping Core, P60 DK079626; Wayne Bradley, UAB Center for Heart Failure Research; and the UAB Animal Resources Program Comparative Pathology Laboratory. This research was supported by grants from the University of Pennsylvania “Improved Therapies for MPS I Grant Program” (MPS I-11-001-01 for KMK and DMB), NIH 1R01GM094792 (TB & DMB), and the US-Israel Binational Science Foundation (2006/301 for TB).

REFERENCES

- [1] H.L. Lee, J.P. Dougherty, Pharmaceutical therapies to recode nonsense mutations in inherited diseases *Pharmacol. Ther.* 136 (2012) 227-266.
- [2] J. Muenzer, J.E. Wraith, L.A. Clarke, Mucopolysaccharidosis I: management and treatment guidelines *Pediatrics* 123 (2009) 19-29.
- [3] L.J. Ashton, D.A. Brooks, P.A. McCourt, V.J. Muller, P.R. Clements, J.J. Hopwood, Immunoquantification and enzyme kinetics of alpha-L-iduronidase in cultured

- fibroblasts from normal controls and mucopolysaccharidosis type I patients *Am J Hum Genet* 50 (1992) 787-794.
- [4] S. Bunge, P.R. Clements, S. Byers, W.J. Kleijer, D.A. Brooks, J.J. Hopwood, Genotype-phenotype correlations in mucopolysaccharidosis type I using enzyme kinetics, immunoquantification and *in vitro* turnover studies *Biochim. Biophys. Acta* 1407 (1998) 249-256.
- [5] D.A. Brooks, V.J. Muller, J.J. Hopwood, Stop-codon read-through for patients affected by a lysosomal storage disorder *Trends in molecular medicine* 12 (2006) 367-373.
- [6] K.M. Keeling, D.A. Brooks, J.J. Hopwood, P. Li, J.N. Thompson, D.M. Bedwell, Gentamicin-mediated suppression of Hurler syndrome stop mutations restores a low level of alpha-L-iduronidase activity and reduces lysosomal glycosaminoglycan accumulation *Hum. Mol. Genet.* 10 (2001) 291-299.
- [7] M.E. Warchol, Cellular mechanisms of aminoglycoside ototoxicity *Current opinion in otolaryngology & head and neck surgery* 18 (2010) 454-458.
- [8] J.M. Lopez-Novoa, Y. Quiros, L. Vicente, A.I. Morales, F.J. Lopez-Hernandez, New insights into the mechanism of aminoglycoside nephrotoxicity: an integrative point of view *Kidney Int.* 79 (2011) 33-45.
- [9] I. Nudelman, D. Glikin, B. Smolkin, M. Hainrichson, V. Belakhov, T. Baasov, Repairing faulty genes by aminoglycosides: development of new derivatives of geneticin (G418) with enhanced suppression of diseases-causing nonsense mutations *Bioorg. Med. Chem.* 18 (2010) 3735-3746.
- [10] D. Wang, V. Belakhov, J. Kandasamy, T. Baasov, S.C. Li, Y.T. Li, D.M. Bedwell, K.M. Keeling, The designer aminoglycoside NB84 significantly reduces glycosaminoglycan accumulation associated with MPS I-H in the Idua-W392X mouse *Mol. Genet. Metab.* 105 (2012) 116-125.
- [11] K.M. Keeling, D. Wang, Y. Dai, S. Murugesan, B. Chenna, J. Clark, V. Belakhov, J. Kandasamy, S.E. Velu, T. Baasov, D.M. Bedwell, Attenuation of nonsense-mediated mRNA decay enhances *in vivo* nonsense suppression *PloS one* 8 (2013) e60478.
- [12] C.M. Simonaro, M. D'Angelo, X. He, E. Eliyahu, N. Shtraizent, M.E. Haskins, E.H. Schuchman, Mechanism of glycosaminoglycan-mediated bone and joint disease: implications for the mucopolysaccharidoses and other connective tissue diseases *Am. J. Pathol.* 172 (2008) 112-122.
- [13] J.E. Wraith, M. Scarpa, M. Beck, O.A. Bodamer, L. De Meirleir, N. Guffon, A. Meldgaard Lund, G. Malm, A.T. Van der Ploeg, J. Zeman, Mucopolysaccharidosis type II (Hunter syndrome): a clinical review and recommendations for treatment in the era of enzyme replacement therapy *Eur. J. Pediatr.* 167 (2008) 267-277.
- [14] G.H. McCracken, Jr., D.F. Chrane, M.L. Thomas, Pharmacologic evaluation of gentamicin in newborn infants *J. Infect. Dis.* 124 (1971) Suppl 214-223.
- [15] A.L. Smith, R.S. Daum, G.R. Siber, D.W. Scheifele, V.P. Syriopoulou, Gentamicin penetration into cerebrospinal fluid in experimental *Haemophilus influenzae* meningitis *Antimicrob. Agents Chemother.* 32 (1988) 1034-1039.
- [16] M. Sardiello, M. Palmieri, A. di Ronza, D.L. Medina, M. Valenza, V.A. Gennarino, C. Di Malta, F. Donaudy, V. Embrione, R.S. Polishchuk, S. Banfi, G. Parenti, E. Cattaneo, A. Ballabio, A gene network regulating lysosomal biogenesis and function *Science* 325 (2009) 473-477.

- [17] F.L. Wilkinson, R.J. Holley, K.J. Langford-Smith, S. Badrinath, A. Liao, A. Langford-Smith, J.D. Cooper, S.A. Jones, J.E. Wraith, R.F. Wynn, C.L. Merry, B.W. Bigger, Neuropathology in mouse models of mucopolysaccharidosis type I, IIIA and IIIB *PloS one* 7 (2012) e35787.
- [18] K. Ohmi, D.S. Greenberg, K.S. Rajavel, S. Ryazantsev, H.H. Li, E.F. Neufeld, Activated microglia in cortex of mouse models of mucopolysaccharidoses I and IIIB *Proc. Natl. Acad. Sci. U. S. A.* 100 (2003) 1902-1907.
- [19] E. Braunlin, S. Mackey-Bojack, A. Panoskaltis-Mortari, J.M. Berry, R.T. McElmurry, M. Riddle, L.Y. Sun, L.A. Clarke, J. Tolar, B.R. Blazar, Cardiac functional and histopathologic findings in humans and mice with mucopolysaccharidosis type I: implications for assessment of therapeutic interventions in hurler syndrome *Pediatr. Res.* 59 (2006) 27-32.
- [20] M. Aldenhoven, J.J. Boelens, T.J. de Koning, The clinical outcome of Hurler syndrome after stem cell transplantation *Biol. Blood Marrow Transplant.* 14 (2008) 485-498.
- [21] D. Wang, C. Shukla, X. Liu, T.R. Schoeb, L.A. Clarke, D.M. Bedwell, K.M. Keeling, Characterization of an MPS I-H knock-in mouse that carries a nonsense mutation analogous to the human IDUA-W402X mutation *Mol. Genet. Metab.* 99 (2010) 62-71.
- [22] A. Nemes, R.G. Timmermans, J.H. Wilson, O.I. Soliman, B.J. Krenning, F.J. ten Cate, M.L. Geleijnse, The mild form of mucopolysaccharidosis type I (Scheie syndrome) is associated with increased ascending aortic stiffness *Heart Vessels* 23 (2008) 108-111.
- [23] J. Tolar, E. Braunlin, M. Riddle, B. Peacock, R.T. McElmurry, P.J. Orchard, B.R. Blazar, Gender-related dimorphism in aortic insufficiency in murine mucopolysaccharidosis type I *J. Heart Valve Dis.* 18 (2009) 524-529.
- [24] C.M. Simonaro, Cartilage and chondrocyte pathology in the mucopolysaccharidoses: The role of glycosaminoglycan-mediated inflammation *Journal of pediatric rehabilitation medicine* 3 (2010) 85-88.
- [25] D.J. Rowan, S. Tomatsu, J.H. Grubb, A.M. Montano, W.S. Sly, Assessment of bone dysplasia by micro-CT and glycosaminoglycan levels in mouse models for mucopolysaccharidosis type I, IIIA, IVA, and VII *J. Inherit. Metab. Dis.* 36 (2013) 235-246.
- [26] S. Wilson, S. Hashamiyan, L. Clarke, P. Saftig, J. Mort, V.M. Dejica, D. Bromme, Glycosaminoglycan-mediated loss of cathepsin K collagenolytic activity in MPS I contributes to osteoclast and growth plate abnormalities *Am. J. Pathol.* 175 (2009) 2053-2062.
- [27] C.B. Landersdorfer, J.B. Bulitta, M. Kinzig, U. Holzgrabe, F. Sorgel, Penetration of antibacterials into bone: pharmacokinetic, pharmacodynamic and bioanalytical considerations *Clin. Pharmacokinet.* 48 (2009) 89-124.
- [28] D. Pan, A. Sciascia, 2nd, C.V. Vorhees, M.T. Williams, Progression of multiple behavioral deficits with various ages of onset in a murine model of Hurler syndrome *Brain Res.* 1188 (2008) 241-253.
- [29] A.A. Lau, A.C. Crawley, J.J. Hopwood, K.M. Hemsley, Open field locomotor activity and anxiety-related behaviors in mucopolysaccharidosis type IIIA mice *Behav. Brain Res.* 191 (2008) 130-136.

- [30] C.D. Heldermon, A.K. Hennig, K.K. Ohlemiller, J.M. Ogilvie, E.D. Herzog, A. Breidenbach, C. Vogler, D.F. Wozniak, M.S. Sands, Development of sensory, motor and behavioral deficits in the murine model of Sanfilippo syndrome type B *PloS one* 2 (2007) e772.
- [31] C.M. McDonald, E.K. Henricson, R.T. Abresch, J.M. Florence, M. Eagle, E. Gappmaier, A.M. Glanzman, R. Spiegel, J. Barth, G. Elfring, A. Reha, S. Peltz, The 6-minute walk test and other endpoints in Duchenne muscular dystrophy: Longitudinal natural history observations over 48 weeks from a multicenter study *Muscle Nerve* (2013) 1-14.
- [32] T.P. Maddatu, S.C. Grubb, C.J. Bult, M.A. Bogue, Mouse Phenome Database (MPD) *Nucleic Acids Res* 40 (2012) D887-894.
- [33] S. Laraway, C. Breen, J. Mercer, S. Jones, J.E. Wraith, Does early use of enzyme replacement therapy alter the natural history of mucopolysaccharidosis I? Experience in three siblings *Mol. Genet. Metab.* 109 (2013) 315-316.
- [34] M.H. de Ru, J.J. Boelens, A.M. Das, S.A. Jones, J.H. van der Lee, N. Mahlaoui, E. Mengel, M. Offringa, A. O'Meara, R. Parini, A. Rovelli, K.W. Sykora, V. Valayannopoulos, A. Vellodi, R.F. Wynn, F.A. Wijburg, Enzyme replacement therapy and/or hematopoietic stem cell transplantation at diagnosis in patients with mucopolysaccharidosis type I: results of a European consensus procedure *Orphanet journal of rare diseases* 6 (2011) 55.
- [35] C. Dupont, C. El Hachem, S. Harchaoui, V. Ribault, M. Amieur, M. Guillot, I. Maire, R. Froissart, N. Guffon-Fouilhoux, [Hurler syndrome. Early diagnosis and successful enzyme replacement therapy: a new therapeutic approach. Case report] *Arch. Pediatr.* 15 (2008) 45-49.
- [36] P.I. Dickson, S. Hanson, M.F. McEntee, C.H. Vite, C.A. Vogler, A. Mlikotic, A.H. Chen, K.P. Ponder, M.E. Haskins, B.L. Tippin, S.Q. Le, M.B. Passage, C. Guerra, A. Dierenfeld, J. Jens, E. Snella, S.H. Kan, N.M. Ellinwood, Early versus late treatment of spinal cord compression with long-term intrathecal enzyme replacement therapy in canine mucopolysaccharidosis type I *Mol. Genet. Metab.* 101 (2010) 115-122.
- [37] A.D. Dierenfeld, M.F. McEntee, C.A. Vogler, C.H. Vite, A.H. Chen, M. Passage, S. Le, S. Shah, J.K. Jens, E.M. Snella, K.L. Kline, J.D. Parkes, W.A. Ware, L.E. Moran, A.J. Fales-Williams, J.A. Wengert, R.D. Whitley, D.M. Betts, A.M. Boal, E.A. Riedesel, W. Gross, N.M. Ellinwood, P.I. Dickson, Replacing the enzyme alpha-L-iduronidase at birth ameliorates symptoms in the brain and periphery of dogs with mucopolysaccharidosis type I *Science translational medicine* 2 (2010) 60ra89.
- [38] R. Nau, F. Sorgel, H. Eiffert, Penetration of drugs through the blood-cerebrospinal fluid/blood-brain barrier for treatment of central nervous system infections *Clin. Microbiol. Rev.* 23 (2010) 858-883.
- [39] M. Howard, R.A. Frizzell, D.M. Bedwell, Aminoglycoside antibiotics restore CFTR function by overcoming premature stop mutations *Nat. Med.* 2 (1996) 467-469.
- [40] G. Laurent, M.B. Carlier, B. Rollman, F. Van Hoof, P. Tulkens, Mechanism of aminoglycoside-induced lysosomal phospholipidosis: *in vitro* and *in vivo* studies with gentamicin and amikacin *Biochem. Pharmacol.* 31 (1982) 3861-3870.
- [41] Y. Qian, M.X. Guan, Interaction of aminoglycosides with human mitochondrial 12S rRNA carrying the deafness-associated mutation *Antimicrob. Agents Chemother.* 53 (2009) 4612-4618.

[42] M. Mort, D. Ivanov, D.N. Cooper, N.A. Chuzhanova, A meta-analysis of nonsense mutations causing human genetic disease *Hum. Mutat.* 29 (2008) 1037-1047.

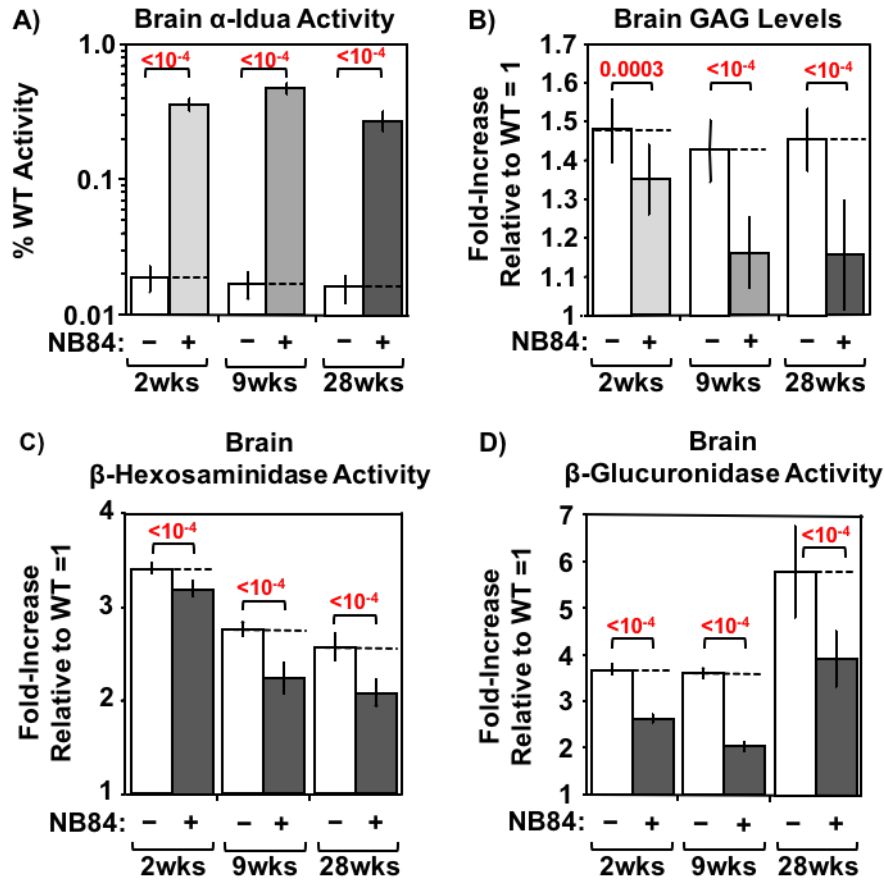


Figure 1. NB84 treatment alleviates MPS I-H biochemical endpoints in mouse brain. **A)** α -L-iduronidase activity, **B)** sulfated GAG levels, **C)** β -hexosaminidase activity, and **D)** β -glucuronidase activity were quantified in whole brain lysates. Data shown are values for untreated (-) and treated (+) MPS I-H mice that have been normalized to WT levels (=1). Dashed lines indicate the average values obtained from untreated mice. n=5 mice per group. p values are indicated above brackets.

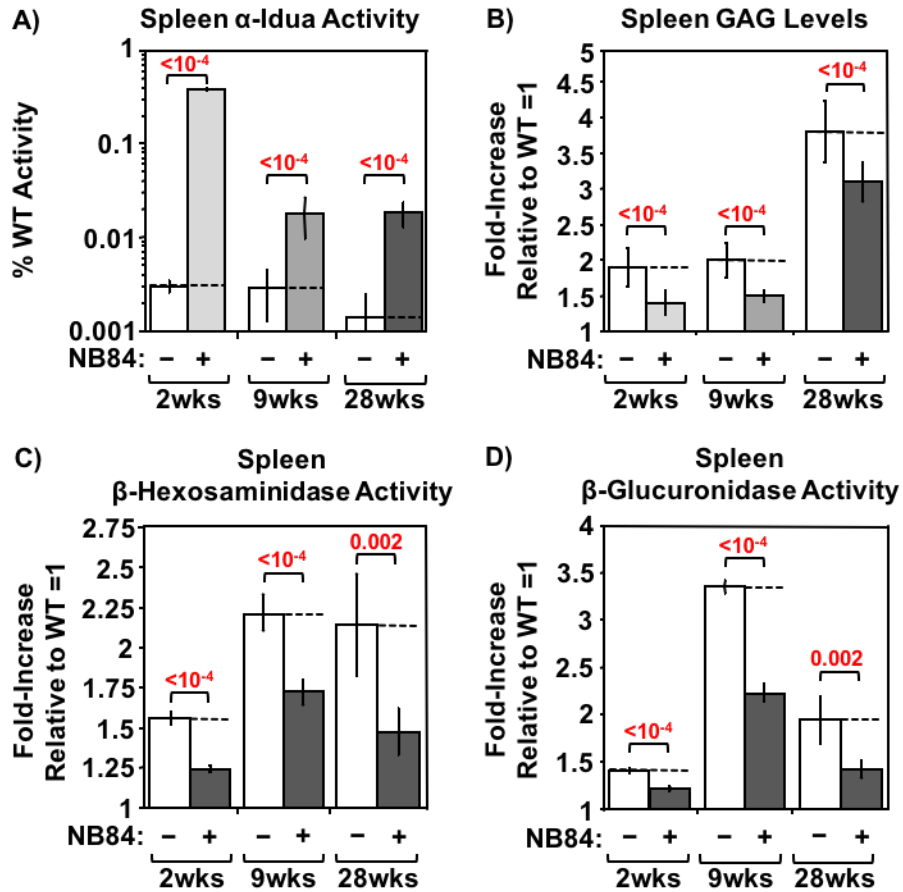


Figure 2. NB84 treatment alleviates MPS I-H biochemical endpoints in mouse spleen.

A) α -L-iduronidase activity, **B)** sulfated GAG levels, **C)** β -hexosaminidase activity, and **D)** β -glucuronidase were quantified in spleen lysates. Data shown are values for untreated (-) and treated (+) MPS I-H mice that have been normalized to WT levels (=1). Dashed lines indicate the average values obtained from untreated mice. n=5 mice per group. p values are indicated above brackets.

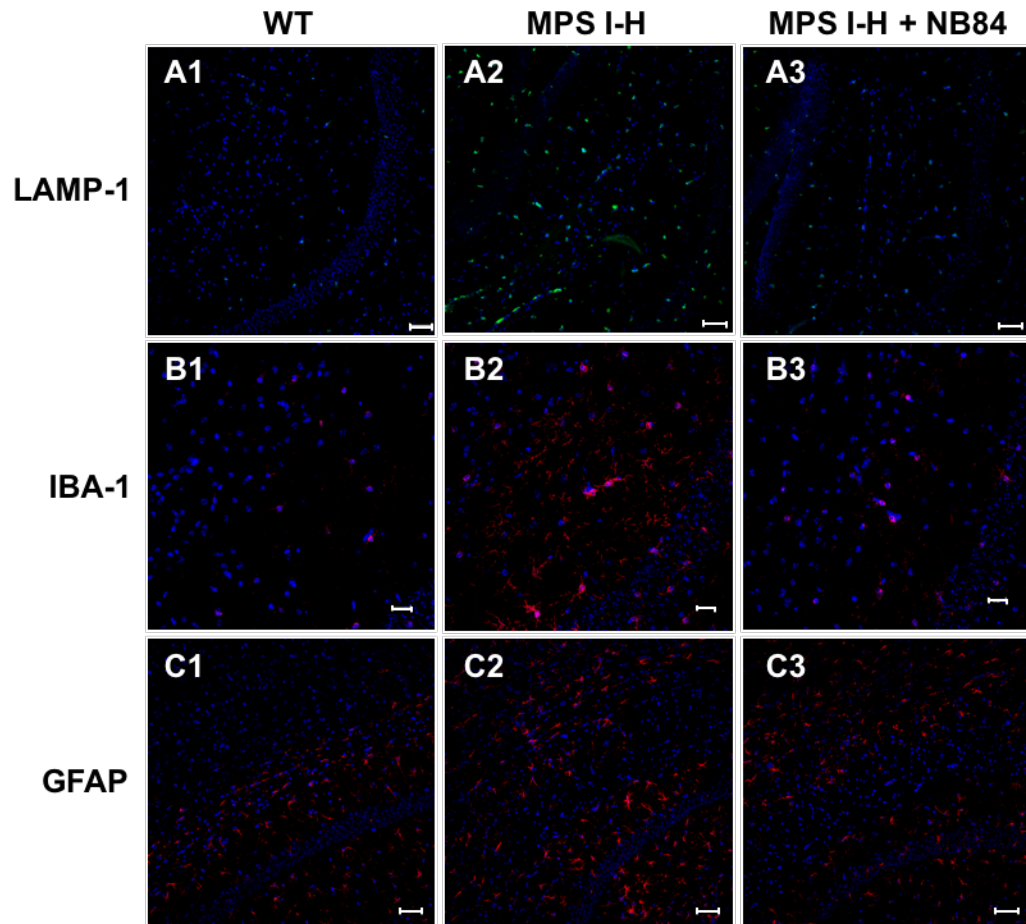


Figure 3. (A-C) *NB84 treatment moderates neuropathology in MPS I-H mice.*

Representative images of immunohistochemistry staining for CNS markers: **A1-3)** LAMP-1 and **B1-3)** IBA-1 in the hippocampus, and **C1-3)** GFAP in the cerebral cortex of 31-week-old untreated WT and MPS I-H male controls and MPS I-H mice treated with NB84 for 28 weeks. All samples were counter-stained with bis-benzamide nuclear stain (blue). LAMP-1 and GFAP are shown at 20X magnification with a scale bar = 50 μ m; IBA-1 is shown at 40X magnification with a scale bar = 20 μ m.

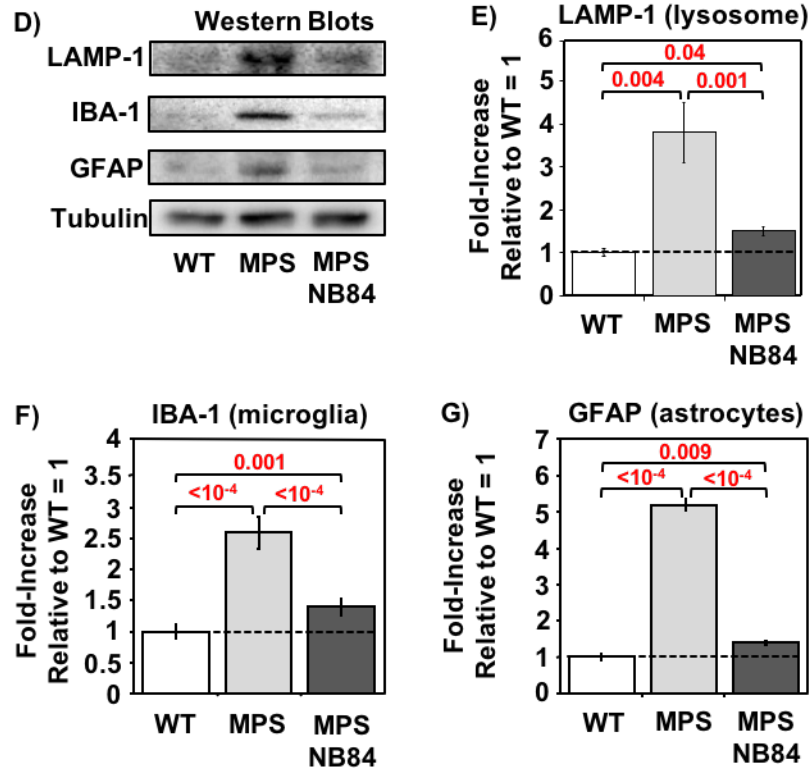


Figure 3. (D-G) NB84 treatment moderates neuropathology in MPS I-H mice. D)

Representative western blots of whole brain lysates from WT mice, untreated MPS I-H mice, or MPS I-H mice treated with NB84 for 28 weeks. Western quantitation data for: **E) LAMP-1; F) IBA-1; G) GFAP.** The data shown is normalized to tubulin levels (=1).

Dashed lines indicate average values obtained from WT mice. n=3 WT mice; n=6 untreated MPS mice; n=5 treated MPS mice. p values are indicated above brackets.

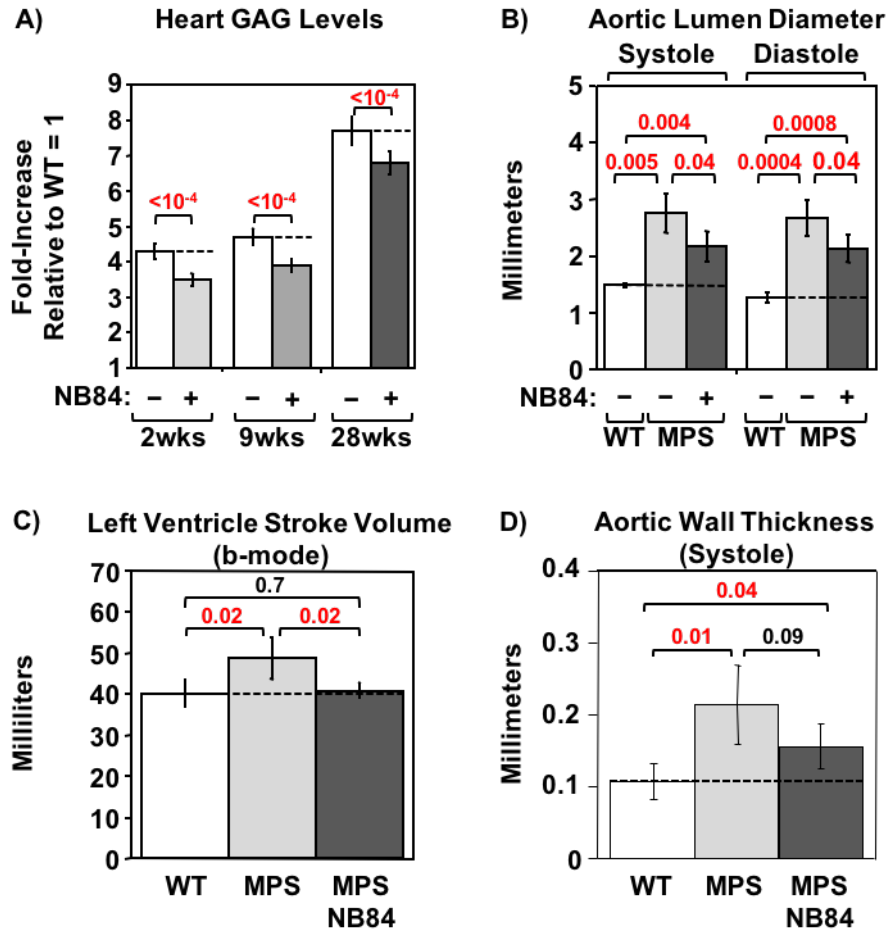


Figure 4. NB84 treatment moderates progression of heart defects in MPS I-H mice. **A)** Sulfated GAGs were quantified in whole heart lysates. Data shown are values for untreated (-) and treated (+) MPS I-H mice that have been normalized to WT levels (=1). Dashed lines indicate average values obtained from untreated mice. n=5 mice per group. Doppler echocardiography measurements of: **B)** aortic lumen diameter at systole (contraction) and diastole (relaxation), **C)** ventricle stroke volume, and **D)** aortic wall thickness in WT mice, untreated MPS I-H mice, and MPS I-H mice treated with NB84 for 28 weeks. Dashed lines indicate average values obtained from WT mice. n= 3-4 WT mice; n= 4-5 untreated or treated MPS mice. p values are indicated above brackets.

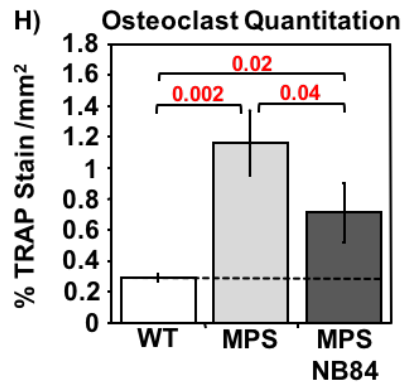
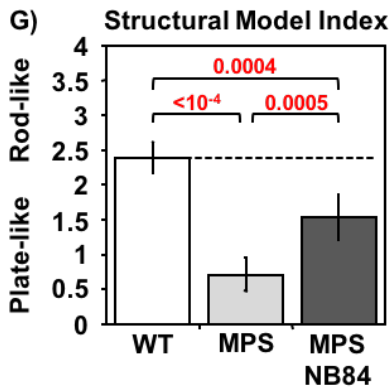
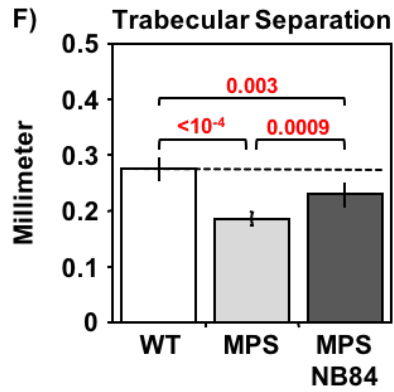
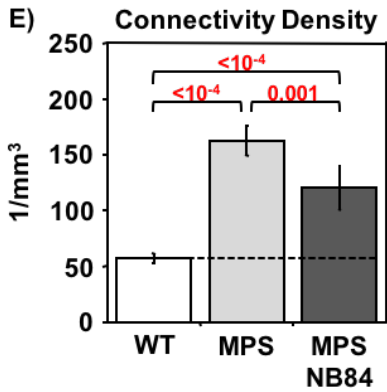
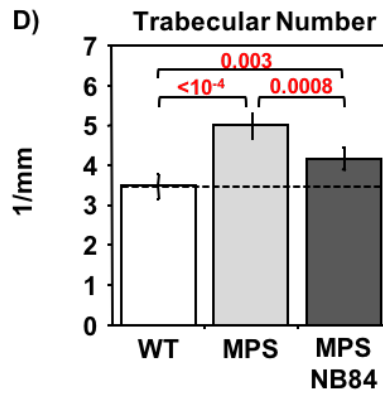
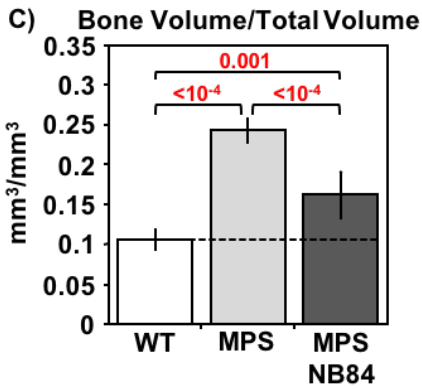
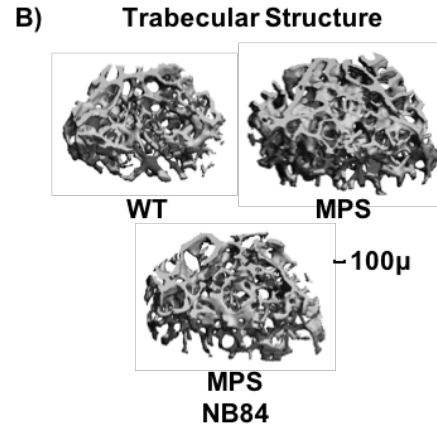
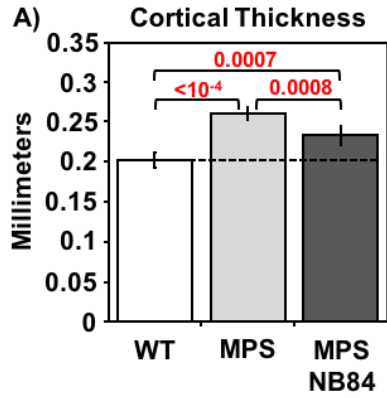


Figure 5. *NB84 treatment moderates progress of bone defects in MPS I-H mice.* Micro-CT measurements of femurs from WT mice, untreated MPS I-H mice, or MPS I-H mice treated with NB84 for 28 weeks: **A)** cortical bone thickness, **B)** representative trabecular bone images, **C)** trabecular bone volume/total volume, **D)** trabecular number; **E)** trabecular connectivity density, **F)** trabecular separation; **G)** trabecular structural model index. **H)** Osteoclast quantification in femoral growth plates using TRAP staining. p values are indicated above brackets. Dashed lines indicate average values obtained from WT mice. For panels A and C-G, n= 5-6 WT mice and n=6 untreated and treated MPS mice. For panel H, n= 3 mice per group. p values are indicated above brackets. See the Methods for detailed descriptions of the micro-CT parameters.

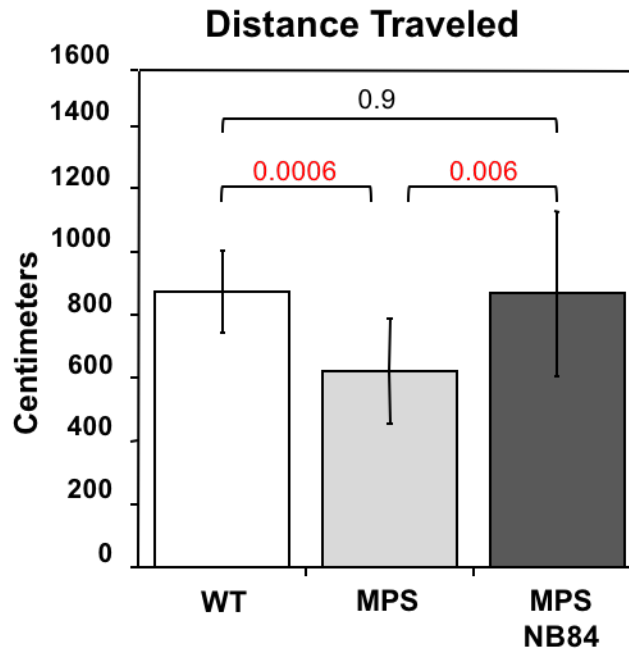


Figure 6. *NB84 treatment improves activity levels in MPS I-H mice.* The distance traveled was measured in 31-week-old WT and MPS I-H mice using the elevated zero maze assay. The dashed line indicates the average value obtained from WT mice. n=9 WT mice; n=17 untreated MPS mice; n=10 NB84-treated MPS mice. p values are indicated above brackets. Additional assay details can be found in the Methods.

Table 1. Comprehensive Serum Clinical Chemistry Analysis to Evaluate NB84 Toxicity

Endpoint	Untreated controls (n=12)	NB84-treated mice (n=6)	p values (treated versus untreated)	Average values for C57BL/6 mice
(ALT) alanine aminotransferase (U/L)	59 ± 36	44 ± 21	0.36	43
albumin (g/dL)	2.7 ± 0.2	2.6 ± 0.2	0.32	3
alkaline phosphatase (U/L)	74 ± 17	103 ± 18	0.004	96
(AST) aspartate aminotransferase (U/L)	136 ± 99	112 ± 39	0.58	157
bilirubin, total (mg/dL)	0.27 ± 0.05	0.20 ± 0.05	0.01	0.45
calcium (mg/dL)	8.6 ± 0.2	8.5 ± 0.2	0.33	9.4
chloride (mEq/L)	112 ± 2	110 ± 3	0.11	115
cholesterol (mg/dL)	95 ± 21	80 ± 25	0.2	84
(CPK) creatine phosphokinase (U/L)	744 ± 640	702 ± 429	0.89	558
creatinine (mg/dL)	0.16 ± 0.05	0.10 ± 0.05	0.03	0.23
globulin (g/dL)	2.5 ± 0.2	2.6 ± 0.2	0.33	
glucose (mg/dL)	210 ± 41	195 ± 24	0.42	184
phosphorous (mg/dL)	6.8 ± 0.7	7.1 ± 0.3	0.34	7.2
potassium (mEq/L)	5.7 ± 0.6	6.1 ± 0.3	0.15	6.3
protein, total (g/dL)	5.2 ± 0.2	5.2 ± 0.3	0.99	5.8
sodium (mEq/L)	150 ± 6	149 ± 4	0.72	150
sodium/potassium ratio	27 ± 3	30 ± 11	0.38	NA
urea nitrogen (mg/dL)	28 ± 6	31 ± 3	0.27	28

ASSESSMENT OF NON-AMINOGLYCOSIDE COMPOUNDS AS NONSENSE
SUPPRESSION AGENTS IN AN *IDUA*-W402X MOUSE MODEL OF MPS I-H

by

GWEN GUNN, SHIRLEY YEH, MARLA WEETALL, ELLEN WELCH, TRENTON
R. SCHOEB, DAVID M. BEDWELL, AND KIM M. KEELING

In preparation

Format adapted for dissertation

ABSTRACT

Nonsense mutations are in-frame single nucleotide changes that alter a sense codon to one of the three eukaryotic nonsense codons resulting in introduction of a premature termination codon (PTC) that cause premature translation termination, rapid mRNA degradation, and reduced or ablated production of functional protein. Such mutations are responsible for ~11% of all disease-associated mutations and are found in ~70% of patients with the severe Hurler form of mucopolysaccharidosis type 1 (MPS I-H).

Nonsense suppression therapy in response to small molecule “read-through” compounds is a therapeutic approach targeting disease-causing PTCs. These compounds increase the rate of incorporation of near-cognate amino acids at the site of a PTC to restore functional protein production to mitigate disease. A number of compounds have been identified that increase the rate of PTC read-through including aminoglycoside antibiotics and non-aminoglycoside small molecule compounds.

Previous studies in our lab demonstrated that long-term, early intervention treatment with the designer aminoglycoside NB84 in the *Idua*-W402X mouse model could effectively ameliorate disease progression, reduced GAG accumulation, slowed disease progression in multiple tissues, and no evidence of toxicity. However, aminoglycosides are associated with both oto- and nephrotoxicity and require further development to offer a viable treatment for chronic disease.

We hypothesized that the 1,2,4-oxadiazole derivative compound, PTC124, its derivative PTC414, and another novel compound PTC415 represent a group of non-aminoglycoside nonsense suppression compounds that may be able to effectively

suppress the W402X PTC and restore sufficient enzyme activity to ameliorate disease in the mouse model of Hurler Syndrome while offering an improved safety profile. We evaluated PTC124, PTC414, and PTC415 *in vitro* to assess mechanism and efficacy, then *in vivo* to further evaluate tolerability and efficacy.

All three compounds resulted in variable but modest efficacy at reducing GAG accumulation. PTC415 was not well-tolerated in short-term administration and was not pursued further. PTC414 produced off-target effects in bone and spleen assays with long-term administration. PTC124 resulted in no undesirable effects and proved modestly effective at improving both short- and long-term endpoints of disease in the nonsense mouse model of Hurler disease.

INTRODUCTION

A nonsense mutation introduces an in-frame premature termination codon (PTC) into the coding region of an mRNA, resulting in premature translation termination and production of a truncated, nonfunctional and/or unstable protein. In addition, PTC-containing mRNAs are often subject to rapid degradation via the nonsense-mediated mRNA decay (NMD) pathway. The presence of a PTC frequently results in clinical disease due to loss or insufficiency of the affected protein. Nonsense mutations represent approximately 11% of all mutations that result in genetic diseases [1].

Nonsense suppression therapy is a developing therapeutic approach that aims to treat genetic diseases caused by nonsense mutations by suppressing translation termination at the PTC to restore full-length, functional protein production. This strategy utilizes low molecular weight compounds that enhance the mispairing of near-cognate

tRNAs with the PTC so that an amino acid is inserted at the site of the PTC and full-length protein production is restored [2]. This mechanism of PTC suppression is also commonly referred to as “readthrough.”

Mucopolysaccharidosis type I-Hurler (MPS I-H) is one of many genetic diseases that could potentially benefit from nonsense suppression therapy. MPS I-H is the most severe form of the autosomal recessive lysosomal storage disease (LSD) caused by mutations in the *IDUA* gene, leading to a deficiency of α -L-iduronidase. Loss of this enzyme results in progressive accumulation of the glycosaminoglycans (GAGs) heparan sulfate and dermatan sulfate within the lysosomes of cells throughout the body [3]. GAG accumulation in various tissues produces a complex and variable disease phenotype. Due to the progressive nature of the disease, patients are born apparently healthy with symptoms gradually emerging within the first year. Initial symptoms include frequent respiratory/ear infections, abdominal hernia, restricted joint mobility, altered facial features, and skeletal abnormalities [4]. Cognitive delays become apparent by the second year followed by progressive involvement of the heart, spleen, liver, the skeletal system, and the central nervous system (CNS). MPS I-H patients who do not receive any treatment intervention typically succumb to the cardiovascular and neurological manifestations of this disease within the first decade [5].

There are a number of factors that indicate MPS I-H may be a good candidate disease for nonsense suppression therapy. First, ~70% of the MPS I-H patient population carries a nonsense mutation in at least one *IDUA* allele [6], suggesting that a nonsense suppression approach could benefit a significant proportion of this patient population. Additionally, the attenuated phenotypes observed in the milder clinical forms of MPS I,

including Hurler-Scheie and Scheie, indicate that the amount of protein function needed to significantly alleviate the severe MPS I-H phenotype is only 0.3-1% of normal [4]. Patients with the attenuated form of MPS I do not develop intellectual disability and have a normal lifespan, thus small amounts of α -L-iduronidase activity restored from readthrough could significantly alleviate the disease phenotype in MPS I-H patients. Hematopoietic stem cell transplantation (HSCT) and enzyme replacement therapy (ERT) are the two therapies currently available to treat MPS I-H. However, the inability of these treatments to access certain tissues suggests that safe, effective treatments are needed to supplement or replace current MPS I-H treatments. Nonsense suppression agents, or readthrough drugs, are low molecular weight compounds that may access tissues such as the brain, bone, heart valves, and cornea for which current treatments are insufficient [7].

The aminoglycosides represent the best characterized readthrough drugs. A subset of aminoglycosides was previously shown to suppress nonsense mutations associated with MPS I-H and restore physiologically significant amounts of α -L-iduronidase in patient fibroblasts that harbor nonsense mutations [8] and in a nonsense mouse model of MPS I-H [9, 10]. Aminoglycosides interact with a region of cytoplasmic ribosomes referred to as the decoding site to stimulate codon misreading and stop codon readthrough [11]. However, aminoglycosides also accumulate disproportionately in certain tissues where they interfere with mitochondrial ribosomes and phospholipase signaling resulting in toxicity to the inner ear and kidneys [12-14]. Recent research has focused on modifying the structure of traditional aminoglycosides to make them more effective at PTC suppression while decreasing toxicity [15]. Although several of these designer

aminoglycosides have been shown to be more effective at suppressing MPS I-H nonsense mutations than traditional aminoglycosides [9, 10], it is not yet known whether these novel compounds will be safe enough for long-term, chronic administration as a nonsense suppression agent.

In the current study, we sought to evaluate and compare the safety and efficacy of three non-aminoglycoside, small-molecule readthrough compounds for long-term nonsense suppression therapy. These compounds, which include PTC124, PTC414 and PTC415, were discovered from high throughput screening of small molecular libraries by PTC Therapeutics, Inc. PTC124 (also known as ataluren or Translarna™) has been shown to be orally bioavailable, non-toxic, and effective at restoring partial protein expression *in vitro* and *in vivo* in a number of nonsense mutation disease models [16-19]. Numerous studies have shown that PTC124 functions as a readthrough drug [17, 20-22]. PTC124 induces readthrough by promoting the incorporation of certain near-cognate tRNAs at PTCs, allowing translation elongation to continue to produce a full-length polypeptide [23]. While computational modeling has posited that PTC124 promotes readthrough by physically overlaying the mRNA and masking PTC recognition so that an alternative amino acid is inserted at the PTC site [24], currently no biochemical evidence exists that support this model. More recent work has demonstrated that concurrent administration of an aminoglycoside reduces the readthrough efficacy of ataluren, raising the possibility that perhaps ataluren, like aminoglycosides, directly binds the ribosome [23]. PTC414 and PTC415 are two other readthrough compounds in development by PTC Therapeutics. A mechanism has not yet been proposed for PTC414, however this drug is a derivative of PTC124 that has been shown to effectively restore functional

protein in a zebrafish model of nonsense mutation choroideremia [25]. Preliminary studies demonstrate higher readthrough efficacy at all three stops in response to PTC414 as well as improved tissue distribution. PTC415 was proposed as a particularly relevant treatment for Hurler syndrome due to its great blood-brain barrier penetrance (personal communication, PTC Therapeutics). We examined these three compounds in the MPS I-H knock-in mouse model that carries a PTC in the mouse *Idua* locus homologous to the human *IDUA* W402X nonsense mutation [26] and assessed whether PTC124, PTC414, or PTC415 could restore enough α -L-iduronidase activity via readthrough to alleviate the MPS I-H phenotype *in vitro* and *in vivo*.

MATERIALS AND METHODS

Cell Culture. Mouse embryonic fibroblasts (MEFs) were cultured from 13-14 day embryos derived by breeding homozygous *Idua*-W402X [26], *Idua*-knockout [27], and wild-type mice. All three cell lines were immortalized through stable expression of the SV40 large T antigen via a lentiviral vector system (ABM, Inc). HEK293T and MEF cells were cultured in Dulbecco's modified Eagle's medium supplemented with 10% fetal bovine serum, 100 IU/ml penicillin, 100ug/ml streptomycin, and 1% v/v nonessential amino acids in 10cm or 6-well culture plates.

Luciferase Assays. The original 2pluc dual luciferase readthrough reporters, gifted from Dr. John Atkins [28], were previously modified by our lab to express the wild-type mouse *Idua* W402 codon (UGG) or the *Idua*-W402X (UAG) premature termination codon in the readthrough cassette. These codons, along with three upstream and three downstream codons of the native mouse *Idua* context, were ligated between the

Sall and BamHI restriction sites of the 2pluc vector [9]. The W402 and W402X dual luciferase constructs were then subcloned into the pcDNA3.1TM/Zeo+ expression vector (ThermoFisher Scientific) to allow stable transfection in HEK293 cells. The original *Renilla* luciferase-based NMD reporters were a gift from Dr. Andreas Kulozik (University of Heidelberg, Germany) [29]. The *Renilla* / β -globin segment was excised from the original pCI-neo vector (Promega) using the restriction sites NheI and NotI and subcloned into the pcDNA3.1TM/Zeo+ expression vector (Fisher), which was used to generate stably transfected HEK293 cells. Cells were grown in the presence of each drug at the indicated doses for 48 hours. Dual luciferase readthrough assays were performed with Dual Luciferase Assay System (Promega) using the GloMax Multi Detection System (Promega) in quadruplicate. The percent readthrough was calculated as the ratio of firefly/*Renilla* luciferase units expressed from the W402X construct relative to the W402 construct x 100. NMD inhibition assays were performed with the Pierce[®] *Renilla* Flash Assay Kit (Fisher) using the GloMax Multi Detection System (Promega) in quadruplicate. NMD inhibition was calculated as *Renilla* luciferase units per milligram protein from the Q39X construct relative to the wild-type construct.

Animal Treatment. This study involved the use and treatment of wild-type C57BL/6J, *Idua*-knockout [27], and *Idua*-W402X mice. In previous studies, *Idua*-W402X mice were referred to as *Idua*-W392X [9, 26] mice or *Idua*^{tm1Kmke} mice [10]. PTC Therapeutics, Inc. synthesized the compounds PTC124, PTC414, and PTC415. PTC124 and PTC414 were then incorporated into chow by OpenSources Diets at a ratio of 0.1% and 0.03% by weight, respectively, and fed *ad libitum* to animals for 2 weeks (from 10 to 12 weeks-old of age), for 4 weeks (from 8 to 12 weeks of age), or for 28

weeks (from 3 to 31 weeks of age). PTC415 was administered as a solution in sterile PBS vehicle at 2.5 mg/kg dose twice weekly via subcutaneous injection to mice for 4 weeks (from 8 to 12 weeks of age). Injection sites were rotated among dorsal locations to minimize injection site irritation. Age-matched control animals were included for all three treatment regimens. All animal protocols used in this study were reviewed and approved by UAB IACUC (protocol number IACUC-10220).

Biochemical Assays. Assays to determine tissue α -L-iduronidase activities were performed using 25% of the brain (left anterior) or 30% of the spleen (anterior end) by size. Tissues were homogenized in T-Per lysis reagent containing protease inhibitors (Roche eComplete) using a Tissue Tearer rotor-stator homogenizer (BioSpec) then centrifuged to obtain clarified lysate. Clarified lysates were then incubated with 0.4 mM 4-methyl-umbelliferyl- α -L-iduronide (FMU-iduronide; Gold Biotech) in 150mM sodium formate (pH 3.5) for 1 hour (wild-type) or 72 hours (W402X or KO) at 37°C. Reactions were quenched with 200uL of glycine buffer (pH 10.8) and free FMU fluorescence was measured in 96-well plates (SOURCE) on the GloMax Multi Detection System (Promega). Total lysate protein concentration was determined using the Bio-Rad Protein Assay reagent. Enzyme specific activity was calculated as nanomoles of FMU released per milligram total protein per hour. Sulfated GAG levels were determined using Blyscan dye binding assays (Biocolor Ltd, UK). MEFs were lysed in Pierce Mammalian Protein Extraction Reagent. Total protein concentration was determined using the Bio-Rad Protein Assay. MEF GAG levels were calculated as the nanograms of GAGs per milligrams total protein. Tissue samples were defatted by homogenizing tissue in 1:1 chloroform methanol using the Tissue Tearer rotor-stator homogenizer (BioSpec) and

subsequently dried in a SpeedVac. Tissue GAG levels were calculated as micrograms of GAGs per milligram of defatted, dried tissue. Spectrophotometric readings for protein and GAG assays were performed using a GloMax Multi Detection System (Promega).

Behavioral Assays

Elevated Zero Maze: The apparatus consisted of a circular maze, 70 centimeters in diameter, raised 40 cm above the platform, and divided into four equal sections. Two opposite sections had 15 cm high sides of non-transparent material, and the other two had only a 0.5 cm high wall. The animal was put in the arena at the center of a low-wall stretch, and observed for 4 minutes, with a camera driven tracker system, (Ethovision, Noldus, The Netherlands).

Open Field: The apparatus consisted of an open-top square box with sides of transparent material measuring 18 inches on a side. The animal was put in the box at the center of one wall, and observed for 10 minutes, with a camera driven tracker system, (Ethovision, Noldus, The Netherlands). For both tests, the system recorded the position of the animal in the arena at 5 frames/second. The test was performed once per animal to prevent habituation. After each testing day and in between animals the apparatus was wiped down with chlorhexidine and 70% ethanol and allowed to air-dry.

Ultrasound Echocardiography. Doppler transthoracic echocardiography was performed by an experienced sonographer using a Visual Sonics Vevo 2100 Imaging System and 30MHz MS400 MicroScan transducer (FUJIFILM VisualSonics, Inc., Toronto). Mice were anesthetized initially with 5% isoflurane and then maintained with 1% to 2% isoflurane. Core temperatures and heart rate were continuously monitored and maintained at ~37 degrees and ~500 beats per minute, respectively. The chests of the

mice were treated with a chemical hair remover to reduce ultrasound attenuation. B-mode guided M-mode measurements of left ventricular wall thickness of the septum and posterior walls were made at the papillary muscle level. An apical four-chamber B-mode color Doppler view was used to position pulse wave Doppler measurement of flow at the tips of the mitral valve leaflets. M-mode was also used to measure ascending aorta lumen diameter and wall thickness at the midpoint between the aortic sinus and the innominate artery. Flow was measured at the aortic root using M-mode Doppler and evaluation of flow turbulence in the aorta was evaluated with color Doppler. When possible, measurements were made on three consecutive beats.

Micro-computed tomography. Excised mouse femurs were scanned using the Scanco uCT40 desktop cone-beam micro-CT scanner. Bones were placed vertically into 12mm diameter holders and scanned at 12 μm resolution, 70kVp, 114 μA with an integration time of 200ms. Cortical bone was scanned at the midshaft and consisted for 25 slices, 12 μm in thickness. Fewer scans are needed for cortical bone due to its uniformity. Scans were reconstructed and the region of interest was drawn at the outside of the cortical bone such that all of the cortical bone and marrow were included. No trabecular bone was included. The threshold for cortical bone was set at 282 and the 3-D reconstruction was performed on all 25 slices. Data was obtained on bone volume (BV), total volume (TV), BV/TV, and cortical thickness. The trabecular bone was scanned from the growth plate and consisted of 200 slices, with each slice 12 μM in thickness. Scans were reconstructed into 2-D slices and 100 slices were analyzed using the μCT Evaluation Program (v5.0A, Sanco Medical). The region of interest was drawn on each of the 100 slices just inside the cortical bone to include only trabecular bone and marrow.

The threshold for trabecular bone was set at 212 to distinguish it from the marrow. The 3-D reconstruction was performed using all the outlined slices. Data was obtained on bone volume (BV), total volume (TV), BV/TV, trabecular number (number of intersections between bone and non-bone components), trabecular thickness, trabecular separation (space between trabeculae), connectivity density (density of trabecular connections), and structural model index (trabecular bone structure characterization: plate-like (SMI=0); rod-like (SMI=3); sphere-like (SMI=4)).

Osteoclast TRAP staining. Mouse femurs were excised and fixed in 70% ethanol, decalcified, embedded in paraffin, and longitudinally sectioned into 5 μ m sections. Osteoclasts within femur sections were stained for tartrate-resistant acid phosphatase (TRAP). Areas of bone and TRAP staining were measured in red and green channel images, respectively, using ImagePro Plus v6.2 software (Media Cybernetics, Rockville, MD). TRAP-stained material was quantitated per area (mm²) of bone examined.

Mass Spectrophotometry GAG Analysis. Dermatan sulphate (DS) and heparan sulphate (HS) were quantified using UPLC-MS/MS to quantify their methanolysis product [30, 31]. An aliquot of the urine was analyzed for creatinine using LC-MS/MS. Another aliquot was dried, then treated with 3M HCL methanol to produce dimeric subunits derived from the principal GAGs. These dimers primarily consist of uronic acid coupled with an N-acetylhexosamine moiety. A mixture of stable isotope-labeled dimers, prepared from standard GAGs by deuteriomethanolysis, enabled their quantification by pseudo-isotope-dilution using UPLC-ESI-MSMS. A Xevo-TQ MS tandem quadrupole mass spectrometer coupled with an Acquity UPLC system plus autosampler equipped

with a Unison UK C18 3 μ m 2.0x 30 mm column (Imtakt, Japan) was utilized. An ion pairing reagent Heptabutyric acid was added in the mobile phase for separations.

LC/MS/MS Analysis for PTC124, PTC124 Glucuronide in mouse urine and liver tissues. An LC/MSMS analytical method was developed for PTC124 & its Glucuronide metabolite in mouse urine or liver tissues. First, PTC124 and its glucuronide metabolite were extracted from its matrix using a standard protein precipitation methods followed by a reverse phase column separation utilizing Waters Acquity UPLC system and a MS detection by Waters XEVO TQ-S Mass spectrometer. Chromatograms were integrated using Masslynx 4.1 software. A weighted ($1/X^2$) where X = concentration) linear regression analysis generated from the reference standards was used to calculate the plasma or urine concentrations in the unknown samples. The following formula was used to characterize the relationship between the peak area ratio and urine concentrations or liver concentrations. Sample Preparation was as follows: Millipore MultiScreen solvinert hydrophilic filter plates were used for the sample extraction. Specifically, a volume of 200 μ L of the internal standard solution was added to the filter plate. For reference standard samples, 20 μ L of the standard solutions in methanol were added to the plate followed by 20 μ L of vehicle treated mouse urine. For unknown samples, 20 μ L of methanol followed by 20 μ L of the properly diluted test urine was added to the plate. The plate was covered with a suitable plate cover and shaken for 5 minutes on a shaker. The plate was then centrifuged for 3 minutes at 2000 rpm using an Eppendorf 5804 centrifuge. After centrifugation, 2 mL of the filtrate was injected into the LC-MS/MS for analysis. Mouse liver samples were homogenized at 100 mg wet weight/mL in 30% methanol in water. The sample preparation procedures for tissues were like those for

urine samples except that replacing 20 uL urine samples with 20 uL of liver tissue homogenates.

Statistics. All statistics were calculated with two-tailed unpaired t-tests using InStat or GraphPad Prism software.

RESULTS

Investigating the ability of PTC124, PTC414, and PTC415 to suppress the Idua-W402X nonsense mutation using luciferase-based reporters. The non-aminoglycoside oxadiazole compound PTC124, or Translarna™, is a small molecular weight compound developed by PTC Therapeutics, Inc. as a nonsense suppression agent [20]. PTC124 is orally bioavailable and was shown to promote readthrough at PTCs associated with numerous genetic diseases [17, 18, 22, 32]. More recently, PTC Therapeutics identified PTC414, a derivative of PTC124, and PTC415, a structurally unrelated small molecule with greater blood-brain barrier penetrance, as two additional low molecular weight readthrough compounds with promising therapeutic potential. PTC414 has been shown to suppress nonsense mutations *in vitro* and *in vivo* in model systems of x-linked chorioretinal dystrophy [25]. Although PTC124 has been studied in a number of disease models, the mechanisms behind nonsense suppression for PTC124 or the new readthrough compounds, PTC414 and PTC415, are not well understood. We currently know of two converging pathways that nonsense suppression compounds can target to enhance protein production from transcripts containing a nonsense mutation. Compounds can increase the rate of readthrough at PTCs through near-cognate aminoacyl tRNA accommodation, increase the mutant mRNA abundance through inhibition of NMD, or

influence both pathways simultaneously.

To directly evaluate the ability of the test compounds to induce PTC readthrough within the native mRNA context of the W402X mutation, we used HEK293 cells expressing dual luciferase readthrough reporters that contained three codons of both upstream and downstream mouse *Idua* sequence context flanking the PTC (or the corresponding sense codon control) (**Figure 1A**). A concentration range was tested for each compound to find the optimal dose that produced the maximum W402X readthrough without cell toxicity as compared to cells treated with vehicle alone. The aminoglycoside G418, a well-characterized readthrough compound, was used as a positive control at its most effective, non-toxic dose. The fold-increase of W402X readthrough obtained for each suppression agent is shown (relative to that of HEK293 cells treated with vehicle alone) (**Figure 1A**). We found that the positive control, G418, induced readthrough by ~30-fold. The effect of PTC124 was much more modest, resulting in a maximal readthrough increase of 2 to 3-fold. PTC414 induced readthrough by nearly 10-fold, while PTC415 did not stimulate readthrough of the W402X PTC in the dual luciferase reporter above basal levels. Thus, PTC414 was most effective at inducing readthrough using the reporter system.

We next investigated the ability of the test compounds to inhibit NMD. To do this, we used HEK293 cells that expressed a *Renilla*- β -globin NMD reporter construct carrying the Q39X PTC within exon 2 of β -globin, which targets the construct for rapid degradation via the NMD pathway [29] (**Figure 1B**). Reporter *Renilla* activity was previously shown to increase when NMD is inhibited due to stabilization of the mRNA. A concentration range was tested for each compound to find the optimal dose that

produced maximum NMD inhibition without significant cell toxicity. The anti-inflammatory compound amlexanox, previously identified as an NMD inhibitor [33] was used as a positive control. The fold-increase in mRNA stability was determined by measuring *Renilla* luciferase units per milligram of total protein in treated cells relative to cells treated with vehicle alone (**Figure 1B**). We found that PTC414 exhibited a slight (25%) increase in *Renilla* signal, suggesting that it may weakly attenuate NMD to increase reporter mRNA abundance (Figure 1B). Neither PTC124 or PTC415 had any effect on *Renilla* levels, suggesting that neither compound affected NMD efficiency (Figure 1B).

Investigating the ability of PTC124, PTC414, and PTC415 to reduce GAG accumulation in Idua-W402X mouse embryonic fibroblasts (MEFs). In order to examine the test compounds in a more physiologically relevant cell-based system, we next examined the ability of the compounds to reduce GAG accumulation in immortalized MEFs derived from the *Idua-W402X* mouse. Loss of α -L-iduronidase activity results in lysosomal GAG accumulation. Accordingly, we found that overall sulfated GAG levels measured using the GAG dye-binding assay were elevated almost 5-fold above normal in untreated *Idua-W402X* MEFs (**Figure 1C**). In *Idua-W402X* MEFs treated with the optimal dose of G418, excess GAG storage was decreased 45%, resulting in a GAG level that was ~2.5-fold above normal. In *Idua-W402X* MEFs treated with PTC124, PTC414 and PTC415, excess GAG levels decreased 56%, 66% and 74%, respectively, at the most effective dose for each compound (**Figure 1C**). Thus, all three non-aminoglycoside compounds were more effective than G418 at reducing GAG storage in MEFs. Of note, PTC415, which showed no effect on the luciferase reporters in HEK293 cells, was the

most effective at reducing GAG accumulation in the MEFs. Additionally, while PTC414 and PTC415 demonstrated a linear dose response in the MEFs, we observed a bell-shaped dose response curve with PTC124, as previously reported [23, 32]. These data provide evidence to support *in vivo* investigation of all three compounds in the *Idua*-W402X mouse.

Examining safety, tolerability, and efficacy of PTC124, PTC414, and PTC415 in Idua-W402X mice. In our preliminary *in vivo* study, we administered PTC124, PTC414, and PTC415 to 8-week-old homozygous *Idua*-W402X mice for a total of 4 weeks for the purpose of evaluating safety, tolerability, and therapeutic efficacy of the test compounds in an animal model of MPS I-H. The study consisted of both male and female W402X and wild-type animals that were treated with each of the three compounds at a single dose that was determined by previous pharmacokinetic studies (**Table 1**). PTC124 and PTC414, which are orally bioavailable, were administered in chow while PTC415 was administered biweekly via subcutaneous injections. To evaluate whether enough α -L-iduronidase function was restored to reduce GAG accumulation, we quantified sulfated GAG levels using a dye-binding assay [10, 26] (**Figure 2A-B**). GAG levels were significantly reduced in the spleen of mice treated with PTC124 and PTC415, but spleen GAG reduction was not observed in response to PTC414. Mass spectrometry evaluation of the specific GAG species that accumulate in MPS I (heparan sulfate and dermatan sulfate) confirmed a significant 12% decrease in dermatan sulfate and a 17% decrease in heparan sulfate in the spleen of mice treated with PTC415 (**Figure 2C, E**). However, no significant changes in spleen GAGs were observed in mice treated with either PTC124 or PTC414 (**Figure 2D, F**). In addition, no changes in GAG levels were observed in the

brain or heart of *Idua*-W402X mice treated with any of the three compounds compared to vehicle only controls (**Supplemental Figure 1A-D**). Notably, a significant fraction of animals receiving PTC415 (75% of the wild-type controls and 50% of the *Idua*-W402X mice) developed lesions at injection sites by the third or fourth dose despite injection site rotation. Lesions worsened throughout treatment and, in several cases, resulted in weight loss. No adverse reactions were detected in mice treated orally with PTC124 or PTC414. Based on these results, we continued evaluation of PTC124 and PTC414 but did not pursue PTC415 in subsequent animal studies.

Evaluating efficacy and specificity of PTC124 and PTC414 in Idua-W402X mice.

In order to further examine the ability of PTC124 and PTC414 to promote PTC readthrough, we carried out a two-week *in vivo* study where we administered PTC124 and PTC414 to the *Idua*-W402X mouse as well as the MPS I-H knock-out mouse (KO), which represents another mouse model of MPS I-H that carries a large insertion mutation that is not amenable to readthrough [27]. Because MPS I-H mice younger than 20-25 weeks do not display many of the more complex morphological and functional phenotypes of MPS I-H, we focused on biochemical endpoint, including α -L-iduronidase activity and GAG storage, for this brief, 2-week study. PTC124 and PTC414 treated *Idua*-W402X showed a statistically significant reduction of brain GAG storage relative to vehicle treated controls, but no changes in GAG levels were detected in treated KO mice compared to controls (**Figure 3A**). This indicates the specificity of PTC124 and PTC414 for nonsense mutations. Analysis of brain enzyme levels did not show statistically significant changes in brain enzyme activity among either the *Idua*-W402X or KO mice (**Figure 3B**). In addition, no change in GAG storage or enzyme activity in the spleen of

Idua-W402X or KO mice was detected in response to either treatment (**Figure 3B and D**).

Evaluation of biochemical endpoints in response to long-term administration of PTC124 or PTC414 in Idua-W402X mice. We next examined whether administration of PTC124 and PTC414 were able to prevent progression of the MPS I-H phenotype in *Idua*-W402X mice. It is broadly agreed that the best treatment course for MPS I-H requires early diagnosis and intervention to prevent damage rather than correct it [4, 34-36]. To that end, and based on the successful time-course of our previous *in vivo* nonsense suppression study [10], we initiated treatment of *Idua*-W402X mice at 3 weeks of age and sustained treatment for 28 weeks to a final age of 31 weeks in an effort to achieve the greatest attenuation of disease progression. The length of this study allowed us to examine more clinically relevant morphological and functional MPS I-H phenotypes in addition to the primary biochemical endpoints.

The lack of α -L-iduronidase function leads to dysfunctional GAG catabolism and progressive GAG accumulation, which leads to secondary morphological and functional phenotypic hallmarks in bone, heart, and brain [5]. As in the short-term studies, we quantified α -L-iduronidase activity and sulfated GAG levels in tissue lysates from treated mice relative to vehicle alone controls. We saw no significant difference in either α -L-iduronidase activity (**Figure 4D-E**) or GAG levels in the brain, spleen, or heart (**Figure 4A**) in response to either PTC124 or PTC414 administered orally in mouse chow. Mass spectrometry analysis of urine samples from PTC124-treated mice demonstrated a trend toward reduction of dermatan sulfate in animals treated for 28 weeks (**Figure 4C**). Quantitative analysis of dermatan sulfate and heparan sulfate GAG levels in liver samples

after 2, 4, or 28 weeks administration of PTC124 was conducted via mass spectrometry. Liver lysate analysis from PTC124-treated mice revealed a statistically significant 24% reduction in dermatan sulfate after 2 weeks treatment (**Figure 5B**) and a statistically significant 25% reduction in heparan sulfate after 28 weeks treatment (**Figure 5E**). Despite the measurable response to PTC124, both species of GAGs continue to accumulate throughout treatment so that treated HS levels increase from 43-fold WT at 12 weeks of age to 448-fold WT at 31 weeks of age and DS levels increase from 28-fold at 12 weeks to 54-fold at 31 weeks of age.

Evaluation of morphological and functional endpoints in response to long-term administration of PTC124 or PTC414 in Idua-W402X mice. In MPS I-H patients, the most common cardiac presentation is valve pathology, involving thickening and associated dysfunction due to GAG accumulation. However, in MPS I-H mice, alterations in aortic elasticity and structure are observed, a phenotype we previously noted in MPS I-H knock out mice [34, 37] and in the *Idua-W402X* mouse model [10]. Examination of mutant, male *Idua-W402X* mice using Doppler echocardiography revealed dilated aortic root with concomitant turbulent flow. Morphological measures showed *Idua-W402X* animals treated with vehicle alone have significantly increased aortic lumen diameter (**Figure 6A**) and aortic wall thickness (**Figure 6B**). While we did not detect any change in lumen diameter in response to either PTC124 or PTC414 (**Figure 6A**), *Idua-W402X* mice treated with PTC124, and to a lesser extent PTC414, resulted in improvement of aortic wall thickness measures (**Figure 6B**). This suggests that PTC124 and PTC414 slowed progression of cardiac deterioration observed in *Idua-W402X* mice.

Skeletal involvement occurs early and ubiquitously among MPS I-H patients due to GAG storage that leads to thickening and malformation of joints and bone through a variety of mechanisms [38]. The *Idua*-W402X mouse model has been shown to have a distinct orthopedic profile as well. Initial characterization of the animal showed thickening of the zygomatic arch, and thickening and shortening of the long bones [26]. Further analysis of bone revealed altered morphological features of the trabecular and cortical bone as well as altered cellular composition [10, 39]. Previously we showed that early intervention with the readthrough compound NB84 could modify disease progression in the bone of *Idua*-W402X mice [10]. We recapitulated those previous analyses, which included micro-computed tomography (**Figure 7; Suppl. Figure 2A**) and osteoblast TRAP staining (**Suppl. Figure 2B**) to evaluate the therapeutic effect of PTC124 and PTC414 on bone in *Idua*-W402X mice after the 28-week administration protocols. We found that neither PTC124 or PTC414 treatment resulted in morphological or cellular improvements in the bone of *Idua*-W402X relative to controls. While PTC124 did not affect bone morphology in wild-type mice, PTC414 treatment caused significant changes in all measures of bone morphology and cellular composition of treated wild-type animals (**Figure 7; Suppl. Figure 2**). These data indicate that PTC124 treatment did not attenuate progression of bone abnormalities. Furthermore, PTC414 may be accumulating disproportionately in bone or interfering with essential processes of bone maintenance.

We also assessed the functionality of mice as measured by the distance travelled in the elevated zero maze and open field tests (**Suppl. Figure 3**). Similar to our previous study [10], we found a significant decrease in the distance travelled by *Idua*-W402X mice

relative to wild-type controls. Treatment with PTC124 and PTC414 did not alter the distance traveled in *Idua*-W402X relative to vehicle alone controls in either the zero maze or the open field test.

Evaluating PTC124 metabolism after 2, 4 and 28 weeks administration in the Idua-W402X mouse model. While our data suggests that the three aminoglycosides are effective at suppressing the *Idua*-W402X nonsense mutation in MEFs, they appear to be far less effective during administration to *Idua*-W402X mice. In order to examine the difference between PTC124 *in vitro* and *in vivo* effectiveness, we performed a preliminary examination of its metabolism and clearance in mice. In humans, PTC124 has been shown to be metabolized to PTC124-O-1 β -acyl glucuronide mainly through conjugation with uridine diphosphate glucuronosyltransferase 1A9 (UGT1A9) in the liver and intestine, which inactivates the drug. Around 50% of an administered PTC124 dose is recovered in the feces, with the remainder excreted in the urine, where unchanged ataluren and the acryl glucuronide metabolite accounts for 1% and 49% of the dose, respectively [16]. We evaluated PTC124 levels in urine from the 2, 4, and 28-week treatment groups to determine the level of glucuronidated PTC124. We found that ~99%, ~82%, and 97% respectively, of the total PTC124 (unchanged and metabolized) found in urine was in the glucuronidated form (**Figure 8A**), which is nearly 2-fold greater the amount of metabolized PTC124 than is excreted in humans. This suggests that metabolism of PTC124 to this inactive form is more robust in mice and may contribute to the generally modest response observed in this study.

DISCUSSION

Current treatments for MPS I-H are insufficient to alleviate all aspects of the disease phenotype. Therapies for MPS I-H include hematopoietic stem cell transplantation (HSCT) as well as enzyme replacement therapy (ERT) with recombinant α -L-iduronidase marketed as AldurazymeTM. Although these methods can significantly attenuate the MPS I phenotype in many somatic tissues and extend the patient lifespan, there are limitations and drawbacks to these techniques. While HSCT has become a significantly safer procedure than in previous years, it remains expensive, invasive, risky, and requires some time to find a match. Recent longitudinal studies demonstrate that HSCT can slow, but not prevent, progression of orthopedic and cardiac phenotypes in patients, indicating that quality of life and life-span are still compromised [40, 41]. Aldurazyme can improve many of the clinical features of MPS I-H though it is unable to adequately penetrate the brain, bone, cornea, and heart valves to alleviate significant aspects of the disease [3, 7]. However, when delivered early enough, Aldurazyme can slow disease progression in the brain and the bone [42]. Longitudinal studies of both HSCT and ERT show that earlier intervention and milder disease progression at the time of intervention are the greatest predictors of improved prognosis later in life, suggesting that a therapy that could be given very early could greatly improve patient outcomes [35, 40, 42]. Nonsense suppression therapy offers the potential of a more affordable, and more easily obtained and administered option that could be combined with existing therapies to augment available options and improve outcomes. Alternatively, if safe and effective nonsense suppression drugs are developed, nonsense suppression therapy alone could potentially alleviate most aspects of the MPS I phenotype.

We have investigated whether nonsense suppression therapy might be an effective treatment for MPS I-H primarily using the *Idua*-W402X mouse, a model that recapitulates many of the phenotypes associated with human disease and requires similar levels of α -L-iduronidase function to attenuate the MPS I-H phenotype [9, 10, 26]. We previously demonstrated that the designer aminoglycoside NB84 effectively restored sufficient α -L-iduronidase activity to reduce GAG accumulation and ameliorate disease progression in several tissues over a 28-week dosing period [10]. We observed sustained enzyme activity with concomitant GAG reduction, improved heart function and morphology, improved behavioral performance, diminished neurological inflammation, and improved bone morphology in *Idua*-W402X mice. These results suggest that nonsense suppression therapy may alleviate many of the phenotypes associated with MPS I-H, including tissues that current therapies are unable to address. However, aminoglycosides are associated with nephrotoxicity and ototoxicity. While NB84 has been shown to produce significantly less cell toxicity than gentamicin [43] and no evidence of NB84 toxicity was observed in our mouse studies, further clinical evaluation is needed to determine whether NB84 and other designer aminoglycosides are safe for chronic, long-term use as nonsense suppression drugs.

PTC124, currently on the market as an orphan drug approved in Europe for the treatment of DMD as Translarna®, was initially identified by high-throughput screening and validated using an *in vitro* luciferase-based assay [20]. Subsequent findings that PTC124 interfered with some luciferase-based systems called into question the readthrough capabilities of the drug [44]. However, multiple *in vivo* results have since recapitulated readthrough efficacy in response to PTC124 [17, 20, 21]. Phase 2 and 3

clinical trials of Translarna® for the treatment of Duchenne Muscular Dystrophy (DMD) gave promising results [45]. One of the factors identified as responsible for the difficulty in identifying therapeutic improvements was the lack of clinically meaningful endpoints for diseases such as DMD [46]. PTC124 Phase 3 trials for DMD are ongoing. Phase 2 for cystic fibrosis (CF) also showed initial promise [47]. Initial findings in the Phase 3 clinical trials for the treatment of CF showed no therapeutic benefit, but post-hoc evaluation showed benefit in a subset of patients [48]. However, more recent Phase 3 results indicated that PTC124 was unable to restore enough protein function in CF patients to improve lung function [47]. Both CF and DMD require between 20-35% of normal protein function to alleviate the disease phenotype. It remains to be examined whether PTC124 can be used to treat other genetic disease for which the threshold for correction is more modest.

The premise of the current study was to investigate the efficacy of more clinically relevant small molecule readthrough compounds in the context of the *Idua*-W402X, a model of Hurler disease for which we have established a broad array of assays to measure numerous biochemical and morphological aspects of the disease, some of which may be amenable for use in clinical trials. While the efficiency of the compounds to suppress the *Idua*-W402X nonsense mutation varied in luciferase reporter assays, we found that all three compounds reduced GAG accumulation in mouse embryonic fibroblasts (MEFs) derived from the *Idua*-W402X mouse. One possible explanation is that all three compounds are contributing, to varying degrees, to both the readthrough pathway and NMD inhibition, as evidenced by the luciferase-based NMD reporter, so that the therapeutic benefit is more robust in the native context where contributions to both PTC

suppression and NMD inhibition augment the therapeutic response. Short-term *in vivo* studies revealed that all three compounds produced modest reductions in GAG levels in multiple mouse tissues but PTC415 was poorly tolerated and resulted in injection site lesions. While adverse effects associated with PTC415 prohibited its long-term evaluation, 28-week administration of PTC124 and PTC414 resulted in modest to negligible benefits in brain, heart, liver, spleen, and bone. However, with long-term administration PTC414 resulted in deleterious changes to WT bone morphology and altered spleen enzyme activity. These unanticipated off-target effects demonstrate that neither PTC415 nor PTC414 represent a viable therapeutic agent for chronic administration to treat MPS I-H patients that harbor the *Idua*-W402X mutation.

Our data indicated that PTC124 mediated marked readthrough induction *in vitro*, but we see only modest efficacy *in vivo*. Short term administration resulted in reduction of brain, spleen and liver GAGs, while long-term administration resulted in reduced liver heparan sulfate levels as well as improvement of both aortic lumen diameter and wall thickness, but no improvement of bone morphology or behavioral endpoints. These results indicated that PTC124 was not as efficient at alleviating MPS I-H endpoints in the *Idua*-W402X mice as observed in our previous study with NB84 [10]. Mass spectrometry (MS) analysis revealed that PTC124 was subject to substantial metabolism as evidenced by its glucuronidated form in liver and urine. We found that >99% of excreted PTC124 was glucuronidated by the end of the 2-week treatment period and >97% by the end of the 28-week treatment period. In humans, PTC124 excreted in the urine was found to be 49% glucuronidated [16]. These results suggest that perhaps the compound is so comprehensively modified and excreted in mice that we cannot achieve

more than minimal therapeutic benefit. Via mass spectrometry evaluation of urine PTC124 levels, we also noted that the samples from the 4-week treatment period reflected much less consistent levels of both metabolized forms of PTC124 (**Figure 8**). We hypothesize that differences in compounding of the drug with chow, which was conducted separately for the 4 versus 2 and 28 week treatments, is responsible for confounding the results of the initial 4-week study.

Although the individual efficacy of PTC124 was modest, this study clearly demonstrated that PTC124 functions as a read-through compound capable of safely restoring functional enzyme in *Idua*-W402X mice. PTC124 showed early efficacy in reducing brain and liver GAG accumulation and was able to improve liver GAG storage and measures of heart morphology and function with long-term administration. The safety, tolerability, affordability, and ease of administration make PTC124 an ideal candidate for combination with existing therapies, particularly in light of its ability to modify the disease in tissues least benefitted by current therapies. Both brain and heart represent systems inadequately improved with available MPS I-H treatments that may benefit from small molecule therapy if metabolism of this compound is more favorable in patients than mice. Unfortunately, we found that metabolism in the mouse model was markedly different from that seen in humans, limiting the usefulness of this animal model in predicting outcomes for human disease. Further evaluation of PTC124 in MPS I-H clinical studies will be required to determine whether this drug will be efficacious enough to alleviate MPS I endpoints in human patients.

REFERENCES

1. Mort, M., et al., *A meta-analysis of nonsense mutations causing human genetic disease*. Hum Mutat, 2008. **29**(8): p. 1037-47.
2. Keeling, K.M., et al., *Therapeutics Based on Stop Codon Readthrough*. Annu Rev Genomics Hum Genet, 2014. **15**: p. 371-394.
3. Pastores, G.M., et al., *The MPS I registry: design, methodology, and early findings of a global disease registry for monitoring patients with Mucopolysaccharidosis Type I*. Mol Genet Metab, 2007. **91**(1): p. 37-47.
4. Oussoren, E., et al., *Residual alpha-L-iduronidase activity in fibroblasts of mild to severe Mucopolysaccharidosis type I patients*. Mol Genet Metab, 2013. **109**(4): p. 377-81.
5. Muenzer, J., J.E. Wraith, and L.A. Clarke, *Mucopolysaccharidosis I: management and treatment guidelines*. Pediatrics, 2009. **123**(1): p. 19-29.
6. Beesley, C.E., et al., *Mutational analysis of 85 mucopolysaccharidosis type I families: frequency of known mutations, identification of 17 novel mutations and in vitro expression of missense mutations*. Hum Genet, 2001. **109**(5): p. 503-11.
7. Valayannopoulos, V. and F.A. Wijburg, *Therapy for the mucopolysaccharidoses*. Rheumatology (Oxford), 2011. **50 Suppl 5**: p. v49-59.
8. Keeling, K.M., et al., *Gentamicin-mediated suppression of Hurler syndrome stop mutations restores a low level of alpha-L-iduronidase activity and reduces lysosomal glycosaminoglycan accumulation*. Hum Mol Genet, 2001. **10**(3): p. 291-9.
9. Wang, D., et al., *The designer aminoglycoside NB84 significantly reduces glycosaminoglycan accumulation associated with MPS I-H in the Idua-W392X mouse*. Mol Genet Metab, 2012. **105**: p. 116-125.
10. Gunn, G., et al., *Long-term nonsense suppression therapy moderates MPS I-H disease progression*. Mol Genet Metab, 2013. **111**(3): p. 374-81.
11. Sachs, A.B., R.W. Davis, and R.D. Kornberg, *A single domain of yeast poly(A)-binding protein is necessary and sufficient for RNA binding and cell viability*. Mol Cell Biol, 1987. **7**(9): p. 3268-76.
12. Sone, M., P.A. Schachern, and M.M. Paparella, *Loss of spiral ganglion cells as primary manifestation of aminoglycoside ototoxicity*. Hear Res, 1998. **115**(1-2): p. 217-23.
13. Martinez-Salgado, C., F.J. Lopez-Hernandez, and J.M. Lopez-Novoa, *Glomerular nephrotoxicity of aminoglycosides*. Toxicol Appl Pharmacol, 2007. **223**(1): p. 86-98.
14. Qian, Y. and M.X. Guan, *Interaction of aminoglycosides with human mitochondrial 12S rRNA carrying the deafness-associated mutation*. Antimicrob Agents Chemother, 2009. **53**(11): p. 4612-8.
15. Sabbavarapu, N.M., et al., *Design of Novel Aminoglycoside Derivatives with Enhanced Suppression of Diseases-Causing Nonsense Mutations*. ACS Med Chem Lett, 2016. **7**(4): p. 418-23.
16. Hirawat, S., et al., *Safety, tolerability, and pharmacokinetics of PTC124, a nonaminoglycoside nonsense mutation suppressor, following single- and multiple-*

- dose administration to healthy male and female adult volunteers. *J Clin Pharmacol*, 2007. **47**(4): p. 430-44.
17. Du, M., et al., *PTC124 is an orally bioavailable compound that promotes suppression of the human CFTR-G542X nonsense allele in a CF mouse model*. *Proc Natl Acad Sci U S A*, 2008. **105**(6): p. 2064-9.
 18. Goldmann, T., et al., *Beneficial read-through of a USH1C nonsense mutation by designed aminoglycoside NB30 in the retina*. *Invest Ophthalmol Vis Sci*, 2010. **51**(12): p. 6671-80.
 19. Haas, M., et al., *European Medicines Agency review of ataluren for the treatment of ambulant patients aged 5 years and older with Duchenne muscular dystrophy resulting from a nonsense mutation in the dystrophin gene*. *Neuromuscul Disord*, 2015. **25**(1): p. 5-13.
 20. Welch, E.M., et al., *PTC124 targets genetic disorders caused by nonsense mutations*. *Nature*, 2007. **447**: p. 87-91.
 21. Goldmann, T., et al., *PTC124 mediated translational read-through of a nonsense mutation causing Usher type 1C*. *Hum Gene Ther*, 2011. **22**(5): p. 537-47.
 22. Sarkar, C., Z. Zhang, and A.B. Mukherjee, *Stop codon read-through with PTC124 induces palmitoyl-protein thioesterase-1 activity, reduces thioester load and suppresses apoptosis in cultured cells from INCL patients*. *Mol Genet Metab*, 2011. **104**(3): p. 338-45.
 23. Roy, B., et al., *Ataluren stimulates ribosomal selection of near-cognate tRNAs to promote nonsense suppression*. *Proc Natl Acad Sci U S A*, 2016. **113**(44): p. 12508-12513.
 24. Lentini, L., et al., *Toward a Rationale for the PTC124 (Ataluren) Promoted Readthrough of Premature Stop Codons: A Computational Approach and GFP-Reporter Cell-Based Assay*. *Mol Pharm*, 2014. **11**: p. 653-64.
 25. Moosajee, M., et al., *Functional rescue of REPI following treatment with PTC124 and novel derivative PTC-414 in human choroideremia fibroblasts and the nonsense-mediated zebrafish model*. *Hum Mol Genet*, 2016.
 26. Wang, D., et al., *Characterization of an MPS I-H knock-in mouse that carries a nonsense mutation analogous to the human IDUA-W402X mutation*. *Mol Genet Metab*, 2010. **99**: p. 62-71.
 27. Clarke, L.A., et al., *Murine mucopolysaccharidosis type I: targeted disruption of the murine alpha-L-iduronidase gene*. *Hum Mol Genet*, 1997. **6**(4): p. 503-11.
 28. Grentzmann, G., et al., *A dual-luciferase reporter system for studying recoding signals*. *RNA*, 1998. **4**(4): p. 479-86.
 29. Boelz, S., et al., *A chemiluminescence-based reporter system to monitor nonsense-mediated mRNA decay*. *Biochem Biophys Res Commun*, 2006. **349**(1): p. 186-91.
 30. Zhang, H., S.P. Young, and D.S. Millington, *Quantification of glycosaminoglycans in urine by isotope-dilution liquid chromatography-electrospray ionization tandem mass spectrometry*. *Curr Protoc Hum Genet*, 2013. **Chapter 17**: p. Unit 17 12.
 31. Zhang, H., et al., *A straightforward, quantitative ultra-performance liquid chromatography-tandem mass spectrometric method for heparan sulfate,*

- dermatan sulfate and chondroitin sulfate in urine: an improved clinical screening test for the mucopolysaccharidoses.* Mol Genet Metab, 2015. **114**(2): p. 123-8.
32. Peltz, S.W., et al., *Ataluren as an agent for therapeutic nonsense suppression.* Annu Rev Med, 2013. **64**: p. 407-25.
33. Gonzalez-Hilarion, S., et al., *Rescue of nonsense mutations by amlexanox in human cells.* Orphanet J Rare Dis, 2012. **7**: p. 58.
34. Braunlin, E.A., et al., *Cardiac disease in patients with mucopolysaccharidosis: presentation, diagnosis and management.* J Inherit Metab Dis, 2011. **34**(6): p. 1183-97.
35. Poe, M.D., S.L. Chagnon, and M.L. Escolar, *Early treatment is associated with improved cognition in Hurler syndrome.* Ann Neurol, 2014. **76**(5): p. 747-53.
36. de Ru, M.H., et al., *Enzyme replacement therapy and/or hematopoietic stem cell transplantation at diagnosis in patients with mucopolysaccharidosis type I: results of a European consensus procedure.* Orphanet J Rare Dis, 2011. **6**: p. 55.
37. Nemes, A., et al., *The mild form of mucopolysaccharidosis type I (Scheie syndrome) is associated with increased ascending aortic stiffness.* Heart Vessels, 2008. **23**(2): p. 108-11.
38. White, K.K., *Orthopaedic aspects of mucopolysaccharidoses.* Rheumatology (Oxford), 2011. **50 Suppl 5**: p. v26-33.
39. Oestreich, A.K., et al., *Characterization of MPS I-H knock-in mouse reveals increased femoral biomechanical integrity with compromised material strength and altered bone geometry.* MGM Rep, 2015. **5**: p. 3-11.
40. Aldenhoven, M., et al., *Long-term outcome of Hurler syndrome patients after hematopoietic cell transplantation: an international multicenter study.* Blood, 2015. **125**(13): p. 2164-72.
41. Yasuda, E., et al., *Molecular Genetics and Metabolism Report Long-term follow-up of post hematopoietic stem cell transplantation for Hurler syndrome: clinical, biochemical, and pathological improvements.* Mol Genet Metab Rep, 2015. **2**: p. 65-76.
42. Laraway, S., et al., *Outcomes of Long-Term Treatment with Laronidase in Patients with Mucopolysaccharidosis Type I.* J Pediatr, 2016. **178**: p. 219-226 e1.
43. Shulman, E., et al., *Designer Aminoglycosides That Selectively Inhibit Cytoplasmic Rather than Mitochondrial Ribosomes Show Decreased Ototoxicity: A STRATEGY FOR THE TREATMENT OF GENETIC DISEASES.* J Biol Chem, 2014. **289**(4): p. 2318-30.
44. Auld, D.S., et al., *Mechanism of PTC124 activity in cell-based luciferase assays of nonsense codon suppression.* Proc Natl Acad Sci U S A, 2009. **106**(9): p. 3585-90.
45. Bushby, K., et al., *Ataluren treatment of patients with nonsense mutation dystrophinopathy.* Muscle Nerve, 2014.
46. McDonald, C.M., et al., *The 6-minute walk test and other endpoints in Duchenne muscular dystrophy: Longitudinal natural history observations over 48 weeks from a multicenter study.* Muscle Nerve, 2013: p. 1-14.
47. Sermet-Gaudelus, I., et al., *Ataluren (PTC124) induces cystic fibrosis transmembrane conductance regulator protein expression and activity in children*

with nonsense mutation cystic fibrosis. Am J Respir Crit Care Med, 2010.
182(10): p. 1262-72.

48. Kerem, E., et al., *Ataluren for the treatment of nonsense-mutation cystic fibrosis: a randomised, double-blind, placebo-controlled phase 3 trial*. Lancet Respir Med, 2014. **2**(7): p. 539-47.

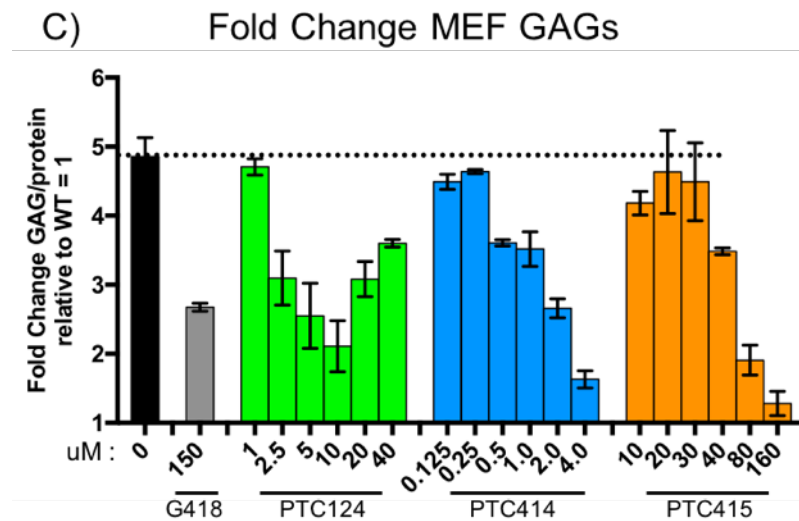
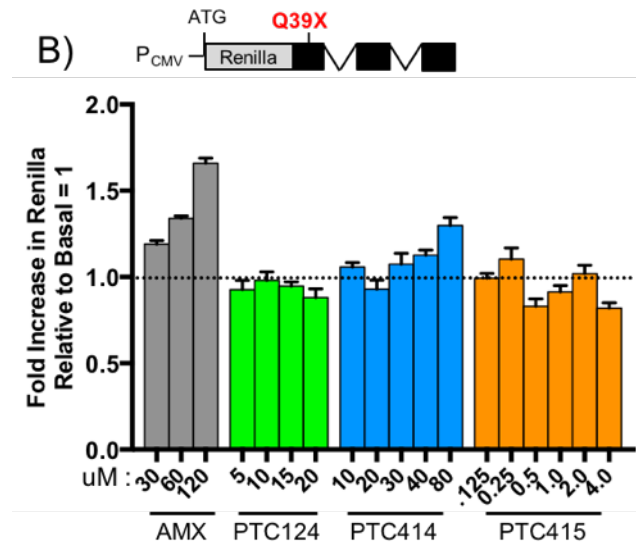
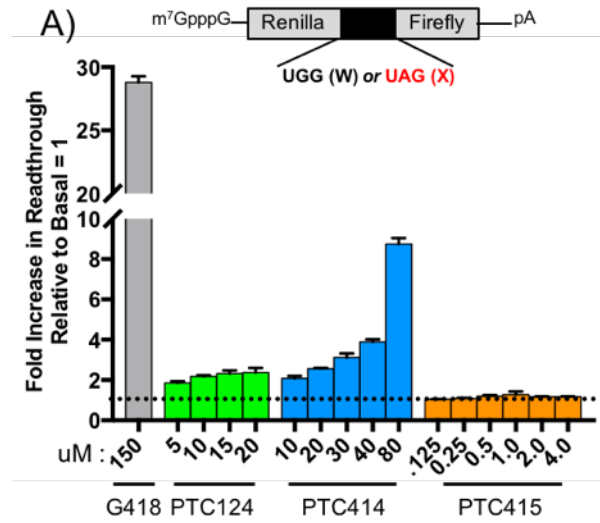
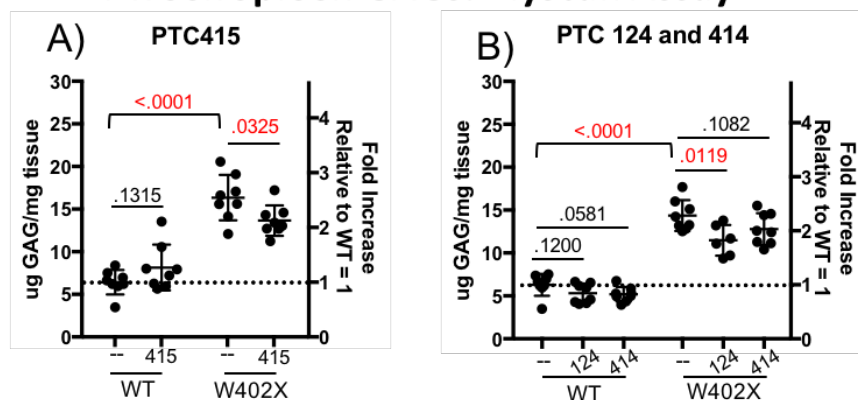


Figure 1: Characterization of the ability of non-aminoglycoside compounds to suppress the *Idua*-W402X nonsense mutation *in vitro*. A) Comparing the ability of test compounds to readthrough the *Idua*-W402X mutation using dual luciferase reporters. Data is expressed as the fold-increase in reporter cells treated with compound relative to cells treated with vehicle only. B) Examining whether test compounds inhibit NMD using a luciferase-based NMD reporter. The level of NMD inhibition is expressed as the level of Renilla luciferase per milligram of total protein in treated cells relative to that of cells treated with vehicle only. C) Examining the ability of test compounds to reduce GAG storage in *Idua*-W402X MEFs. Data is expressed as the level of GAGs quantified in treated cells relative to GAGs quantified in wild-type MEFs. Dotted lines represent baseline reading of relevant control. All of the data shown in A-C are from representative experiments performed in quadruplicate.

4 week Spleen GAGs: Blyscan Assay



4 week Spleen GAGs: Mass Spec

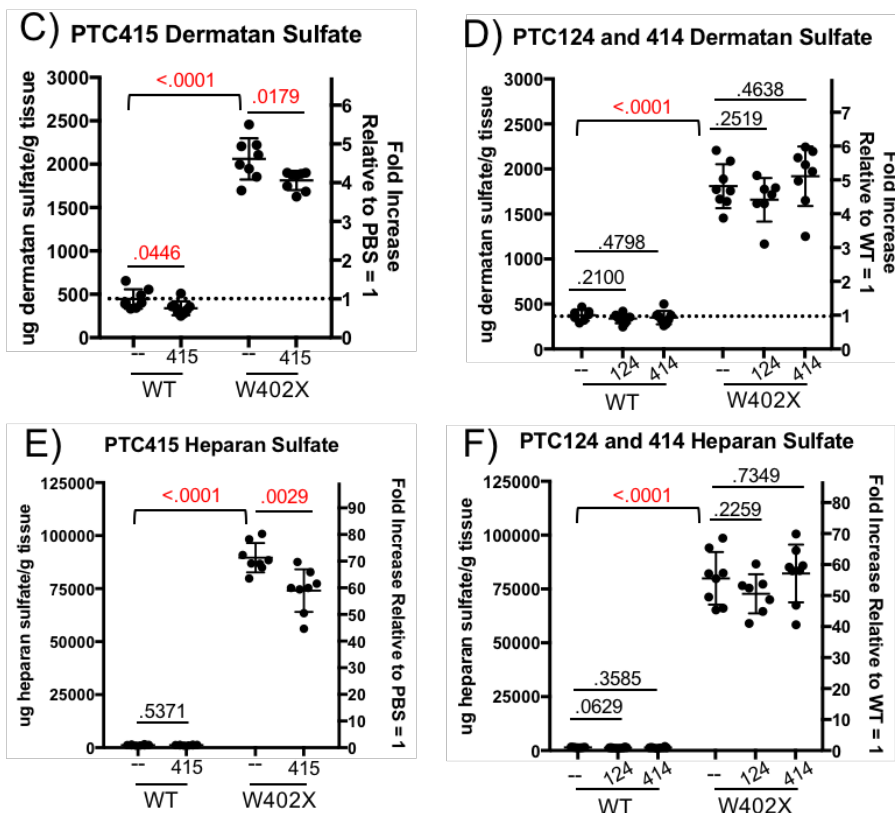
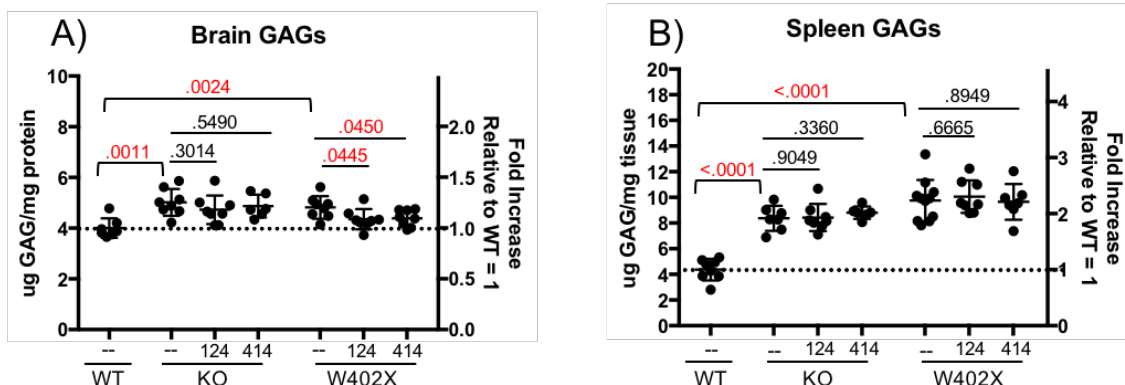


Figure 2: Examination of compound efficacy and tolerability after 4 weeks of treatment in *Idua-W402X* mice. Quantitative analysis of sulfated spleen GAGs measured via the Blyscan dye binding assay in response to: A) PTC415, and B) PTC124 and PTC414. Quantitative analysis of the specific GAG species dermatan sulfate and heparan sulfate by mass spectrometry in response to: C) & E) PTC415, and D) & F) PTC124 and PTC414. Dotted lines indicate GAG levels obtained from untreated WT mice age 12 weeks. n = 8 mice per group. P values from two-tailed t-tests are indicated above brackets.

2 week GAGs



2 week Enzyme

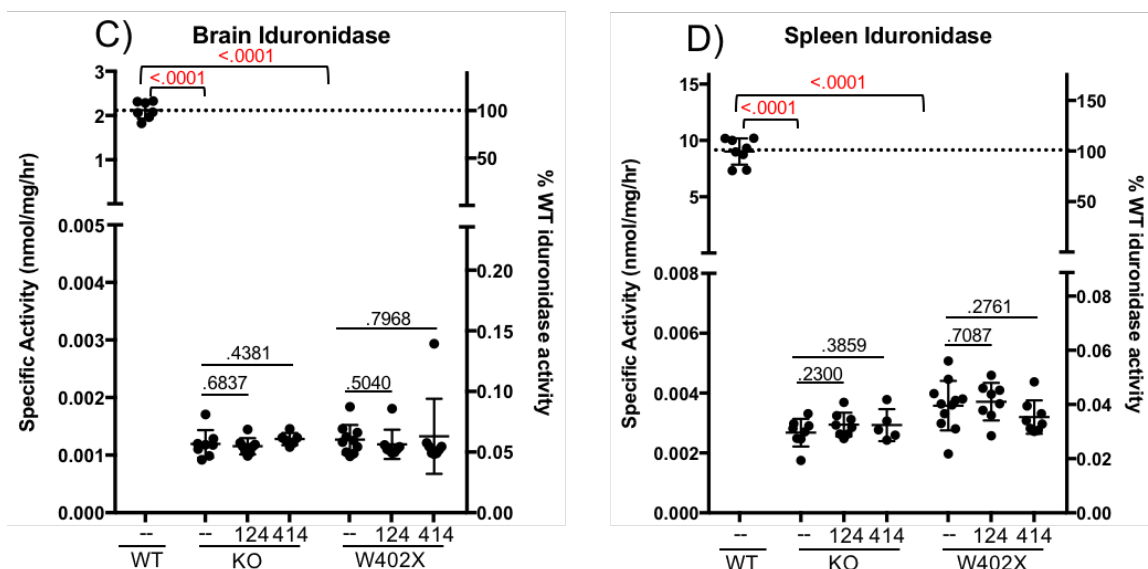


Figure 3: Examination of compound specificity after 2 weeks of treatment in *Idua-W402X* and KO MPS I-H mice. Quantitative analysis of sulfated GAGs measured via the Blyscan assay in: A) brain, and B) spleen of knockout (KO) and *Idua-W402X* (W402X) MPS I-H mice. α -L-iduronidase specific activity in: C) brain, and D) spleen of KO and W402X mice. Dotted lines indicate levels obtained from untreated, 12-week-old wild-type mice. $n = 8$ mice per group. P values from two-tailed t-tests are indicated above brackets.

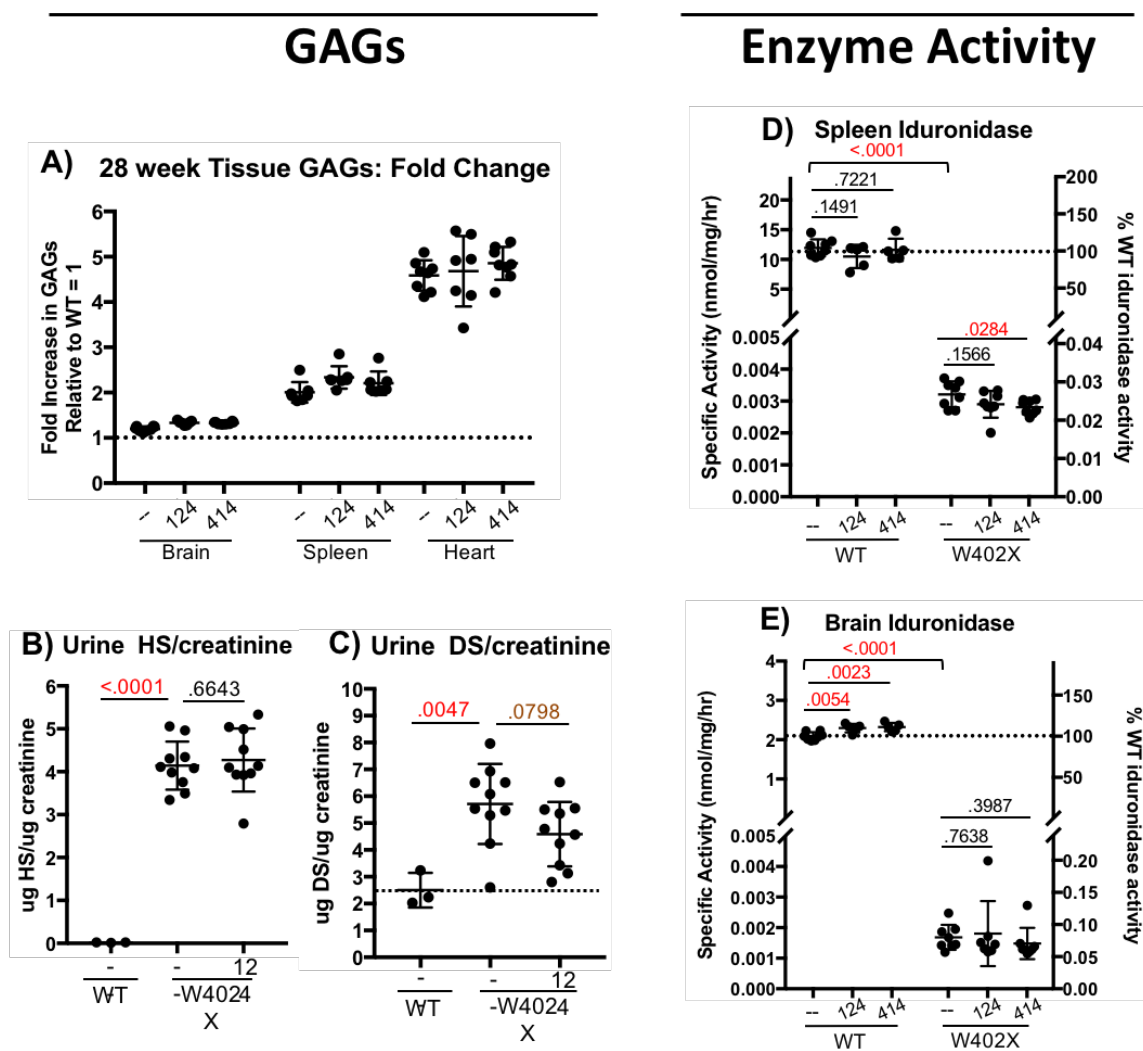


Figure 4: Examination of biochemical endpoints after 28 weeks of treatment in *Idua-W402X* mice. A) Quantitative analysis of sulfated tissue GAGs measured via Blyscan dye binding assay in response to PTC124 and PTC414. Quantitative analysis by mass spectrometry of the specific urine GAG species heparan sulfate (B) and dermatan sulfate (C) in response to PTC124. α -L-iduronidase specific activity in: D) spleen, and E) brain mice response to PTC124 and PTC414. Dotted lines indicate levels obtained from untreated, 31-week-old wild-type mice. n = 3 for wild-type mass spec. n = 7-10 mice per group for all other measures. P values from two-tailed t-tests are indicated above brackets.

Heparan Sulfate

Dermatan Sulfate

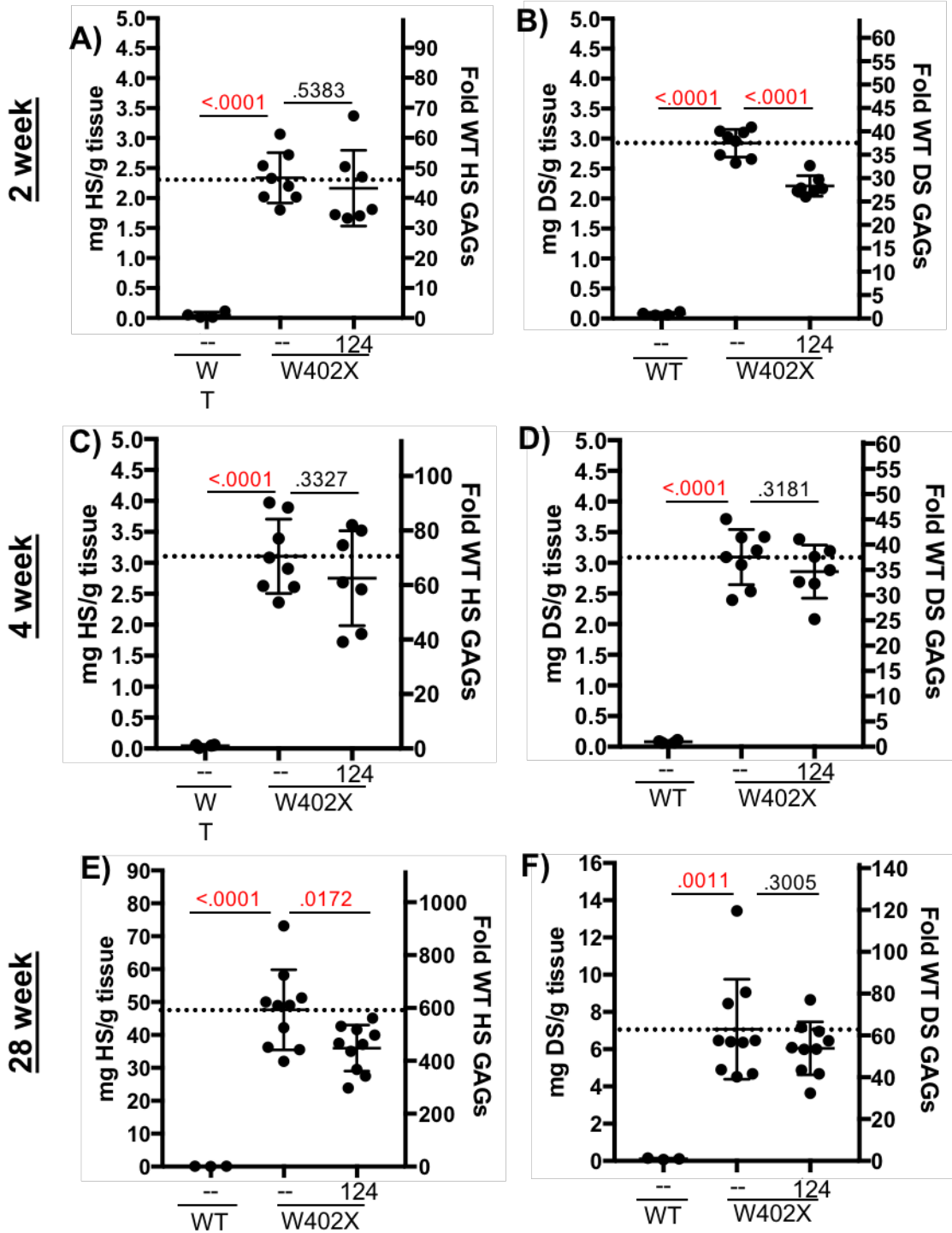


Figure 5: Mass spectrometry analysis of liver GAGs in response to PTC124.

Quantitative analysis by mass spectrometry of the specific liver GAG species heparan sulfate and dermatan sulfate in response to PTC124 after 2 (**A, B**), 4 (**C, D**), or 28 (**E, F**) weeks administration. n = 3 for wild-type mass spec. n = 7-10 mice per group for all other measures. P values from two-tailed t-tests are indicated above brackets.

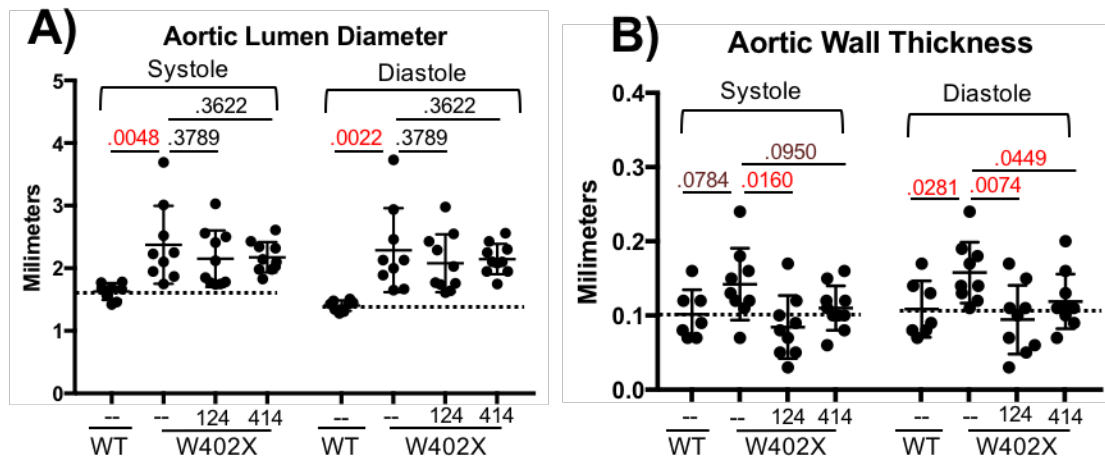
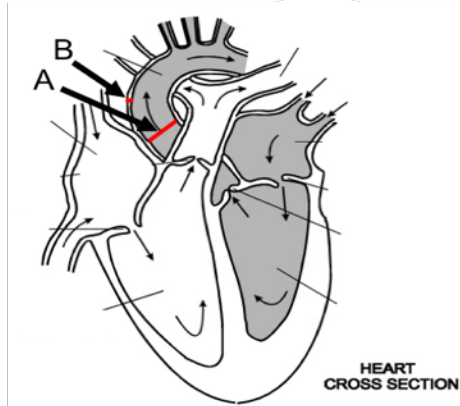


Figure 6: Functional and morphological heart analysis after 28 weeks of treatment in *Idua-W402X* mice. Echocardiography measurements for: A) Aortic lumen diameter, and B) aortic wall thickness at systole (contraction) and diastole (relaxation). Dotted lines indicate levels obtained from untreated, 31-week-old wild-type mice. n = 8-9 mice for all other measures. P values from two-tailed t-tests are indicated above brackets.

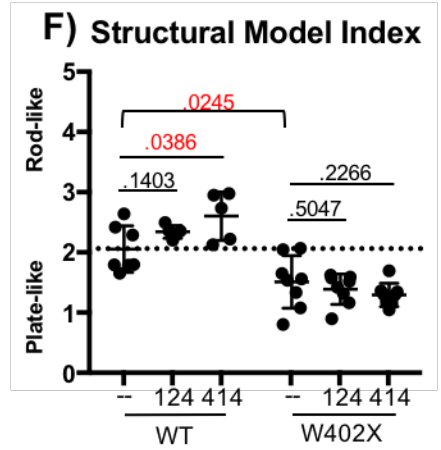
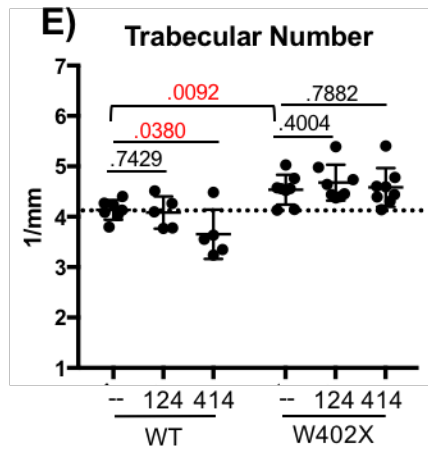
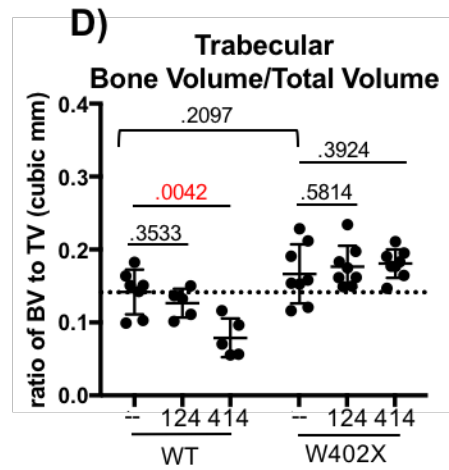
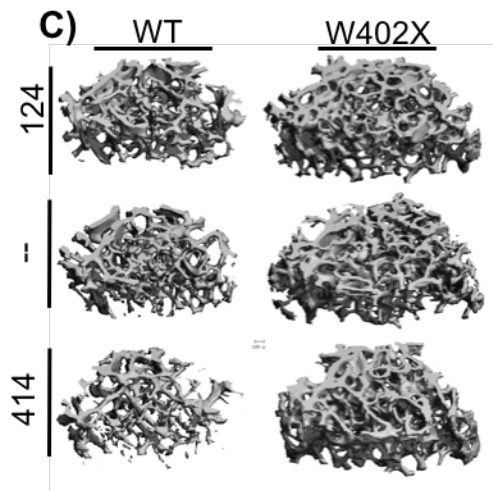
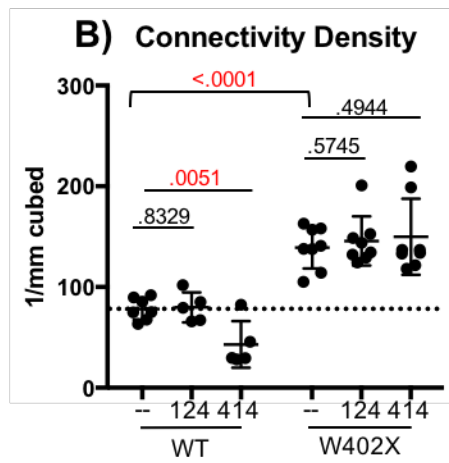
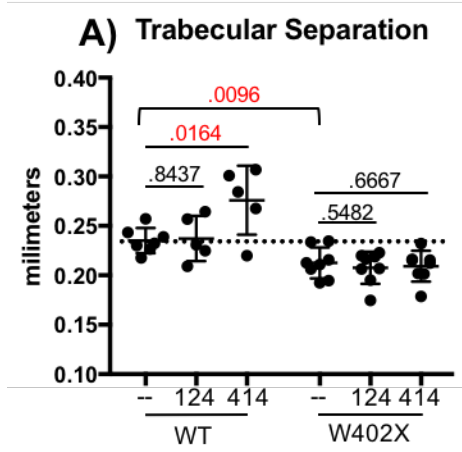


Figure 7: Bone morphological parameters after 28 weeks of treatment in *Idua-W402X* mice. Micro-computed tomography measurements of femurs from wild-type (WT) and *Idua-W402X* (W402X) mice treated for 28 weeks with PTC124 or PTC414. A) trabecular separation, B) trabecular connectivity density, C) representative trabecular bone images, D) trabecular bone volume/total volume; E) trabecular number, F) trabecular structural model index. Dotted lines indicate levels obtained from untreated, 31-week-old wild-type mice. n = 5-8 mice for all other measures. P values from two-tailed t-tests are indicated above brackets.

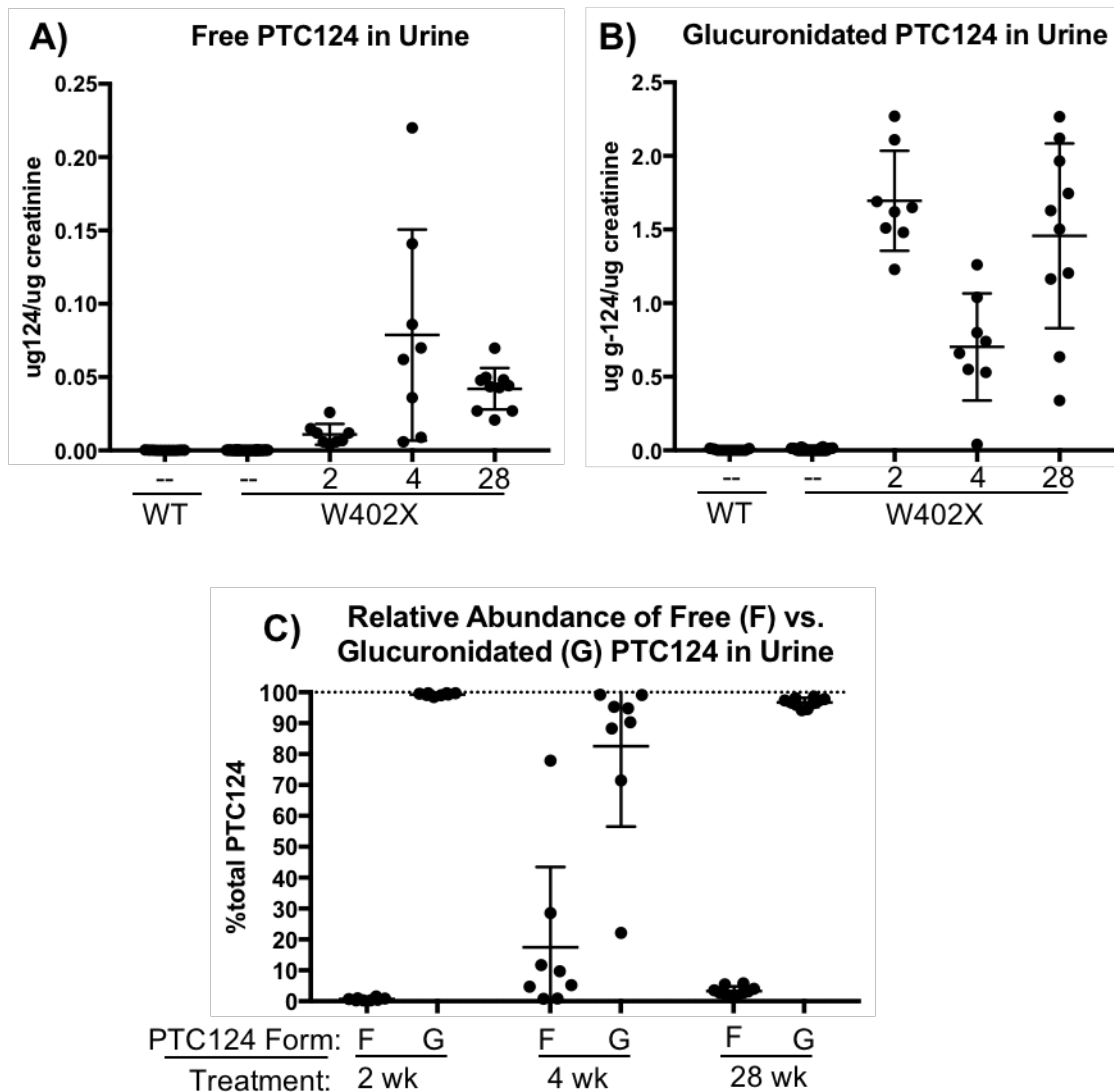
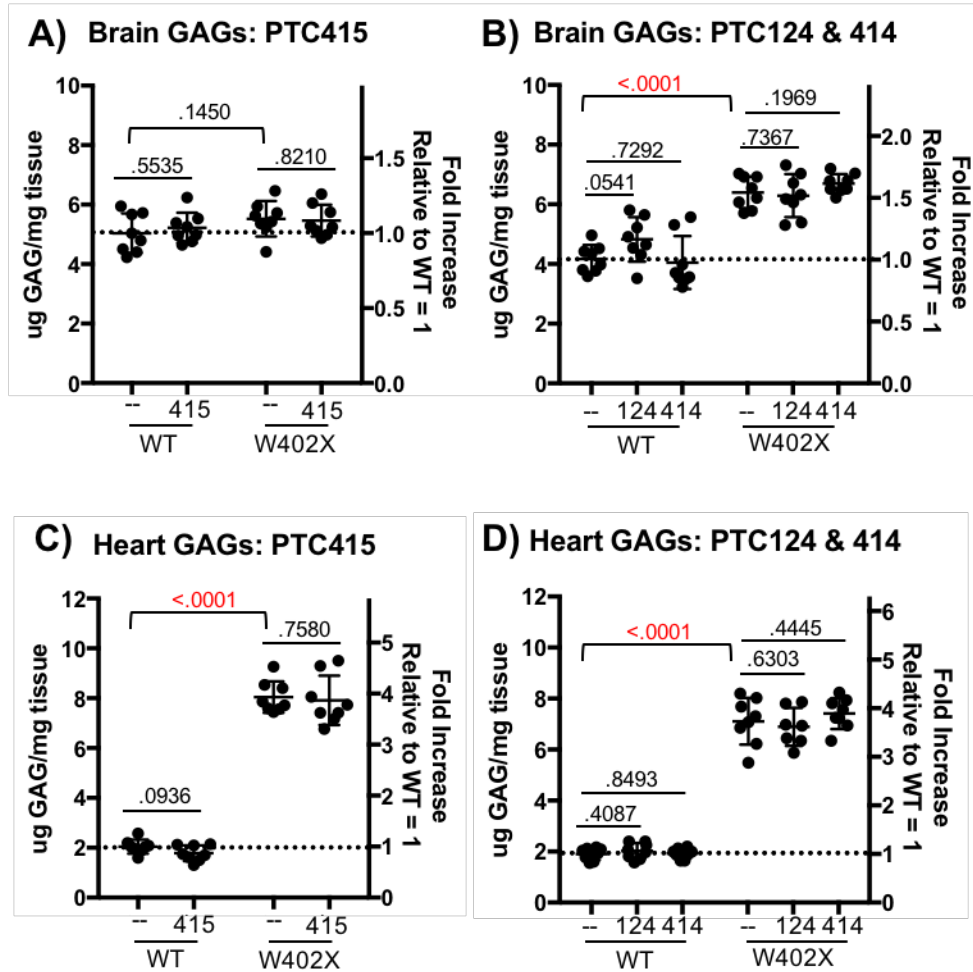
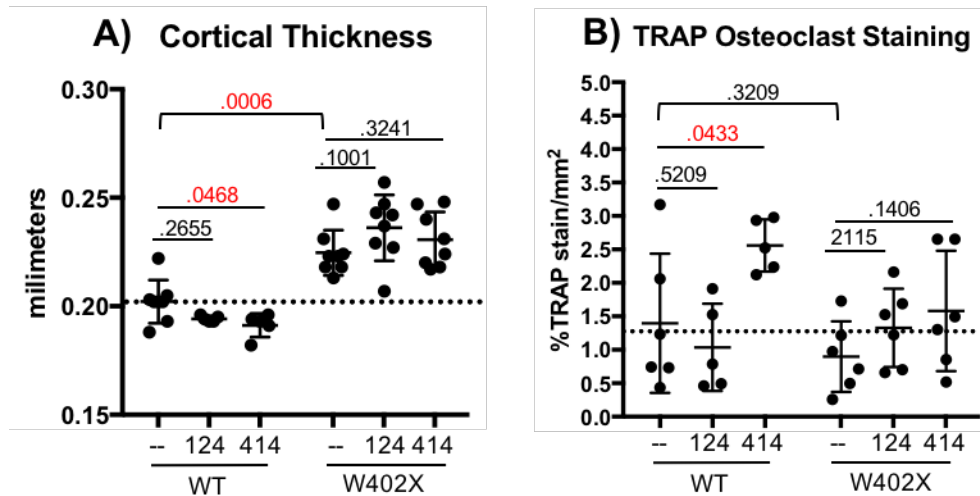


Figure 8: Examination of PTC124 metabolites in mouse urine. Free PTC124 (A) and glucuronidated PTC124 (B) were quantitated via mass spectrometry evaluation of urine samples and normalized to urine creatinine. These two metabolites are represented as the percent of total urine PTC after 2, 4, or 28-week administration in the W402X mouse (C). n = 11 or 26 mice for WT and untreated W402X, respectively. n = 8-10 mice for each treated group.

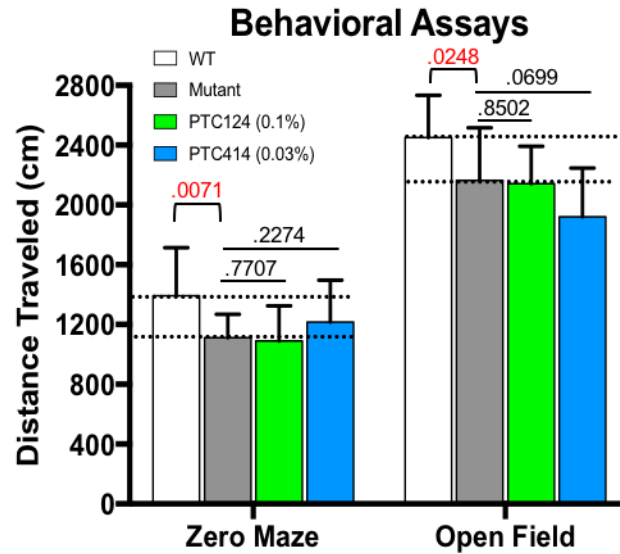
Tissue GAGs: Blyscan Assay



Supplemental Figure 1: Four-week treatment does not reduce GAG accumulation in heart and brain. Quantitative analysis of sulfated GAGs measured via the Blyscan dye binding assay. Brain GAGs in response to A) PTC415, and B) PTC124 and PTC414 and heart GAGs in response to C) PTC415, and D) PTC124 and PTC414 represented as ug GAG per mg dried, defatted tissue. Dotted lines indicate GAG levels obtained from untreated WT mice age 12 weeks. n = 8 mice per group. P values from two-tailed t-tests are indicated above brackets.



Supplemental Figure 2.: Additional bone morphological and histological parameters after 28-week treatment in *Idua*-W402X mice. Analysis of wild type (WT) and *Idua*-W402X (W402X) mice treated for 28 weeks with PTC124 or PTC414. A) Micro-computed tomography measurement of femur cortical bone thickness. B) Quantitation of TRAP staining of slide-mounted femur cross-sections. Dotted lines indicate levels obtained from untreated, 31-week-old wild-type mice. n = 5-8 mice for all measures. P values from two-tailed t-tests are indicated above brackets.



Supplemental Figure 3: Behavioral analysis after 28-week treatment in *Idua-W402X* mice. Zero maze distance traveled (left) and open field distance traveled (right) in response to 28 weeks treatment with PTC124 and PTC414 in WT and *Idua-W402X* mice. Dotted lines indicate levels obtained from untreated, 31-week-old wild-type mice and W402X mice. n = 20 mice for all measures. P values from two-tailed t-tests are indicated above brackets.

Table 1. *In vivo* study design details and study endpoints.

Treatment Duration (weeks)	Age (weeks)	PTC Test Compounds	Study Endpoints	Animals
4	8-12	415 (2.5mg/kg) subQ BIW 124 (0.1% wt/wt in chow) ad lib 414 (0.03% wt/wt in chow) ad lib	Initial efficacy/tolerability	M & F MPS I-H
2	10-12	124 (0.1% wt/wt in chow) ad lib 414 (0.03% wt/wt in chow) ad lib	Mechanistic specificity and efficacy	M & F MPS I-H and KO
28	3-31	124 (0.1% wt/wt in chow) ad lib 414 (0.03% wt/wt in chow) ad lib	Biochemical, morphological and functional endpoints	All Male MPS I-H

SUMMARY

Major Findings and Significance

Current treatments for MPS I-H include HSCT and ERT, both of which are prohibitively expensive and, though promisingly effective, still fail to address all aspects of the disease, particularly in CNS, heart and bone [50, 56]. ERT cannot cross the blood-brain barrier and is therefore not a viable long-term treatment for the severe Hurler form of MPS I. Additionally, early intervention has been demonstrated to predict much more promising health prognosis [47, 57]. Longitudinal studies of HSCT indicate that the disease continues to progress in heart and bone of patients, though earlier intervention and milder disease burden at time of treatment predict better long-term prognosis. The time delay prior to treatment and incomplete efficacy of existing treatments demonstrates the need for alternative therapies that address these short-comings. With nonsense mutations accounting for ~70% of gene lesions associated with Hurler syndrome [1] and ~ 11% of all gene lesions associated with genetic diseases [17], the pursuit of less toxic, more effective read-through drugs has become the focus of much research [36, 37, 39], including in our own lab. In this work, we investigated the ability of nonsense suppression drugs to ameliorate disease progression *in vivo* in a nonsense mouse model of Hurler Syndrome. This project follows from previous *in vitro* [52] and *in vivo* [54] work in which it was demonstrated that nonsense suppression drugs could restore functional enzyme to levels sufficient to ameliorate cellular and biochemical disease

phenotypes. Success in these earlier investigations have led to the hypothesis that, with early and sustained administration, nonsense suppression therapy can prevent or ameliorate disease progression *in vivo* in a nonsense model of Hurler disease.

Our initial investigation discussed in Chapter 2 involved the *in vivo* administration of the designer aminoglycoside NB84 to animals 10-12 weeks of age, or animals 3 weeks of age and continuing for 9 or 28 weeks. The goal of this study was to demonstrate that nonsense suppression therapy could result in detectable improvements in the Hurler phenotype seen in our nonsense mouse model. Our primary biochemical endpoints, lysosomal enzyme activity and glycosaminoglycan (GAG) accumulation, demonstrated that NB84 restored significant levels of iduronidase enzyme activity resulting in sustained reduction of GAG accumulation in multiple tissues, including the brain. However, as discussed, Hurler disease has a very complex and progressive onset with disease manifestations in a diverse set of tissues including brain, heart, and bone. To assess the ability of nonsense suppression therapy to truly alter the progression of disease, we developed a diverse set of assays for the comprehensive evaluation of MPS I-H disease burden in the *Idua*-W402X mouse model. Evaluation of brain sections with the use of antibody staining allowed us to clearly demonstrate that astrocytosis and gliosis occur in mutant animals concomitantly with increased lysosomal size and abundance. Western blot analysis of whole brain lysates demonstrated a reduction in lysosomal and inflammatory biomarkers in response to long-term treatment with NB84. This data demonstrated that neuroinflammation is a consequence of Hurler disease in the *Idua*-W402X mouse model and that this aspect of the disease can be improved through the administration on nonsense suppression drugs. The finding that nonsense suppression

therapy can reduce disease progression in the CNS is incredibly important as the only other therapy currently available with this capability is HSCT. One of the most important hurdles in moving therapeutic options forward is the existing of clinically relevant endpoints amenable to assessment during clinical trials. Skeletal anomalies in Hurler patients represent one of the most difficult-to-treat aspects of the disease. We employed micro-computed tomography to evaluate the three-dimensional structure of the mouse femurs. This technique revealed differential morphology between normal and mutant mice, a phenotype independently observed in both the MPS I-H mouse model and human patients [58-60], with significantly decreased pathology in mutant animals treated long-term with NB84. Through the use of micro-computed tomography, we demonstrated that aminoglycoside therapy was able to reduce the progression of disease in bone, a tissue that has responded poorly to all existing treatments. Additionally, the application of this technique for assessment of disease progression could easily be adapted to a clinical setting for the evaluation of potential therapies for MPS I. To corroborate the morphological findings, and elucidate some of the potential underlying disease mechanisms, we performed histology analysis to evaluate osteoclasts. Osteoclasts are the cells responsible for bone resorption and remodeling, and rely on specialized lysosomes for the excretion of enzymes capable of digesting bone [61]. We found an increased number of osteoclasts, though the thickened bone phenotype was more suggestive of reduced osteoclast activity. This could be the result of impaired osteoclast function [60-62] or irregular function of the osteoblast cells responsible for laying down new mineralized bone. In addition, we assessed mobility in our animals using the elevated zero maze to induce locomotion in our animals. This is an assessment easily adapted to a

clinical setting that does not necessarily identify the specific aspect of disease alleviated, but clearly demonstrates improved overall phenotypic improvement. However, we can hypothesize that reduced GAG accumulation in joints, improved bone morphology, and improved CNS pathology could all contribute directly to improved physical activity [63]. Another major aspect of Hurler disease, and one poorly addressed by existing therapies, is cardiac involvement. We adapted echocardiography with Doppler for the non-invasive evaluation of heart structure and function in the mouse model of Hurler disease. We were able to clearly identify the morphological defects of dilated ascending aorta and thickened vessel walls, hallmarks of Hurler disease identified both in mice and in human Hurler patients [64] [65] and found that they resulted in functional changes in left ventricular stroke volume in the mouse model. In response to long-term NB84 administration we saw greatly reduced morphological differences and normalized heart function, clearly demonstrating that small molecule nonsense suppression therapy penetrates heart tissue to ameliorate disease. We developed a robust set of assays, many of which are non-invasive, that can be easily adapted for evaluation of clinically relevant endpoints of Hurler disease in clinical settings. This study definitely demonstrated that nonsense suppression therapy can modify progression of a nonsense-associated disease in an animal model of MPS I-H, particularly in tissues inadequately addressed by current therapies, such as CNS, heart, and bone.

The aminoglycoside antibiotics represent the most well-known and characterized small molecule read-through compounds currently available [26-29]. However, their toxic effects upon long-term administration are equally well-documented [32-34].

Though we saw no sign of toxicity in our *in vivo* studies, there still exists concern about the safety of early and chronic administration of these historically toxic compounds.

To address this concern and further investigate nonsense suppression as a viable option for the treatment of Hurler disease, we looked to the non-aminoglycoside compounds PTC124, PTC414, and PTC415. In Chapter 3 we characterized the non-aminoglycoside read-through drug PTC124 [40], its derivative PTC414, and the promising read-through compound PTC415 to evaluate mechanism, tolerability, and efficacy. *In vitro* assays revealed that each of these three compounds contributes differentially to the two pathways of nonsense suppression, read-through and NMD. All three compounds showed robust reduction of GAGs in *Idua*-W402X-derived MEFs in contrast to the modest efficacy seen in the HEK293-based read-through reporter system, indicating that perhaps the interplay of read-through and NMD, in a physiologically relevant context, results in greater therapeutic efficacy. Short-term *in vivo* administration revealed acute toxic effects from the compound PTC415, neutral results in response to PTC414, and modest therapeutic efficacy in response to PTC124. Based on short-term tolerability, we investigated both PTC414 and PTC124 efficacy with long-term *in vivo* administration. PTC414 resulted in off-target negative effects in bone and spleen without producing any evidence of therapeutic benefit. However, PTC124 was well-tolerated and maintained the modest efficacy demonstrated in short-term studies, producing modest benefit in cardiac and liver findings. Metabolic analysis of PTC124 revealed significant glucuronidation of the drug, providing a possible explanation for the modest therapeutic benefits achieved.

Although PTC124 produced modest therapeutic efficacy, its well-established safety profile was maintained [42, 43, 66] suggesting that, if combined with existing therapies, it might contribute to improved therapeutic benefit to patients particularly in light of the fact that PTC124 metabolism appears to be less active in patients than in the animal model [16]. Though trepidation remains concerning chronic administration of even designer aminoglycosides, the vastly superior therapeutic efficacy achieved with the use of NB84 clearly demonstrates the mechanistic superiority of these compounds over current alternative small molecule nonsense suppression compounds and justifies further pursuit of these compounds as therapeutic agents.

Future Directions

There is a growing body of evidence demonstrating the validity of nonsense suppression therapy as an effective treatment for nonsense-associated diseases. However, these studies have been ongoing for upwards of 30 years with minimal success at providing tangible benefit to the patient population. There are two primary avenues for the advancement of nonsense suppression therapy (NST). One approach is to optimize the therapeutic efficacy of NST drugs by identifying the compounds capable of safely inducing the highest level of read-through. We demonstrated that NST appears to be most effective at addressing tissues currently resistant to existing therapies, suggesting that another promising approach would be the combination of NST with alternative therapies to enhance the overall improvement in disease prognosis. One of the things most clearly demonstrated by the two studies represented in this work is the need for the identification and development of safer, more effective compounds for nonsense

suppression therapy. High throughput screens, medicinal chemistry, and improved compound validation are all techniques being employed to advance the identification of nonsense suppression compounds [37, 40, 67].

One aspect of nonsense suppression therapy that is only just beginning to be investigated is the question of which near-cognate amino acid gets inserted during PTC read-through and what factors determine the amino acid identity. Recent analysis of amino acid insertion in response to PTC124 or in response to G418 indicates that all read-through-inducing compounds are constrained to a finite set of near-cognate amino acids [68, 69]. Preliminary evidence also demonstrates that the degree of read-through induction, as well as the identity of the amino acid inserted, depends more on the genetic context rather than the nature of the nonsense drug [69], though there is evidence to suggest that a specific compound can be more effective in a particular context [39]. Additionally, some read-through products resulted in nonfunctional protein products for which function could be restored through the use of available complementary therapies known as modulators [69]. These results demonstrate that nonsense suppression therapy could benefit from a personalized medicine approach in which a patient's particular mutation dictated the best treatment drug or combination.

Co-administration of NSTs with ERT or HSCT in MPS I-H animal models could give essential evidence in the feasibility and efficacy of combining existing therapies to enhance their benefit and achieve comprehensive improvement to all affected tissues. Substrate reduction therapy (SRT) is also a promising therapy that might produce greater benefit from combination approaches. SRT targets the pathways by which biogenesis and abundance of the substrate of the deficient enzyme is reduced. Genestein is a plant-

derived isoflavone compound that has demonstrated modest substrate reduction capability in animal models and is thought to be exerting its effects through the TFEB pathway that regulates lysosomal biogenesis [70].

Nonsense-mediated mRNA decay is a surveillance pathway responsible for the rapid degradation of mRNAs that meet certain criteria that result in stalled ribosomal translation. NMD will occur if 1) exon junction complexes are detected downstream of the stalled ribosome and 2) the transcript has an abnormally long 3'UTR resulting in lack of association between the translating ribosome and poly-A-binding protein (PABP) [71, 72]. NMD efficiency has been shown to be inversely correlated with the response of CF patients to aminoglycoside nonsense suppression therapy due to its impact on availability of PTC-containing mRNA [73]. This study also demonstrated that *in vitro* inhibition of NMD, via downregulation of key NMD factors, correlated with increased response to aminoglycoside nonsense suppression. Additionally, it was shown that co-administration of a nonsense-mediated decay inhibitor (NMDI) with the aminoglycoside gentamicin resulted in greater restoration of functional enzyme and amelioration of disease *in vivo* in a mouse model of MPS I-H [74]. These results demonstrate that NMD inhibition, through targeting of NMD factors or small molecule therapy, represents a logical approach to enhance nonsense suppression therapy.

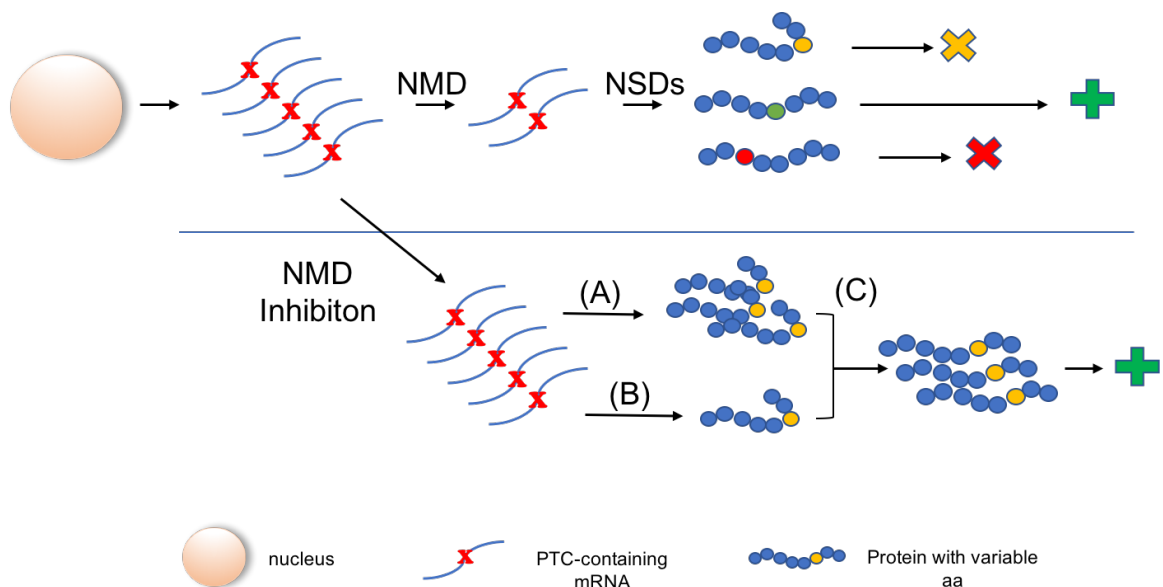


Figure 1. *Opportunities for enhancing or modifying nonsense suppression therapy.* So far nonsense suppression therapy has failed to achieve clinically beneficial levels of functional enzyme restoration. Factors such as NMD, inserted amino acid identity, mutation context, and protein stability diminish the impact of nonsense suppression. However, each of these factors also represent a potential therapeutic target to enhance the efficacy of nonsense suppression drugs (NSDs) in the restoration of functional protein. (A) and (B) represent different NSDs and (C) represents drugs such as CF potentiators, activators, and other protein chaperones.

In recent years, we have begun to understand that there are many variables involved in restoring protein from PTC-containing mRNA. First, mRNA containing a PTC are subject to rapid degradation via the nonsense-mediated mRNA decay pathway (NMD), reducing the availability of PTC-containing mRNA from which enzyme can be produced. Second, the identity of the drug used can result in variable efficacy depending on the context of the mutation and the amino acid(s) inserted at the site of the PTC. Finally, although read-through drugs may restore protein production, that protein may not represent the native protein due to differences in translation rate or amino acid insertion and thus may be non-functional or require additional intervention to achieve functionality. Though these variables create increased complexity they also represent additional therapeutic targets to enhance efficacy of nonsense suppression therapy (Figure 1). Nonsense suppression therapy represents a promising approach for the treatment of diseases caused by nonsense mutations. The advancement of this therapeutic technique has the potential to benefit millions and represents a personalized medicine approach.

GENERAL LIST OF REFERENCES

1. Beesley, C.E., et al., *Mutational analysis of 85 mucopolysaccharidosis type I families: frequency of known mutations, identification of 17 novel mutations and in vitro expression of missense mutations*. Hum Genet, 2001. **109**(5): p. 503-11.
2. Oussoren, E., et al., *Residual alpha-L-iduronidase activity in fibroblasts of mild to severe Mucopolysaccharidosis type I patients*. Mol Genet Metab, 2013. **109**(4): p. 377-81.
3. Haas, M., et al., *European Medicines Agency review of ataluren for the treatment of ambulant patients aged 5 years and older with Duchenne muscular dystrophy resulting from a nonsense mutation in the dystrophin gene*. Neuromuscul Disord, 2015. **25**(1): p. 5-13.
4. Moosajee, M., et al., *Functional rescue of REPI following treatment with PTC124 and novel derivative PTC-414 in human choroideremia fibroblasts and the nonsense-mediated zebrafish model*. Hum Mol Genet, 2016.
5. Pestova, T.V., et al., *Molecular mechanisms of translation initiation in eukaryotes*. Proc Natl Acad Sci U S A, 2001. **98**(13): p. 7029-36.
6. Jackson, R.J., C.U. Hellen, and T.V. Pestova, *The mechanism of eukaryotic translation initiation and principles of its regulation*. Nat Rev Mol Cell Biol, 2010. **11**(2): p. 113-27.
7. Wohlgemuth, I., et al., *Evolutionary optimization of speed and accuracy of decoding on the ribosome*. Philos Trans R Soc Lond B Biol Sci, 2011. **366**(1580): p. 2979-86.
8. Pisarev, A.V., et al., *The role of ABCE1 in eukaryotic posttermination ribosomal recycling*. Mol Cell, 2010. **37**(2): p. 196-210.
9. Shoemaker, C.J. and R. Green, *Translation drives mRNA quality control*. Nat Struct Mol Biol, 2012. **19**(6): p. 594-601.
10. Shao, S., et al., *Decoding Mammalian Ribosome-mRNA States by Translational GTPase Complexes*. Cell, 2016. **167**(5): p. 1229-1240 e15.
11. Schmeing, T.M., et al., *The Crystal Structure of the Ribosome Bound to EF-Tu and Aminoacyl-tRNA*. Science, 2009. **326**: p. 688-94.
12. Brown, A., et al., *Structural basis for stop codon recognition in eukaryotes*. Nature, 2015. **524**: p. 493-496.
13. Blanchet, S., et al., *New insights into stop codon recognition by eRF1*. Nucleic Acids Res, 2015. **43**(6): p. 3298-308.
14. Wells, S.E., et al., *Circularization of mRNA by eukaryotic translation initiation factors*. Mol Cell, 1998. **2**(1): p. 135-40.
15. Ivanov, A., et al., *PABP enhances release factor recruitment and stop codon recognition during translation termination*. Nucleic Acids Res, 2016. **44**(16): p. 7766-76.

16. Heuer, A., et al., *Structure of the 40S-ABCE1 post-splitting complex in ribosome recycling and translation initiation*. Nat Struct Mol Biol, 2017. **24**(5): p. 453-460.
17. Mort, M., et al., *A meta-analysis of nonsense mutations causing human genetic disease*. Hum Mutat, 2008. **29**(8): p. 1037-47.
18. Zund, D., et al., *Translation-dependent displacement of UPF1 from coding sequences causes its enrichment in 3' UTRs*. Nat Struct Mol Biol, 2013. **20**(8): p. 936-43.
19. Serdar, L.D., D.L. Whiteside, and K.E. Baker, *ATP hydrolysis by UPF1 is required for efficient translation termination at premature stop codons*. Nat Commun, 2016. **7**: p. 14021.
20. Chamieh, H., et al., *NMD factors UPF2 and UPF3 bridge UPF1 to the exon junction complex and stimulate its RNA helicase activity*. Nat Struct Mol Biol, 2008. **15**(1): p. 85-93.
21. Silva, A.L., et al., *Proximity of the poly(A)-binding protein to a premature termination codon inhibits mammalian nonsense-mediated mRNA decay*. RNA, 2008. **14**(3): p. 563-76.
22. Manuvakhova, M., K. Keeling, and D.M. Bedwell, *Aminoglycoside antibiotics mediate context-dependent suppression of termination codons in a mammalian translation system*. RNA, 2000. **6**(7): p. 1044-55.
23. Floquet, C., et al., *Statistical analysis of readthrough levels for nonsense mutations in mammalian cells reveals a major determinant of response to gentamicin*. PLoS Genet, 2012. **8**(3): p. e1002608.
24. Roy, B., et al., *Nonsense suppression by near-cognate tRNAs employs alternative base pairing at codon positions 1 and 3*. Proc Natl Acad Sci U S A, 2015. **112**(10): p. 3038-43.
25. Moazed, D. and H.F. Noller, *Transfer RNA shields specific nucleotides in 16S ribosomal RNA from attack by chemical probes*. Cell, 1986. **47**(6): p. 985-94.
26. Palmer, E., J.M. Wilhelm, and F. Sherman, *Phenotypic suppression of nonsense mutants in yeast by aminoglycoside antibiotics*. Nature, 1979. **277**(5692): p. 148-50.
27. Hobbie, S.N., et al., *Engineering the rRNA decoding site of eukaryotic cytosolic ribosomes in bacteria*. Nucleic Acids Res, 2007. **35**(18): p. 6086-93.
28. Howard, M., R.A. Frizzell, and D.M. Bedwell, *Aminoglycoside antibiotics restore CFTR function by overcoming premature stop mutations*. Nat Med, 1996. **2**(4): p. 467-9.
29. Barton-Davis, E.R., et al., *Aminoglycoside antibiotics restore dystrophin function to skeletal muscles of mdx mice*. J Clin Invest, 1999. **104**(4): p. 375-81.
30. Politano, L., et al., *Gentamicin administration in Duchenne patients with premature stop codon. Preliminary results*. Acta Myol, 2003. **22**(1): p. 15-21.
31. Wilschanski, M., et al., *Gentamicin-induced correction of CFTR function in patients with cystic fibrosis and CFTR stop mutations*. N Engl J Med, 2003. **349**(15): p. 1433-41.
32. Sone, M., P.A. Schachern, and M.M. Paparella, *Loss of spiral ganglion cells as primary manifestation of aminoglycoside ototoxicity*. Hear Res, 1998. **115**(1-2): p. 217-23.

33. Carlier, M.B., et al., *Inhibition of lysosomal phospholipases by aminoglycoside antibiotics: in vitro comparative studies*. *Antimicrob Agents Chemother*, 1983. **23**(3): p. 440-9.
34. Martinez-Salgado, C., F.J. Lopez-Hernandez, and J.M. Lopez-Novoa, *Glomerular nephrotoxicity of aminoglycosides*. *Toxicol Appl Pharmacol*, 2007. **223**(1): p. 86-98.
35. Qian, Y. and M.X. Guan, *Interaction of aminoglycosides with human mitochondrial 12S rRNA carrying the deafness-associated mutation*. *Antimicrob Agents Chemother*, 2009. **53**(11): p. 4612-8.
36. Sabbavarapu, N.M., et al., *Design of Novel Aminoglycoside Derivatives with Enhanced Suppression of Diseases-Causing Nonsense Mutations*. *ACS Med Chem Lett*, 2016. **7**(4): p. 418-23.
37. Shulman, E., et al., *Designer Aminoglycosides That Selectively Inhibit Cytoplasmic Rather than Mitochondrial Ribosomes Show Decreased Ototoxicity: A STRATEGY FOR THE TREATMENT OF GENETIC DISEASES*. *J Biol Chem*, 2014. **289**(4): p. 2318-30.
38. Rowe, S.M., et al., *Suppression of CFTR premature termination codons and rescue of CFTR protein and function by the synthetic aminoglycoside NB54*. *J Mol Med (Berl)*, 2011. **89**: p. 1149-1161.
39. Xue, X., et al., *Synthetic aminoglycosides efficiently suppress cystic fibrosis transmembrane conductance regulator nonsense mutations and are enhanced by ivacaftor*. *Am J Respir Cell Mol Biol*, 2014. **50**(4): p. 805-16.
40. Welch, E.M., et al., *PTC124 targets genetic disorders caused by nonsense mutations*. *Nature*, 2007. **447**: p. 87-91.
41. Du, M., et al., *PTC124 is an orally bioavailable compound that promotes suppression of the human CFTR-G542X nonsense allele in a CF mouse model*. *Proc Natl Acad Sci U S A*, 2008. **105**(6): p. 2064-9.
42. Hirawat, S., et al., *Safety, tolerability, and pharmacokinetics of PTC124, a nonaminoglycoside nonsense mutation suppressor, following single- and multiple-dose administration to healthy male and female adult volunteers*. *J Clin Pharmacol*, 2007. **47**(4): p. 430-44.
43. Bushby, K., et al., *Ataluren treatment of patients with nonsense mutation dystrophinopathy*. *Muscle Nerve*, 2014.
44. Trowbridge, J.M. and R.L. Gallo, *Dermatan sulfate: new functions from an old glycosaminoglycan*. *Glycobiology*, 2002. **12**(9): p. 117R-25R.
45. Brooks, D.A., V.J. Muller, and J.J. Hopwood, *Stop-codon read-through for patients affected by a lysosomal storage disorder*. *Trends Mol Med*, 2006. **12**(8): p. 367-73.
46. Muenzer, J., J.E. Wraith, and L.A. Clarke, *Mucopolysaccharidosis I: management and treatment guidelines*. *Pediatrics*, 2009. **123**(1): p. 19-29.
47. de Ru, M.H., et al., *Enzyme replacement therapy and/or hematopoietic stem cell transplantation at diagnosis in patients with mucopolysaccharidosis type I: results of a European consensus procedure*. *Orphanet J Rare Dis*, 2011. **6**: p. 55.
48. Matern, D., et al., *Newborn screening for lysosomal storage disorders*. *Semin Perinatol*, 2015. **39**(3): p. 206-16.

49. Schielen, P.C.J.I., E.A. Kemper, and M.H. Gelb, *Newborn Screening for Lysosomal Storage Diseases: A Concise Review of the Literature on Screening Methods, Therapeutic Possibilities and Regional Programs*. Int. J. Neonatal Screen, 2017. **3**(2): p. 6.
50. Laraway, S., et al., *Outcomes of Long-Term Treatment with Laronidase in Patients with Mucopolysaccharidosis Type I*. J Pediatr, 2016. **178**: p. 219-226 e1.
51. Pastores, G.M., *Laronidase (Aldurazyme): enzyme replacement therapy for mucopolysaccharidosis type I*. Expert Opin Biol Ther, 2008. **8**(7): p. 1003-9.
52. Keeling, K.M., et al., *Gentamicin-mediated suppression of Hurler syndrome stop mutations restores a low level of alpha-L-iduronidase activity and reduces lysosomal glycosaminoglycan accumulation*. Hum Mol Genet, 2001. **10**(3): p. 291-9.
53. Wang, D., et al., *Characterization of an MPS I-H knock-in mouse that carries a nonsense mutation analogous to the human IDUA-W402X mutation*. Mol Genet Metab, 2010. **99**: p. 62-71.
54. Wang, D., et al., *The designer aminoglycoside NB84 significantly reduces glycosaminoglycan accumulation associated with MPS I-H in the Idua-W392X mouse*. Mol Genet Metab, 2012. **105**: p. 116-125.
55. Bedwell, D.M., et al., *The nonsense suppression drug PTC124 restored alpha-l-iduronidase activity and reduces glycosaminoglycan accumulation in MPS IH mice carrying the Idua-W402X mutation*. Molecular Genetics and Metabolism, 2015. **114**(2): p. S20.
56. Aldenhoven, M., et al., *Long-term outcome of Hurler syndrome patients after hematopoietic cell transplantation: an international multicenter study*. Blood, 2015. **125**(13): p. 2164-72.
57. Poe, M.D., S.L. Chagnon, and M.L. Escolar, *Early treatment is associated with improved cognition in Hurler syndrome*. Ann Neurol, 2014. **76**(5): p. 747-53.
58. Aldenhoven, M., J.J. Boelens, and T.J. de Koning, *The clinical outcome of Hurler syndrome after stem cell transplantation*. Biol Blood Marrow Transplant, 2008. **14**(5): p. 485-98.
59. Oestreich, A.K., et al., *Characterization of MPS I-H knock-in mouse reveals increased femoral biomechanical integrity with compromised material strength and altered bone geometry*. MGM Rep, 2015. **5**: p. 3-11.
60. Wilson, S. and D. Bromme, *Potential role of cathepsin K in the pathophysiology of mucopolysaccharidoses*. J Pediatr Rehabil Med, 2010. **3**(2): p. 139-46.
61. Charles, J.F. and A.O. Aliprantis, *Osteoclasts: more than 'bone eaters'*. Trends Mol Med, 2014. **20**(8): p. 449-459.
62. Mellis, D.J., et al., *The skeleton: a multi-functional complex organ: the role of key signalling pathways in osteoclast differentiation and in bone resorption*. J Endocrinol, 2011. **211**(2): p. 131-43.
63. Pan, D., et al., *Progression of multiple behavioral deficits with various ages of onset in a murine model of Hurler syndrome*. Brain Res, 2008. **1188**: p. 241-53.
64. Nemes, A., et al., *The mild form of mucopolysaccharidosis type I (Scheie syndrome) is associated with increased ascending aortic stiffness*. Heart Vessels, 2008. **23**(2): p. 108-11.

65. Jordan, M.C., et al., *Cardiac manifestations in the mouse model of mucopolysaccharidosis I*. Mol Genet Metab, 2005. **86**(1-2): p. 233-43.
66. Kerem, E., et al., *Ataluren for the treatment of nonsense-mutation cystic fibrosis: a randomised, double-blind, placebo-controlled phase 3 trial*. Lancet Respir Med, 2014. **2**(7): p. 539-47.
67. Mutyam, V., et al., *Discovery of Clinically Approved Agents That Promote Suppression of CFTR Nonsense Mutations*. Am J Respir Crit Care Med, 2016.
68. Roy, B., et al., *Ataluren stimulates ribosomal selection of near-cognate tRNAs to promote nonsense suppression*. Proc Natl Acad Sci U S A, 2016. **113**(44): p. 12508-12513.
69. Xue, X., et al., *Identification of the Amino Acids Inserted During Suppression of CFTR Nonsense Mutations and Determination of Their Functional Consequences*. Hum Mol Genet, 2017.
70. Coutinho, M.F., J.I. Santos, and S. Alves, *Less Is More: Substrate Reduction Therapy for Lysosomal Storage Disorders*. Int J Mol Sci, 2016. **17**(7): p. 1-22.
71. Fatscher, T., et al., *The interaction of cytoplasmic poly(A)-binding protein with eukaryotic initiation factor 4G suppresses nonsense-mediated mRNA decay*. RNA, 2014. **20**(10): p. 1579-92.
72. Schweingruber, C., et al., *Nonsense-mediated mRNA decay - mechanisms of substrate mRNA recognition and degradation in mammalian cells*. Biochim Biophys Acta, 2013. **1829**(6-7): p. 612-23.
73. Linde, L., et al., *The efficiency of nonsense-mediated mRNA decay is an inherent character and varies among different cells*. Eur J Hum Genet, 2007. **15**(11): p. 1156-62.
74. Keeling, K.M., et al., *Attenuation of nonsense-mediated mRNA decay enhances in vivo nonsense suppression*. PLoS One, 2013. **8**(4): p. e60478.

APPENDIX

IACUC APPROVAL FOR ANIMAL STUDIES



THE UNIVERSITY OF ALABAMA AT BIRMINGHAM

Institutional Animal Care and Use Committee (IACUC)

NOTICE OF APPROVAL

DATE: January 24, 2011

TO: DAVID M BEDWELL, Ph.D.
BBRB-432A 2170
FAX: (205) 975-5482

FROM: 
Judith A. Kapp, Ph.D., Chair
Institutional Animal Care and Use Committee (IACUC)

SUBJECT: Title: Investigating Suppression Therapy to Treat MPS I-H
Sponsor: University Of Pennsylvania
Animal Project Number: 110109344

As of January 24, 2011, the animal use proposed in the above referenced application is approved. The University of Alabama at Birmingham Institutional Animal Care and Use Committee (IACUC) approves the use of the following species and numbers of animals:

Species	Use Category	Number in Category
Mice	A	360

Animal use must be renewed by January 23, 2012. Approval from the IACUC must be obtained before implementing any changes or modifications in the approved animal use.

Please keep this record for your files, and forward the attached letter to the appropriate granting agency.

Refer to Animal Protocol Number (APN) 110109344 when ordering animals or in any correspondence with the IACUC or Animal Resources Program (ARP) offices regarding this study. If you have concerns or questions regarding this notice, please call the IACUC office at (205) 934-7692.

Institutional Animal Care and Use Committee
CH19 Suite 403
933 19th Street South
205.934.7692
FAX 205.934.1188

Mailing Address:
CH19 Suite 403
1530 3RD AVE S
BIRMINGHAM AL 35294-0019

UAB THE UNIVERSITY OF ALABAMA AT BIRMINGHAM
Institutional Animal Care and Use Committee (IACUC)

MEMORANDUM

DATE: 10-Aug-2015
TO: Bedwell, David M
FROM: 
Robert A. Kesterson, Ph.D., Chair
Institutional Animal Care and Use Committee (IACUC)
SUBJECT: **NOTICE OF APPROVAL**

The following application was approved by the University of Alabama at Birmingham Institutional Animal Care and Use Committee (IACUC) on 10-Aug-2015.

Protocol PI: Bedwell, David M

Title: New Nonsense Suppression Drugs to Treat MPS I

Sponsor: National Institute of Neurological Disorders and Stroke/NIH/DHHS

Animal Project Number (APN): IACUC-10220

This institution has an Animal Welfare Assurance on file with the Office of Laboratory Animal Welfare (OLAW), is registered as a Research Facility with the USDA, and is accredited by the Association for Assessment and Accreditation of Laboratory Animal Care International (AAALAC).

Institutional Animal Care and Use Committee (IACUC)		Mailing Address:
CH19 Suite 403		CH19 Suite 403
933 19th Street South		1530 3rd Ave S
(205) 934-7692		Birmingham, AL 35294-0019
FAX (205) 934-1188		